University of Camerino

School of Advanced Studies

Doctoral thesis in

Life and Health Sciences - Nutrition, Food and Health

Encapsulation of bioactive nutraceutical compounds in donkey and bovine milk β-casein-based carriers

PhD Student:

Dr. Jingjing Zhang

Supervisors:

Prof. Paolo Polidori

Prof. Silvia Vincenzetti

XXXVI CYCLE

2020/2021 - 2022/2023

CONTENTS

ABSTRACT

The use of self-assembled β-caseins from bovine origin as nanocarriers for the delivery of nutraceutical compounds or drugs has been widely investigated. Concerning β-caseins from other milk sources, the use of hypoallergenic donkey β-CN as a potential delivery vehicle for nutraceutical hydrophobic compounds is beginning to generate interest. Therefore, the purpose of this study was to characterize the self-assembly properties and structural changes of purified β-CN obtained from hypoallergenic donkey milk under different conditions of pH, temperature, and ionic strength, with the comparison of commercial bovine β-CN. Based on this knowledge, the interaction mechanisms between donkey β-CN with vitamin D2, and resveratrol, were studied, as well as the encapsulation efficiency of resveratrol within β-CN micelles. These data can provide a theoretical basis for promoting the enrichment and bioavailability of hydrophobic bioactive compounds in food products. This thesis work has been structured as follows:

CHAPTER 1 delves into the structure and attributes of casein micelles while highlighting bovine β-CN's favored role as an encapsulation material due to its unique structure. Intriguingly, similarities in self-assembly patterns between donkey and bovine β-CN were detected, seen through comparable CMC and CMT behaviors. It is interesting to further explore donkey milk-derived β-CN with hypoallergenic properties as nanocarriers for bioactive substances. Therefore, **CHAPTER 2** examined the self-assembly, secondary structure, and surface hydrophobicity of isolated donkey β-CN under varying pH, temperature, and buffer concentration conditions, then was compared with commercial bovine β-CN. The results offer valuable insights into the factors that influence molecular interactions driving donkey β-CN self-association, which could be applied to the development of nanocarriers for bioactive compound encapsulation in pharmaceutical and nutraceutical contexts. Based on this concept, **CHAPTER 3** studied the interaction mechanisms between both donkey and bovine β-CN, and vitamin D2 (VD2) were explored using fluorescence and Dynamic Laser Light Scattering (DLS) techniques at elevated vitamin/protein ratios. Furthermore, the mechanism of interaction between both β-CNs and resveratrol, as well as the

ability of these protein micelles to encapsulate resveratrol are studied in **CHAPTER 4**. Lastly, **CHAPTER 5** imparts the general discussion to declare the main findings of this thesis, and their potential applications in donkey β-CN encapsulating or delivering bioactive substances with the purpose of enhancing their stability and bioactivity.

Keywords: Donkey β-casein; Critical micelle concentration; Critical micelle temperature; Secondary structure; Surface hydrophobicity**; V**itamin D2**;** Resveratrol; Encapsulation.

CHAPTER 1 - General introduction and thesis outline

1.1. Introduction

The use of biopolymer in the in the field of controlled drug-delivery systems has increased dramatically over the past decade (Lu & Chen, 2004). Novel drug-delivery systems, as the key biomedical application of biopolymers, could potentially change the future of numerous therapies via enabling precise molecular targeting and prolong drug delivery (Muthu et al., 2009). Compared to synthetic biopolymers, natural biopolymers are generally considered a safe carrier due to their non-toxic, degradable and metabolizable characteristics (Chasin & Langer, 1990). In recent years, the trend of utilizing food protein-based nanomicelles as carriers to enhance the solubility of hydrophobic drugs or bioactive substances (such as antioxidants, vitamins, probiotics, and fatty acids) in their core has become prevalent. Food protein based delivery vehicles could enhance the stability and bioavailability of these hydrophobic molecules through binding or encapsulating them, protecting them from external influences and degradation, and facilitating their release at the specific location within human tissues (El‐Salam & El‐Shibiny, 2012; Chen et al., 2006).

Milk proteins and milk protein aggregates are regarded as highly favorable nanocarriers due to their predominantly hydrophobic structure, allowing them to function as innate carrier proteins for hydrophobic bioactive substances. Milk proteins are an economical and easily accessible option with good nutritional value and satisfying sensory qualities, which are usually grouped into two main fractions: caseins and whey proteins (Livney, 2010). Caseins (CNS), responsible for 80% of the total protein content in bovine milk, were considered the phosphate-containing proteins with low solubility at their isoelectric point of pH 4.6 (Holt et al., 2013). Four distinctive proteins that make up caseins have been identified till now. They were known as alpha s1 (α_{s1}, 39-46% of total caseins), alpha s2 (α_{s2}, 8-11%), beta (β, 25-35%), and kappa-casein (k, 8–15%), based on their different

amino acid sequences and functions (Swaisgood, 2003). These proteins with molecular weights ranging from 19 to 25 kDa, can exhibit amphiphilic activity due to their hydrophilic and hydrophobic fragments as well (Elzoghby et al., 2011; Ranadheera et al., 2016).

The β-casein (β-CN) fraction serves as a vital protein component, making up roughly 30% of the total bovine casein protein, which is two times less than that (~85%) in human milk. As far as we know, β-CN can be self-assembled into micelles through its highly hydrophobic C-terminus and hydrophilic N-terminus (Atamer et al., 2017; Chia et al., 2017). The β-CN micelles have been widely used as natural vehicles of bioactive compounds such as polyphenols (Esmaili et al., 2011; T. Li et al., 2020), vitamins (Forrest et al., 2005), and flavonoids (Li et al., 2019; M. Li et al., 2020). Additionally, it has also been demonstrated that the drugs can be successfully entrapped into β-CN based micelles such as mitoxantrone, celecoxib, and paclitaxel. These bioactive substances and drugs, once encapsulated, can increase their stability and bioavailability (Rehan et al., 2019).

The research regarding self-assembling behaviour, as well as encapsulation of bioactive compounds and drugs of β-CN has mostly focused on the bovine origin. However, bovine β-CN is identified as one of the key factors in Cow Milk Protein Allergy (CMPA), which occurs initially in infants, but may also persist throughout adulthood with serious symptoms (Lam et al., 2008). In light of this, there has been an increasing number of studies devoted to exploring the use of β-CN protein derived from the milk of various animal species (donkey, equine, camel, and caprine), as an alternative source for hypoallergenic bovine milk alternatives.

Therefore, this thesis chapter provides a detailed account of casein nano micelles, the molecular structure, and physical-chemical properties of donkey and bovine β-CNs, as well as the applications in encapsulation fields based on both β-CN protein micelles. Moreover, the difference between donkey, bovine, and human β-CNs focused on their structure and hypoallergenic properties are also presented and critically discussed.

1.2. Composition of casein and casein micelles models

Globally, milk proteins are crucial components of the human diet, with important nutritional functions. The separation of two types of protein in milk by acidification at pH 4.6 has been a recognized fact since 1830. The protein fractions that are insoluble at pH 4.6 are referred to as caseins, accounting for roughly 78% of the total nitrogen in bovine milk. On the other hand, the remaining soluble protein fractions are known as whey or serum proteins (Fox & Kelly, 2012). Originally, the casein fraction of milk proteins was thought to be uniform; however, since the 1960s, it has been discovered that caseins are highly heterogeneous due to their composition of different sub-fractions, namely αs1-, αs2-, β-, and κ-caseins. These sub-fractions make up approximately 38%, 10%, 36%, and 12% of the entire casein, respectively. Moreover, about 85% of the total casein is comprised of the three caseins, αs1-, αs2-, and β-CNs, which can be precipitated by calcium when concentrations exceed 6.0 mM and temperatures rise above 20 °C (Swaisgood, 2003).

The two primary caseins, αs1- and β-CNs, lack cysteine or cystine residues, while the two lesser caseins, αs2- and κ-CNs, contain two intermolecular disulfide bonds. The principal role of caseins is to produce large macromolecular structures, known as casein micelles, which supply significant amounts of calcium to newborns. Table 1 illustrates and compares the concentrations of caseins and whey proteins found in donkey and human milk with those present in bovine milk.

Table 1. Caseins and whey protein concentrations ($g.kg^{-1}$) in donkey, human and bovine milk.

	Donkey	**Human**	**Bovine**
Total caseins	7.8	2.4	26
αs1-casein	identified	0.77	10.7
αS2-casein	unknown	--	2.8
β-casein	identified	3.87	8.6
k-casein	unknown	0.14	3.1
ɤ-casein	unknown	---	0.8

Total whey proteins	5.8	6.2	6.3
β-lactoglubulin	3.3	---	3.2
α-lactalbumin	1.9	2.5	1.2
Serum albumin	0.4	0.48	0.4
Immunoglobulins	1.30	0.96	0.80
Lactoferrin	0.37	1.65	0.10
Lysozyme	1.00	0.34	0.01
Casein micelle size (nm)	100-200	64	182

Source: (Uniacke‐Lowe & Fox, 2012).

In aqueous solutions, caseins, as amphiphilic proteins, form stable micelle structures through self-assembly. The micelles comprise the four phosphoproteins mentioned above, which are bound together through hydrophobic interactions and the calcium phosphate nanoclusters (CCP) that bridge between phosphorylated serine residues of the casein side chains. In 1921, Beau was the first to use the term "casein micelle". In the past half-century, there have been several proposals for models of casein micelle structure, which were developed based on the information regarding their physicochemical properties and the behavior exhibited by the four casein fractions. Various models have been proposed to elucidate the structure of caseins and casein micelles, with a focus on their functional properties. However, the most widely accepted models for their structure are the subunit model (Walstra, 1999), the Holt model (De Kruif & Holt, 2003), and the dual-binding model that has been introduced to overcome criticisms leveled at the first two (Horne, 2011; Horne, 2002). These three models are illustrated in Fig. 1.

The submicelle is regarded as the primary unit in the submicelle model, where individual caseins aggregated in the correct proportions to form submicelles that are predominantly stabilized by κ-casein (Walstra, 1999). The calcium-phosphate clusters, represented as dark dots in Figure 1B, are essential for cross-linking the proteins and providing stability to the network in the other two models.

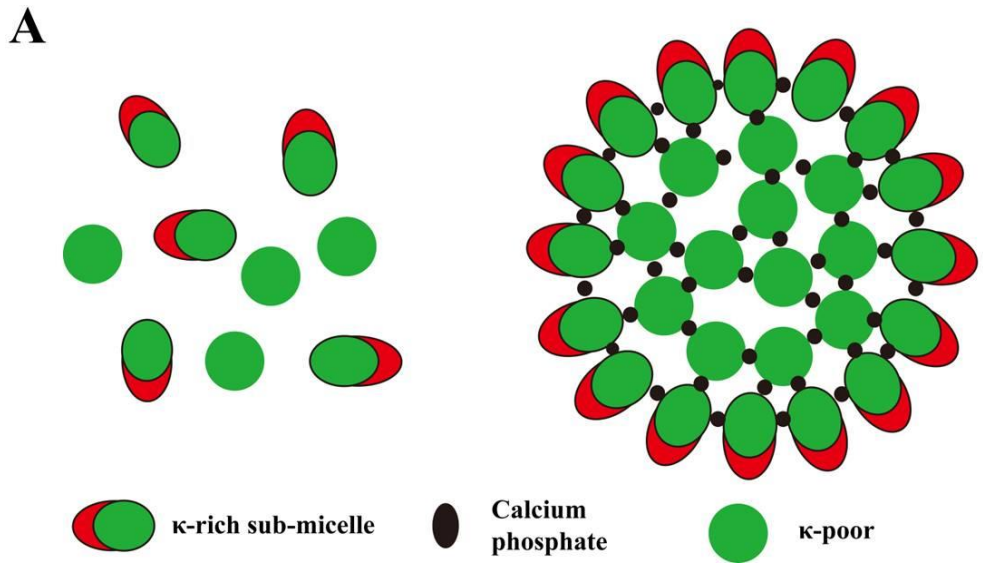
A
κ-rich sub-micelle
Calcium phosphate
κ-poor

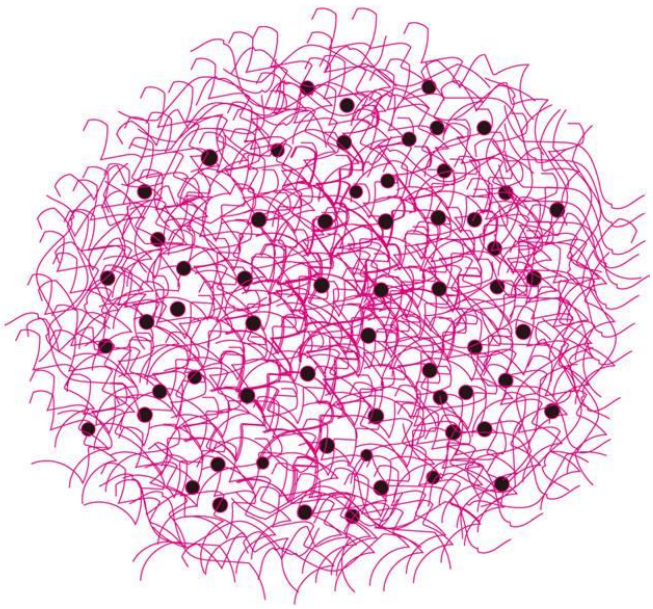
B

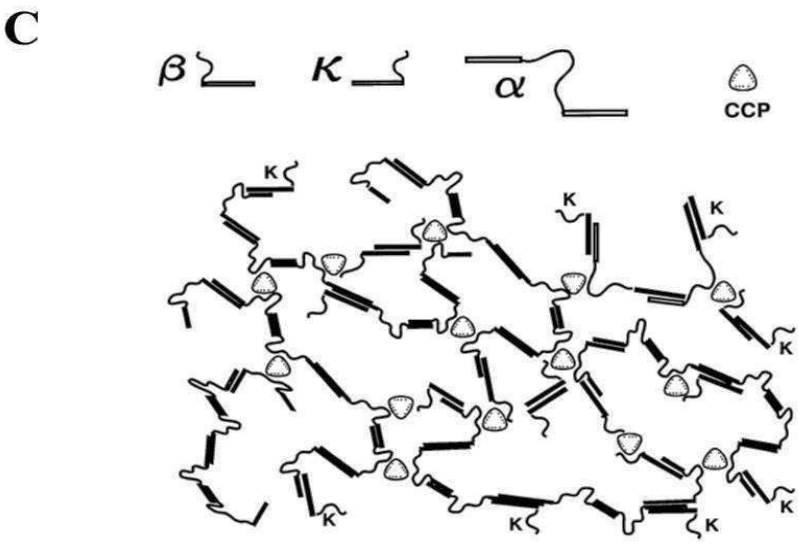
C
β
κ
α
CCP
K

Fig. 1. (A) submicelle model of the casein micelle. (B) Holt model of casein monomers where the dark circles represent calcium phosphate nanoclusters. (C) Horne model of casein micelle representing dual bonding, where the rectangular bars represent hydrophobic regions in which protein–protein interactions occur while the loops represent the protein hydrophilic regions that bind to calcium phosphate clusters shown as triangles, and κ-casein is monomeric and on the surface. Adapted and modified from (Farrell Jr et al., 2006).

In particular, the dual-binding model proposed by Horne (2016) suggests that the stability and integrity of casein micelles are maintained through localized hydrophobic interactions rather than electrostatic repulsions. In this model, it is postulated that the hydrophobic sections of casein fractions (depicted as rectangular bars in Fig. 1C) promote protein-protein interactions, while the hydrophilic segments (represented as loops in Fig. 1C) engage with hydrophilic calcium phosphate clusters (illustrated as triangles in Fig. 1C). During the formation of casein micelles, each casein molecule can interact with different behaviors as they do in their self-association equilibrium and exist as a block copolymer of micelles (Horne, 2016). In summary, αs1-casein undergoes polymerization through hydrophobic interactions, forming a wormlike chain, while the negative charges in the hydrophilic regions are neutralized by calcium phosphate nanoclusters, allowing for the formation of crosslinks with other polymerization pathways. β-casein can utilize both hydrophobic interactions and bridging across calcium phosphate nanoclusters by virtue of its possession of a phosphoserine cluster and a hydrophobic region. However, αs2-casein is capable of sustaining micelle growth by interacting through its two phosphoserine clusters and two hydrophobic regions. Furthermore, κ-casein uses its hydrophobic N-terminal block to form links in the growing chains but cannot extend the polymer chain due to the lack of a phosphoserine cluster in its hydrophilic C-terminal region, which prevents bridging across calcium phosphate nanoclusters. In other words, the micelle stops growing and is stabilized resulting in the formation of an outer "hairy" layer of κ-casein molecules, as depicted in Figure 1C.

1.3. Characteristics of bovine β-CN

1.3.1. Molecular structure of bovine β-CN

β-CN plays a crucial role as a protein component due to its high abundance, making up approximately 30% of the total bovine casein protein, which is less than 85% of the total casein in human milk (Atamer et al., 2017). Characterized by an isoelectric point spanning from pH 4.8 to 5.1, β-CN is an acidic protein composed of 209 amino acid residues and possesses a molecular weight of approximately 24 kDa. In the 1990s report, it was noted that the N-terminal portion of β-CN, with its substantial charge, harbors four out of the five phosphates in the molecule, seven carboxyl groups, and just two positive groups (Dalgleish, 1998).

Taking into account gene polymorphisms and variations in protein sequences, there are a total of 12 unique genetic β-CN variants, including A1, A2, A3, B, C, D, E, F, G, H1, H2, and I, with A1 and A2 being the most frequently found and well-characterized variants (Caroli et al., 2009; Farrell Jr et al., 2004). Amino acid residues associated with the mutational distinctions identified in these 12 genetic bovine β-CN variants are presented in Table 2. Barnett et al, (2014) have observed that the two primary variants A1 and A2 types differ from each other because of the substitution of a single amino acid: specifically, A1 β- CN has histidine at position 67, while A2 β-CN has proline, as illustrated in Fig 2 (Barnett et al., 2014).

Table 2. Positions and amino acid differences in genetic variants of bovine β-CN.

		18	25	35	36		67	72	88	93	106	122	137/138	152	?
β-CN	**A[1]**						His								
(209)	**A[2]**	***SerP***	*Arg*	***SerP***	*Glu*	*Glu*	*Pro*	*Gln*	*Leu*	*Met*	*His*	*Ser*	*Leu/Pro*	*Pro*	*Gln*
	A[3]										Gln				
	B						His					Arg			
	C			Ser		Lys	His								
	D	Lys													
	E				Lys										

F		His					Leu	
G		His				Leu		
H^1	Cys			Ile				
H^2			Glu		Leu			Glu
I					Leu			

Adapted from (Farrell Jr et al., 2004)

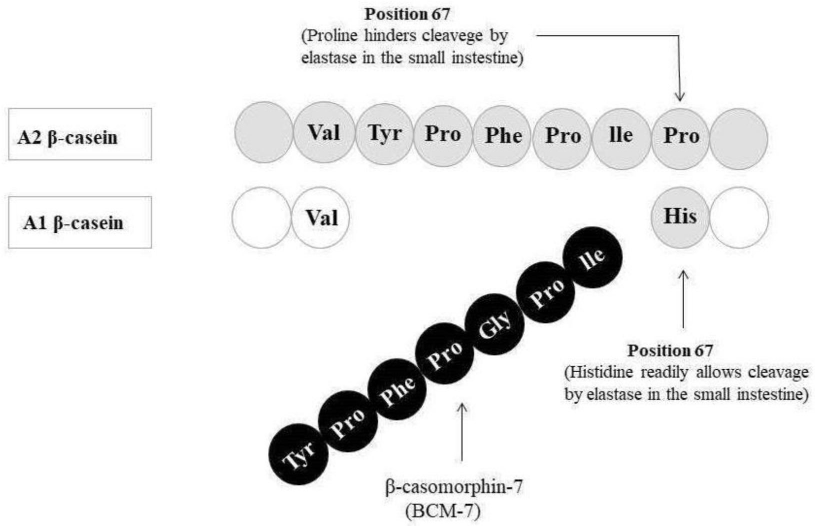

Fig. 2. Systematic diagram of the two variants of the β-casein being varied by the two amino acids at position 67. Adapted from (Chia et al., 2017).

β-CN is regarded as a member of intrinsically unstructured/disordered proteins, which can adopt either a random coil or a molten globule state, with some degree of secondary structure remained in the latter (Dunker et al., 2001). In the study conducted by Dickinson et al. (2003), it was determined that β-CN displays a flexible linear structure and does not possess any internal covalent linkages. The N-terminal sequence of β-CN, which includes charged amino acids and a phosphoserine cluster, is distinct from the neutral and hydrophobic amino acid residues found abundantly in the second half of the molecule, making it the most hydrophobic protein of the casein (Dickinson, 2003). The first 21 amino acids at the N-terminal sequence of β-CN have a net charge at pH 6.6, whereas the C-terminal 21 amino acids are uncharged, creating an atypical distribution of

charged and hydrophobic amino acids that causes β-CN to be released from CN micelles in cold temperatures (Aoki et al., 1990).

1.3.2. Physical and chemical properties of bovine β-CN

Hydrophobic interactions induce the spontaneous self-assembly of β-CN into spherical micelles, although this process faces resistance from electrostatic repulsions and steric hindrances. Due to its amphiphilic nature, β-CN can be spontaneously self-assembled into globular micelles driven by hydrophobic interactions, although this process faces resistance from electrostatic repulsions and steric hindrances (Crowley et al., 2019; Euston & Horne, 2005). These globular micelles have a central hydrophobic core surrounded by a charged hydrophilic coating, exhibiting a structure similar to that of micelles formed by amphiphilic block-copolymers and surfactants (Faizullin et al., 2017). The β-CN critical micellization concentration (CMC) fluctuates within the range of 0.05% to 0.2% w/v, which was affected mainly by pH, temperature, and the ionic strength of their solution.

Generally, alteration in pH values of a solution can weaken or strengthen the intermolecular electrostatic and hydrophobic interactions, which are crucial for determining the structure and function of proteins. Increasing the pH to alkaline values increases inter-residue repulsion, leading to predominantly a disordered coil structure of the polypeptide chain. Conversely, reducing the pH to acidic values neutralizes the negative charges on the caseins with added protons, which progressively decreases the ratio of charge to hydrophobicity, leading to protein folding (Chakraborty & Basak, 2007).

Portnaya et al (2008) reported the β-CN protein is present in micelles when the pH is above pI (around 5.3), whereas it can form round disk-like assemblies below the pI (pH 2.6) with a width of 3-4 nm and a diameter of 20-25 nm (Portnaya et al., 2008). Phoebe et al (2004) investigated the self-association process of β-CN under low concentrations (1-2 mg/mL) and reduced ionic strength (50 mM) at neutral pH 6.75 as well as extreme pH 10.5 (Qi et al., 2004). The results of the analytical

ultracentrifugation experiments conducted under conditions of low ionic strength (50 mM) and extreme pH (10.5) indicated that β-CN remains predominantly in its monomeric form irrespective of temperature within the range of 2-37 ℃, as there was no apparent formation of polymers observed. The self-association process of β-CN has been mostly eliminated at high pH (10.5) is likely attributed to the neutralization or alkaline denaturation of its positively charged side chains, which could shift the net charges of this protein from -12 per molecule at neutral pH to -22 at pH 10.5 (Moitzi et al., 2008; Swaisgood, 1992).

The self-assembly behavior has also been demonstrated to exhibit a strongl dependence on the temperature. Previous research reported the solubility of β-CN was observed to be low at a temperature of 20 °C within the pH range of 4.0 to 5.0. When the temperature is lowered to 2 °C, β-CN is more soluble at pH 5.0, with a slight decrease in solubility at neutral pH (Lucey et al., 1996). Moitzi et al (2008) investigated how temperature impacts the self-assembly of bovine β-CN above and below its isoelectric pH using both Cryogenic-Transmission Electron Microscopy and Small-Angle X-ray Scattering techniques (Moitzi et al., 2008). At pH 2.6, an increase in temperature from 4 to 25 °C leads to a decrease of in the CMC from 0.05 to 0.2% (w/v), which is due to strong hydrophobic interactions at high temperatures. Similarly, the CMC was significantly reduced from 0.36 to 0.06% (w/v) with the temperature rising from 16 to 25 °C at pH 6.7. Furthermore, due to the absence of clear separation between the hydrophobic and hydrophilic domains below its isoelectric pH, β-CN cannot be viewed as a conventional amphiphilic block copolymer with head and tail regions like it at neutral pH. Confirmation of the restructuring of β-CN was obtained at 4 °C, as the content of α-helical structure decreased while the content of random coils increased. This can be explained by the breaking of hydrogen bonds and the attenuation of hydrophobic interactions within the system (Markoska et al., 2021).

An increase in temperature can shift the equilibrium towards the micelle form by elevating the monomer density within the micelles; however, ionic strength can shift the equilibrium position which has a minimal impact on the number of monomers present in the micelle. In addition, the

formation of β-CN micelle can be affected by adding Ca^{2+} which neutralizes the net-negative charge on the protein, leading to the association of phosphoseryl residues (Rollema, 1992). Recently, Li (2019) evaluated the aggregation behaviour of β-CN in the presence of $CaCl_2$, showing that the aggregation behavior of β-CN samples was comparable in water and imidazole buffer, while it exhibited variability in sodium phosphate buffer, particularly when exposed to higher ionic calcium concentrations of 2.5 mM at pH 6.8 (Li et al., 2019). The introduction of $CaCl_2$ stimulated the thermal aggregation of β-CN, which resulted in the formation of larger aggregates with particle sizes larger than 500 nm that were observable under light microscopy. Moreover, the addition of dephosphorylated bovine β-CN for emulsion stabilization reduces the aggregation induced by calcium, as even with the inclusion of 15 or 30 mM CaCl2, dephosphorylated β-CN shows less susceptibility to aggregation compared to phosphorylated β-CN, according to McCarthy et al (2013) (McCarthy et al., 2013). More recently, it was also reported that compared to native β-CN (<100 nm), partially dephosphorylated bovine β-CN was more susceptible to forming large protein aggregates (>1 μm) as increases in $CaCl_2$ concentration from 0 to 9 mM; however, the aggregation behavior of partially dephosphorylated β-CN was exceptional, as it formed smaller aggregates (< 30 nm) than native beta-casein (>300 nm) at pH 4 (Song et al., 2023).

1.3.3. Bovine β-CN micelle-based delivery systems (use in encapsulation)

β-CN micelles, known for their extreme hydrophobicity and high amphipathic properties, have been widely investigated as nanocarriers to encapsulate bioactive molecules and some disease-related drugs, which can enhance their bioavailability, stability, and control delivery. The inner core of β-CN micelles contains hydrophobic residues that can engage in hydrophobic interactions with hydrophobic compounds, while the outer layer is primarily composed of hydrophilic residues, leading to the formation of an electrostatic repulsion layer. Literature has proposed that β-CN exhibited similarities to a diblock copolymer, resulting in its micelles being significantly more stable compared to those formed by low-molecular-weight surfactants, and the release of hydrophobic

substances confined within would exhibit a considerably slower rate, differing by several orders of magnitude compared to those released from surfactants with low molecular weights (Shapira et al., 2010).

Esmaili et al. (2011) reported that curcumin, entrapped into β-CN micelles using the solvent evaporation method, showed higher antioxidant activity compared to that of free curcumin. In comparison to the effective concentration of free curcumin evaluated on the K-562 human leukemia cell line, the median effective concentration of curcumin within capsules was reduced to 17.7 μmol/L

(Esmaili et al., 2011). Naringenin (4', 5, 7-trihydroxyflavonone), known as a flavonoid, naturally presents in citrus fruits such as grapefruit. It has been demonstrated to have an important role in biology and pharmacology, including anti-inflammatory, antimutagenic, anticancer, antimicrobial, antiatherogenic, antioxidative, and hepatoprotective agent. Previous research has indicated that the inclusion of naringenin within β-CN micelles leads to increased stability, a reduced critical micelle concentration (CMC), and an elevated aggregation number (Nagg) when compared to micelles consisting solely of pure β-CN. Furthermore, this inclusion induces a transformation in the shape of β-CN micelles, shifting them from elliptical to spherical structures. Due to its hydrophobic nature, the solubility of naringenin in aqueous solution could be improved significantly after its uptake into the β-CN micelles (Li et al., 2019). Recently, Cheng and co-workers (2020), demonstrated that both trans- and cis- resveratrol could be entrapped by β-CN micelles with encapsulation efficiencies of approximately 69% and 57%, respectively. The isomerization of trans-resveratrol was delayed by β-CN micelles, but the photostability of the cis-isomer was reduced (Cheng et al., 2020). Furthermore, lipid-soluble vitamins such as vitamin D, polyunsaturated fatty acids like omega-3, and various polyphenols such as folic acid exhibit notable encapsulation efficiency and provide significant protection against degradation when incorporated within β-CN micelles (Ranadheera et al., 2016).

Specifically, β-CN can act as a protective barrier for the upper gastrointestinal tract against drug toxicity, making it an ideal candidate for utilization in oral drug delivery systems. Celecoxib

has been shown to be efficiently encapsulated into β-CN nanomicelles which could improve the bioavailability of this drug by improving its solubility in intestinal fluid. Heating-induced celecoxib-β-CN micelles were found to exhibit almost complete drug release, potentially attributed to the reduced colloidal stability of these micelles caused by the heat treatment (Elzoghby et al., 2015). β-CN micelles have been employed to encapsulate various hydrophobic anticancer drugs, such as mitoxantrone, vinca alkaloids (vinblastine), and taxanes (paclitaxel and docetaxel) (Ranadheera et al., 2016).

1.4. Characteristics of Donkey β-CN

1.4.1. Molecular structure of donkey β-CN

In donkey milk, β-CN is the most abundant casein fraction compared to other milk types (Vincenzetti et al., 2012). Various variants of β-CN have been identified in donkey milk, with pI values ranging from 4.63 to 4.95, which are closely resembled those observed in equine β-CN (pI=4.4 to 5.9), but more acidic than the pI of human β-CN (ranging from 4.9 to 5.8) and bovine β-CN (ranging from 5.20 to 5.85) (Poth et al., 2008). Chianese and co-workers (Chianese et al., 2010), showed that donkey milk contains full-length β-CN and spliced variants with 7, 6, and 5-bound phosphate groups, which was later confirmed by two-dimensional studies conducted by Vincenzetti et al. (2012). Indeed, at least three isoforms of full-length β-CNs were discovered in donkey milk, which had comparable molecular weight (around 33.5 kDa) but varied isoelectric points (pIs: 4.72, 4.82, and 4.92, respectively). Additionally, three spliced variants were identified with a smaller molecular weight (about 31.5 kDa) and variable pIs (4.68, 4.80, and 4.88, respectively). Moreover, a new variant with a molecular weight 28 kDa higher than the most prevalent one and an identical phosphorylation pattern was identified.

Three β-CN sequences from *Equus asinus* (donkey) were discovered through research on protein sequence databases such as https://www.uniprot.org/. These sequences are presented in Fig. 3, along with their alignment, which was conducted using the T-COFFEE software, Version_11.00,

Cedric Notredame available at https://tcoffee.crg.eu/apps/tcoffee/do:expresso.

```
BAD AVG GOOD


D2EC27          MKILILACLVALALAREKEELNVSSETVESLSSNEPDSSSEESITHINKEKVQKFKHEGQQQREVEHQD
A0A9L0K6S3      MKILILACLVALALAREKEELNVSSETVESLSSNEPDSSSEESITHINKEKVQKFKHEGQQQREVEHQD
A0A8C4ME87      MKILILACLVALALAREKEELNVSSETVESLSSNEPDSSSE--------EKVQKFKHEGQQQREVEHQD

cons            ****************************************        *********************


D2EC27          KISRFVQPQPVVYPYAEPVPYAVVPQNILPLAQPPIVPFLQPEIMEVSQAKETLLPKRKVMPFLKSPIV
A0A9L0K6S3      KISRFVQPQPVVYPYAEPVPYAVVPQNILPLAQPPIVPFLQPEIMEVSQAKETLLPKRKVMPFLKSPIV
A0A8C4ME87      KISRFVQPQPVVYPYAEPVPYAVVPQNILPLAQPPIVPFLQPEIMEVSQAKETLLPKRKVMPFLKSPIV

cons            ************************************************************************


D2EC27          PFSERQILNPTNGENLRLPVHLIQPFMHQVPQSLLQTLMLPSQPVLSPPQSKVAPFPQPVVPYPQRDTP
A0A9L0K6S3      PFSERQILNPTNGENLRLPVHLIQPFMHQVPQSLLQTLMLPSQPVLSPPQSKVAPFPQPVVPYPQRDTP
A0A8C4ME87      PFSERQILNPTNGENLRLPVHLIQPFMHQVPQSLLQTLMLPSQPVLSPPQSKVAPFPQPVVPYPQRDTP

cons            ************************************************************************


D2EC27          VQAFLLYQDPQLGLTGEFDPATQPIVPVHNPVIV
A0A9L0K6S3      VQAFLLYQDPQLGLTGEFDPATQPIVPVHNPVIN
A0A8C4ME87      VQAFLLYQDPQLGLTGEFDPATQPIVPVHNPVIN

cons            ********************************
```

Fig. 3. Multiple sequence alignment of β-caseins isoforms from *Equus asinus* (donkey). The analysis was performed by using the T-COFFEE software, Version_11.00, Cedric Notredame available at https://tcoffee.crg.eu/apps/tcoffee/do:expresso. The serine, tyrosine and threonine residues evidenced in bold red are those in which there is a high percentage of probability of phosphorylation, calculated by the software NetPhos - 3.1 (Generic phosphorylation sites in eukaryotic proteins) available at https://services.healthtech.dtu.dk/service.php?NetPhos-3.1.

The amino acid residues cut by chymosin are highlighted in blue.

Looking at the sequences, it can be noticed that in the sequences GenBank Acc. No. A0A8C4ME87 the peptide $_{41}$ESITHINK$_{49}$ is not present compared to the other two isoforms, and that the other two forms GenBank Acc. No. D2EC27and A0A9L0K6S3 differ only for the last aminoacidic residue at the C-terminal. Concerning the phosphorylation sites, the analysis performed by the software NetPhos - 3.1 (Generic phosphorylation sites in eukaryotic proteins, https://services.healthtech.dtu.dk/service.php?NetPhos-3.1) revealed that the isoforms GenBank Acc. No. D2EC27and A0A9L0K6S3 have at least 23 potential phosphorylated residues (15 serine, 1 tyrosine and 7 threonine) of which 9 serine residues and 1 threonine lie in the first 45 amino acids of the N-terminal region (Figure 2).

The isoform GenBank Acc. No. A0A8C4ME87, lacking the peptide $_{41}$ESITHINK$_{49}$, is less phosphorylated with respect to the other two full-length isoforms since has 18 potential phosphorylation sites (13 serine, 1 tyrosine, 4 threonine).

Furthermore, at the C terminal region of donkey β-casein (all three isoforms), it can be noticed the presence of the two amino acids $_{213}$LY$_{214}$ which have been identified, in the equine and bovine β-casein, as a site recognized by the chymosin (Egito et al., 2001). In the donkey β-casein this site sensitive to the chymosin action seems to be located in an aminoacidic region not accessible to the solvent, contrary to the bovine β-casein (Figure 4, red box). This could explain the fact that the formation of the curd is very slow when donkey milk is used for cheesemaking.

Donkey

Bovine

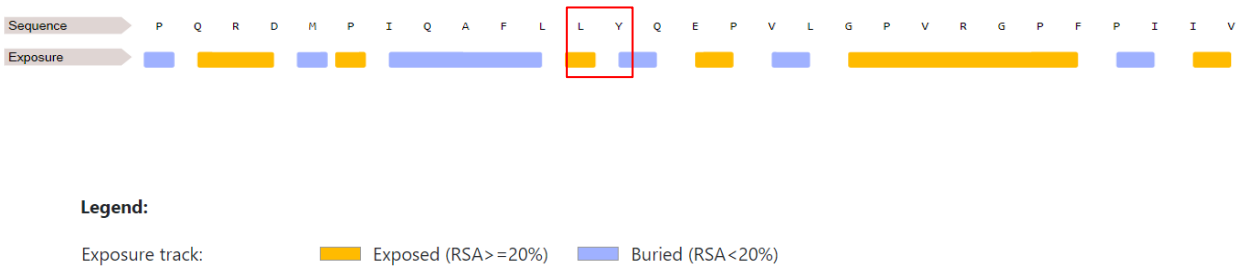

Figure 4. Prediction of residue solvent exposure of the C-terminal region sequence of donkey β-casein (GenBank Acc. No. D2EC27) and bovine β-casein. The analysis has been performed by the software DeepREx-WS available at: https://deeprex.biocomp.unibo.it/home/.

Since donkey milk has very little amount of k-CN which has the fundamental function to stabilize casein micelles (see1.2. Composition of casein and casein micelles models), it has been suggested that non-phosphorylated β-CN present in equid milk may perform a role similar to that of k-CN in bovine milk, which involves stabilizing casein micelles (Doreau & Martin Rosset, 2002; Horne, 2016). However, in donkey milk the presence of a dephosphorylated β-casein isoform has not been found until now.

1.4.2. Physical and chemical properties of donkey β-CN

Perinelli et al. (2019) studied the self-assembling behaviour of β-CN purified from donkey milk for the first time, and the results were compared to those of commercial bovine β-CN, whose concentration and temperature aggregation behaviour has been extensively investigated. The critical micelle concentration (CMC) of donkey β-CN was determined as 0.44 mg/mL in HEPES buffer (50

mM, pH 7.3) by spectrofluorimetry, which was similar to that calculated for bovine β-CN (0.56 mg/mL). As for CMC, the critical micelle temperature (CMT) values of donkey β-CN at concentrations of 2 mg/mL and 5 mg/mL were found to be 24.74 °C and 20.42 °C, respectively, which were comparable to those of bovine β-CN at both concentrations. Additionally, an initial assessment of the potential immunogenicity of β-CN from donkey milk has been conducted via cross-reaction experiments using bovine anti-β-CN antibodies. These results showed donkey β-CN proteins could not be recognized by the bovine anti-β-CN antibodies (Perinelli et al., 2019).

1.5. Difference between donkey, bovine, and human β-CN

Generally, the β-CNs sequences of donkeys, humans and cattle have very high homology. However, the C-terminal sequence of 20 amino acids (ATQPIVPVHNP) present in donkey and human β-CNs makes them different from bovine, as demonstrated in previous study (Perinelli et al., 2019). Looking at Fig. 3 this sequence is present in the three donkey β-CN isoforms (GenBank Acc. No. A0A9L0K6S3; D2EC27 and A0A8C4ME87).

The absence of cross-reactivity between bovine anti-β-CN antibodies and β-CN from human and donkey milk observed by Perinelli and co-workers ((Perinelli et al., 2019) could be attributed to these sequence differences. Among IgE and IgG epitopes of β-CN identified in allergic patients, there were 6 primary and 3 secondary IgE binding epitopes, and 8 primary and 1 secondary IgG binding epitopes for bovine β-CN. Notably, two specific amino acid sequences (VVVPPFLQPEV and LPLPLLQSWM) in β-CN have strong cumulative intensity of IgE binding, while two regions (LPLPLLQSWM and MPIQAFLLYQEPVLGPVRGP-FPII) could be recognized by all patients with CMPA due to their high cumulative intensity of IgG binding. Furthermore, donkey and human β-CN proteins differ in partial amino acid sequence (VVVPPFLQPEV) and C-terminal region (MPIQAFLLYQEPVLGPVRGPFPII), in comparison to the bovine counterpart. These findings highlighted the remarkable similarity between donkey and human milk, further supporting the well-established evidence of donkey milk's hypoallergenic properties (Fig 4.).

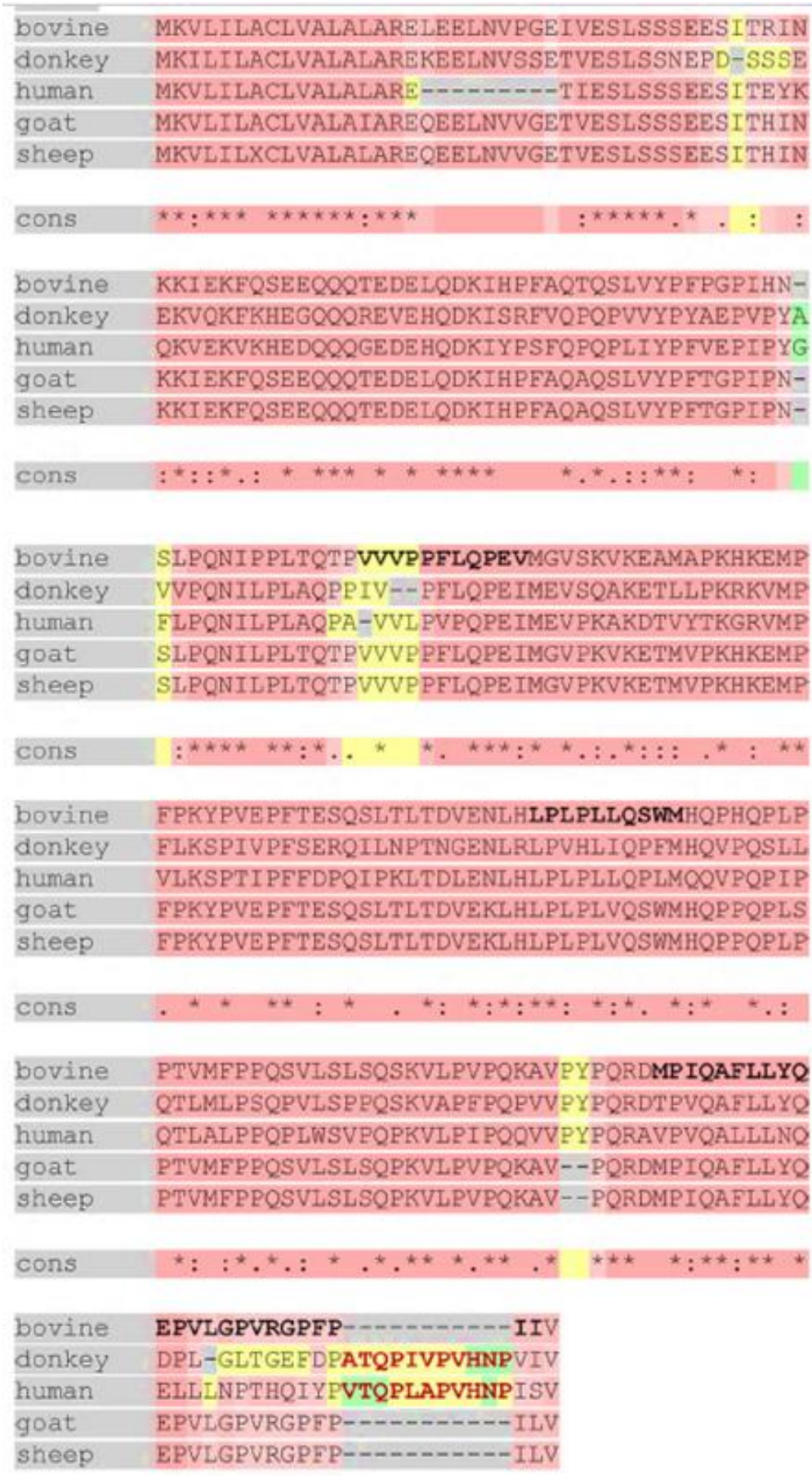
bovine MKVLILACLVALALARELEELNVPGEIVESLSSSEESITRIN
donkey MKILILACLVALALAREKEELNVSSETVESLSSNEPD-SSSE
human MKVLILACLVALALARE---------TIESLSSSEESITEYK
goat MKVLILACLVALAIAREQEELNVVGETVESLSSSEESITHIN
sheep MKVLILXCLVALALAREQEELNVVGETVESLSSSEESITHIN
cons **:*** ******:*** :*****.* . : :
bovine KKIEKFQSEEQQQTEDELQDKIHPFAQTQSLVYPFPGPIHN-
donkey EKVQKFKHEGQQQREVEHQDKISRFVQPQPVVYPYAEPVPYA
human QKVEKVKHEDQQQGEDEHQDKIYPSFQPQPLIYPFVEPIPYG
goat KKIEKFQSEEQQQTEDELQDKIHPFAQAQSLVYPFTGPIPN-
sheep KKIEKFQSEEQQQTEDELQDKIHPFAQAQSLVYPFTGPIPN-
cons :*::*.: * *** * * **** *.*.::**: *:
bovine SLPQNIPPLTQTPVVVPPFLQPEVMGVSKVKEAMAPKHKEMP
donkey VVPQNILPLAQPPIV--PFLQPEIMEVSQAKETLLPKRKVMP
human FLPQNILPLAQPA-VVLPVPQPEIMEVPKAKDTVYTKGRVMP
goat SLPQNILPLTQTPVVVPPFLQPEIMGVPKVKETMVPKHKEMP
sheep SLPQNILPLTQTPVVVPPFLQPEIMGVPKVKETMVPKHKEMP
cons :**** **:*.. * *. ***:* *.:.*::: .* : **
bovine FPKYPVEPFTESQSLTLTDVENLHLPLPLLQSWMHQPHQPLP
donkey FLKSPIVPFSERQILNPTNGENLRLPVHLIQPFMHQVPQSLL
human VLKSPTIPFFDPQIPKLTDLENLHLPLPLLQPLMQQVPQPIP
goat FPKYPVEPFTESQSLTLTDVEKLHLPLPLVQSWMHQPPQPLS
sheep FPKYPVEPFTESQSLTLTDVEKLHLPLPLVQSWMHQPPQPLP
cons . * * ** : * . *: *:*:**: *:*. *:* *.:
bovine PTVMFPPQSVLSLSQSKVLPVPQKAVPYPQRDMPIQAFLLYQ
donkey QTLMLPSQPVLSPPQSKVAPFPQPVVPYPQRDTPVQAFLLYQ
human QTLALPPQPLWSVPQPKVLPIPQQVVPYPQRAVPVQALLLNQ
goat PTVMFPPQSVLSLSQPKVLPVPQKAV--PQRDMPIQAFLLYQ
sheep PTVMFPPQSVLSLSQPKVLPVPQKAV--PQRDMPIQAFLLYQ
cons *: :*.*.: * .*.** *.** .* *** *:**:** *
bovine EPVLGPVRGPFP----------IIV
donkey DPL-GLTGEFDPATQPIVPVHNPVIV
human ELLLNPTHQIYPVTQPLAPVHNPISV
goat EPVLGPVRGPFP----------ILV
sheep EPVLGPVRGPFP----------ILV

Fig 4. Sequence alignment of β-caseins from the bovine, donkey, human, goat, and sheep milk. The analysis was performed by using the T-COFFEE software, Version_11.00, Cedric Notredame available at https://tcoffee.crg.eu/apps/tcoffee/do:expresso. Evidenced in bold are the sequences of the IgE and IgG allergenic epitopes of the bovine milk β-caseins found in the cow's milk allergic patients. From: Perinelli et al., 2019.

In human milk, β-CN is found in multi-phosphorylated forms having 0-5 phosphate groups per molecule, whereas bovine β-CN usually presents in fully phosphorylated forms (Greenberg et al., 1984). The 2-P and 4-P isoforms of human β-CN are usually more abundant compared to those of 0-P, 1-P, 3-P, and 5-P isoforms (Yang et al., 2022). By forming calcium bridges with colloidal calcium phosphates, the phosphate groups in caseins play a crucial role in preserving the structural integrity of casein micelles. Differences in phosphorylation levels may also explain that the temperature-dependent dissociation behavior of human β-CN form micelles was more significant than that of bovine counterpart (Sood et al., 1997).

1.6. Conclusions

This review presents comprehensive information related to the structure and properties of casein micelles, along with the various proposed models that describe their internal organization. Bovine β-CN has been popularly utilized as an encapsulation material for various bioactive substances, primarily due to its special structure and physicochemical properties. A similar self-assembling profile on the basis of critical micelle concentration (CMC) and temperature (CMT) was discovered between β-CN purified from donkey milk and bovine β-CN. Additionally, donkey and human β-CN did not cross-react with bovine β-CN antibodies, suggesting a possible use of donkey β-CN as nanocarrier as an alternative to the bovine one. However, there have been no studies on applications of donkey β-CN in particular encapsulation to date. Therefore, further research is encouraged on the use of β-CN from donkey milk nanocarriers for bioactive substances.

References

EL-Salam, M. H. A, & El-Shibiny, S. (2012). Formation and potential uses of milk proteins as nano delivery vehicles for nutraceuticals: a review. *International journal of dairy technology*, *65*(1), 13-21.

Aoki, T., Yamada, N., & Kako, Y. (1990). Relation between colloidal calcium phosphate cross-linkage and release of β-casein from bovine casein micelles on cooling. *Agricultural and biological chemistry*, *54*(9), 2287-2292.

Atamer, Z., Post, A. E., Schubert, T., Holder, A., Boom, R. M., & Hinrichs, J. (2017). Bovine β-casein: Isolation, properties and functionality. A review. *International dairy journal*, *66*, 115-125.

Barnett, M. P., McNabb, W. C., Roy, N. C., Woodford, K. B., & Clarke, A. J. (2014). Dietary A1 β-casein affects gastrointestinal transit time, dipeptidyl peptidase-4 activity, and inflammatory status relative to A2 β-casein in Wistar rats. *International journal of food sciences and nutrition*, *65*(6), 720-727.

Caroli, A., Chessa, S., & Erhardt, G. (2009). Invited review: Milk protein polymorphisms in cattle: Effect on animal breeding and human nutrition. *Journal of dairy science*, *92*(11), 5335-5352.

Chakraborty, A., & Basak, S. (2007). pH-induced structural transitions of caseins. *Journal of Photochemistry and Photobiology B: Biology*, *87*(3), 191-199.

Chasin, M., & Langer, R. S. (1990). Biodegradable polymers as drug delivery systems. *(No Title)*.

Chen, L., Remondetto, G. E., & Subirade, M. (2006). Food protein-based materials as nutraceutical delivery systems. *Trends in Food Science & Technology*, *17*(5), 272-283.

Cheng, H., Dong, H., & Liang, L. (2020). A comparison of β-casein complexes and micelles as vehicles for trans-/cis-resveratrol. *Food chemistry*, *330*, 127209.

Chia, J., McRae, J., Kukuljan, S., Woodford, K., Elliott, R., Swinburn, B., & Dwyer, K. (2017). A1 beta-casein milk protein and other environmental pre-disposing factors for type 1 diabetes.

Nutrition & Diabetes, *7*(5), e274-e274.

Chianese, L., Calabrese, M. G., Ferranti, P., Mauriello, R., Garro, G., De Simone, C., Quarto, M., Addeo, F., Cosenza, G., & Ramunno, L. (2010). Proteomic characterization of donkey milk "caseome". *Journal of Chromatography A*, *1217*(29), 4834-4840.

Crowley, S. V., Kelly, A. L., O'Mahony, J. A., & Lucey, J. A. (2019). Colloidal properties of protein complexes formed in β-casein concentrate solutions as influenced by heating and cooling in the presence of different solutes. *Colloids and Surfaces B: Biointerfaces*, *174*, 343-351.

Dalgleish, D. (1998). Casein micelles as colloids: surface structures and stabilities. *Journal of dairy science*, *81*(11), 3013-3018.

De Kruif, C., & Holt, C. (2003). Casein micelle structure, functions and interactions. In *Advanced Dairy Chemistry—1 Proteins: Part A/Part B* (pp. 233-276). Springer.

Dickinson, E. (2003). Interfacial, emulsifying and foaming properties of milk proteins. *Advanced Dairy Chemistry—1 Proteins: Part A/Part B*, 1229-1260.

Doreau, M., & Martin Rosset, W. (2002). Dairy animals: horse. U: Encyclopedia of dairy scineces (ur. Roginski H., Fuquay JA, Fox PF). In: Academic Press, London, UK.

Dunker, A. K., Lawson, J. D., Brown, C. J., Williams, R. M., Romero, P., Oh, J. S., Oldfield, C. J., Campen, A. M., Ratliff, C. M., & Hipps, K. W. (2001). Intrinsically disordered protein. *Journal of molecular graphics and modelling*, *19*(1), 26-59.

Egito, A., Girardet, J.-M., Miclo, L., Mollé, D., Humbert, G., & Gaillard, J.-L. (2001). Susceptibility of equine κ-and β-caseins to hydrolysis by chymosin. *International dairy journal*, *11*(11-12), 885-893.

Elzoghby, A. O., El-Fotoh, W. S. A., & Elgindy, N. A. (2011). Casein-based formulations as promising controlled release drug delivery systems. *Journal of controlled release*, *153*(3), 206-216.

Elzoghby, A. O., Elgohary, M. M., & Kamel, N. M. (2015). Implications of protein-and peptide-based nanoparticles as potential vehicles for anticancer drugs. *Advances in protein chemistry*

and structural biology, *98*, 169-221.

Esmaili, M., Ghaffari, S. M., Moosavi-Movahedi, Z., Atri, M. S., Sharifizadeh, A., Farhadi, M., Yousefi, R., Chobert, J.-M., Haertlé, T., & Moosavi-Movahedi, A. A. (2011). Beta casein-micelle as a nano vehicle for solubility enhancement of curcumin; food industry application. *LWT-food science and technology*, *44*(10), 2166-2172.

Euston, S. R., & Horne, D. S. (2005). Simulating the self-association of caseins. *Food Hydrocolloids*, *19*(3), 379-386.

Faizullin, D. A., Konnova, T. A., Haertlé, T., & Zuev, Y. F. (2017). Secondary structure and colloidal stability of beta-casein in microheterogeneous water-ethanol solutions. *Food Hydrocolloids*, *63*, 349-355.

Farrell Jr, H., Jimenez-Flores, R., Bleck, G., Brown, E., Butler, J., Creamer, L., Hicks, C., Hollar, C., Ng-Kwai-Hang, K., & Swaisgood, H. (2004). Nomenclature of the proteins of cows' milk—Sixth revision. *Journal of dairy science*, *87*(6), 1641-1674.

Farrell Jr, H., Malin, E., Brown, E., & Qi, P. (2006). Casein micelle structure: What can be learned from milk synthesis and structural biology? *Current opinion in colloid & interface science*, *11*(2-3), 135-147.

Forrest, S. A., Yada, R. Y., & Rousseau, D. (2005). Interactions of vitamin D3 with bovine β-lactoglobulin A and β-casein. *Journal of agricultural and food chemistry*, *53*(20), 8003-8009.

Fox, P., & Kelly, A. (2012). Chemistry and biochemistry of milk constituents. *Food biochemistry and food processing*, 442-464.

Greenberg, R., Groves, M. L., & Dower, H. J. (1984). Human beta-casein. Amino acid sequence and identification of phosphorylation sites. *Journal of Biological Chemistry*, *259*(8), 5132-5138.

Holt, C., Carver, J., Ecroyd, H., & Thorn, D. (2013). Invited review: Caseins and the casein micelle: Their biological functions, structures, and behavior in foods. *Journal of dairy science*, *96*(10), 6127-6146.

Horne, D. (2011). Milk proteins| Casein, micellar structure.

Horne, D. (2016). Casein: Micellar structure (Dual-binding model).

Horne, D. S. (2002). Casein structure, self-assembly and gelation. *Current opinion in colloid & interface science*, *7*(5-6), 456-461.

Lam, H. Y., Van Hoffen, E., Michelsen, A., Guikers, K., Van Der Tas, C., Bruijnzeel-Koomen, C., & Knulst, A. (2008). Cow's milk allergy in adults is rare but severe: both casein and whey proteins are involved. *Clinical & Experimental Allergy*, *38*(6), 995-1002.

Li, M., Fokkink, R., Ni, Y., & Kleijn, J. M. (2019). Bovine beta-casein micelles as delivery systems for hydrophobic flavonoids. *Food Hydrocolloids*, *96*, 653-662.

Li, M., Wang, K., Wang, Y., Han, Q., Ni, Y., & Wen, X. (2020). Effects of genipin concentration on cross-linked β-casein micelles as nanocarrier of naringenin: Colloidal properties, structural characterization and controlled release. *Food Hydrocolloids*, *108*, 105989.

Li, T., Li, X., Dai, T., Hu, P., Niu, X., Liu, C., & Chen, J. (2020). Binding mechanism and antioxidant capacity of selected phenolic acid-β-casein complexes. *Food Research International*, *129*, 108802.

Livney, Y. D. (2010). Milk proteins as vehicles for bioactives. *Current opinion in colloid & interface science*, *15*(1-2), 73-83.

Lu, Y., & Chen, S. (2004). Micro and nano-fabrication of biodegradable polymers for drug delivery. *Advanced drug delivery reviews*, *56*(11), 1621-1633.

Lucey, D. R., Clerici, M., & Shearer, G. M. (1996). Type 1 and type 2 cytokine dysregulation in human infectious, neoplastic, and inflammatory diseases. *Clinical microbiology reviews*, *9*(4), 532-562.

Manfredi, M., Savojardo, C., Martelli, P. L., & Casadio, R. (2021). DeepREx-WS: A web server for characterising protein–solvent interaction starting from sequence. *Computational and Structural Biotechnology Journal*, *19*, 5791-5799.

Markoska, T., Daniloski, D., Vasiljevic, T., & Huppertz, T. (2021). Structural changes of β-casein induced by temperature and pH analysed by nuclear magnetic resonance, Fourier-transform

infrared spectroscopy, and chemometrics. *Molecules*, *26*(24), 7650.

McCarthy, N. A., Kelly, A. L., O'Mahony, J. A., & Fenelon, M. A. (2013). The physical characteristics and emulsification properties of partially dephosphorylated bovine β-casein. *Food chemistry*, *138*(2-3), 1304-1311.

Moitzi, C., Portnaya, I., Glatter, O., Ramon, O., & Danino, D. (2008). Effect of temperature on self-assembly of bovine β-casein above and below isoelectric pH. Structural analysis by cryogenic-transmission electron microscopy and small-angle X-ray scattering. *Langmuir*, *24*(7), 3020-3029.

Muthu, M. S., Rajesh, C. V., Mishra, A., & Singh, S. (2009). Stimulus-responsive targeted nanomicelles for effective cancer therapy. *Nanomedicine*, *4*(6), 657-667.

Perinelli, D. R., Cespi, M., Bonacucina, G., & Palmieri, G. F. (2019). PEGylated polylactide (PLA) and poly (lactic-co-glycolic acid)(PLGA) copolymers for the design of drug delivery systems. *Journal of pharmaceutical investigation*, *49*, 443-458.

Portnaya, I., Ben-Shoshan, E., Cogan, U., Khalfin, R., Fass, D., Ramon, O., & Danino, D. (2008). Self-assembly of bovine β-casein below the isoelectric pH. *Journal of agricultural and food chemistry*, *56*(6), 2192-2198.

Poth, A. G., Deeth, H. C., Alewood, P. F., & Holland, J. W. (2008). Analysis of the human casein phosphoproteome by 2-D electrophoresis and MALDI-TOF/TOF MS reveals new phosphoforms. *Journal of proteome research*, *7*(11), 5017-5027.

Qi, P. X., Wickham, E. D., & Farrell, H. M. (2004). Thermal and alkaline denaturation of bovine β-casein. *The protein journal*, *23*, 389-402.

Ranadheera, C., Liyanaarachchi, W., Chandrapala, J., Dissanayake, M., & Vasiljevic, T. (2016). Utilizing unique properties of caseins and the casein micelle for delivery of sensitive food ingredients and bioactives. *Trends in Food Science & Technology*, *57*, 178-187.

Rehan, F., Ahemad, N., & Gupta, M. (2019). Casein nanomicelle as an emerging biomaterial—A comprehensive review. *Colloids and Surfaces B: Biointerfaces*, *179*, 280-292.

Rollema, H. (1992). Casein association and micelle formation. *Advanced dairy chemistry-1: Proteins.*(Ed. 2), 111-140.

Shapira, A., Markman, G., Assaraf, Y. G., & Livney, Y. D. (2010). β-casein–based nanovehicles for oral delivery of chemotherapeutic drugs: drug-protein interactions and mitoxantrone loading capacity. *Nanomedicine: Nanotechnology, Biology and Medicine*, *6*(4), 547-555.

Song, S., Lin, Y., Zhang, Y., Luo, Y., & Guo, H. (2023). The self-association properties of partially dephosphorylated bovine beta-casein. *Food Hydrocolloids*, *134*, 108019.

Sood, S. M., Herbert, P. J., & Slatter, C. W. (1997). Structural studies on casein micelles of human milk: Dissociation of β-casein of different phosphorylation levels induced by cooling and ethylenediaminetetraacetate. *Journal of dairy science*, *80*(4), 628-633.

Swaisgood, H. (2003). Chemistry of the Caseins Advanced Dairy Chemistry. In: New York: Plenum Publishers.

Swaisgood, H. E. (1992). Chemistry of the caseins. *Advanced dairy chemistry-1: Proteins.*(Ed. 2), 63-110.

Uniacke-Lowe, T., & Fox, P. F. (2012). Equid milk: Chemistry, biochemistry and processing. *Food biochemistry and food processing*, 491-530.

Vincenzetti, S., Amici, A., Pucciarelli, S., Vita, A., Micozzi, D., Carpi, F., Polzonetti, V., Natalini, P., & Polidori, P. (2012). A proteomic study on donkey milk. *Biochem Anal Biochem*, *1*(109), 2161-1009.1000109.

Walstra, P. (1999). Casein sub-micelles: do they exist? *International dairy journal*, *9*(3-6), 189-192.

Yang, T., Liu, D., & Zhou, P. (2022). Temperature-dependent dissociation of human micellar β-casein: Implications of its phosphorylation degrees and casein micelle structures. *Food chemistry*, *376*, 131935.

CHAPTER 2 - The effects of pH, temperature, and buffer concentration on the self-assembling behavior, secondary structure, and surface hydrophobicity of donkey and bovine β-casein

This article has been published as:

Zhang, Jingjing , Silvia Vincenzetti, Paolo Polidori, Valeria Polzonetti, Alessandro Di Michele, Diego Romano Perinelli, Guiqin Liu, Lanjie Li, Stefania Pucciarelli. "The effects of pH, temperature, and buffer concentration on the self-assembling behavior, secondary structure, and surface hydrophobicity of donkey and bovine β-casein." *Food Chemistry* 433 (2024): 137285.

Supplementary data to this article can be found online at https://doi.org/10.1016/j.foodchem.2023.137285.

Abstract

The self-assembling behavior, secondary structure, and surface hydrophobicity of purified donkey β-casein in terms of pH, temperature, and buffer concentration were investigated in comparison with commercial bovine β-casein. Critical micelle concentration of both β-caseins decreased with the lowering of pH (pH 8.0-6.0) and the increasing temperatures (25 ℃-50 ℃). Critical micelle temperature of both β-caseins increased moving from pH 6.0 to 8.0 and aggregates larger than micelles formed at pH 6.0 that is close to their isoelectric point. Fluorescence spectroscopy analysis demonstrated that the maximum surface hydrophobicity was achieved at pH 6.0. The secondary structure was examined using circular dichroism spectroscopy, highlighting an increase of α-helix content and a decrease of unordered structures with the decrease of pH and increase of temperature. This work provides insights on parameters promoting molecular interactions involved in donkey β-CN self-association, useful to develop nanocarriers for encapsulating bioactive compounds in pharmaceutical and nutraceutical applications.

Keywords: Donkey β-casein; Critical micelle concentration; Critical micelle temperature; Secondary structure; Surface hydrophobicity

2.1. Introduction

Caseins represent the major fractions (50-80%, w/w) of total milk proteins and have attracted much interest thanks to their peculiar structure and appealing functional properties (Tidona et al., 2014). The four caseins in milk that differ markedly in terms of structure and function are αs1-caseins (~38%), αs2-caseins (~10%), β-caseins (~34%) and k-caseins (~15%) (Ranadheera et al., 2016). In an aqueous environment, as in milk, they associate into supramolecular colloidal structures known as casein micelles, which are approximately spherical in shape with an average diameter of about 120 nm and a mass in the range of 10^6-10^9 Da (Holt, 2013).

β-casein (β-CN) is the major protein constituent, accounting for around 30% of the total bovine caseins. Differently from the other caseins, β-CN can self-assemble into a micellar structure under appropriate (e.g., physiological) conditions thanks to its amphiphilic structure, leading to the formation of energetically favored intermolecular hydrophobic interactions (Chia et al., 2017). Bovine β-CN consists of 224 amino acids and shows a molecular weight of ~24 kDa, and the secondary structure is widely represented by a random coil with considerable flexibility due to the lack of disulfide bonds (Raynes et al., 2015). The β-CN unique structural properties can depend on the presence of large amounts of proline residues, which strongly affect the protein structure due to their tendency to impair the formation of α-helixes and β-sheets and arrange in short segments of polyproline II-helices in a temperature-dependent behavior (Hasni et al., 2011). The formation of β-casein's self-assembled micelles in an aqueous environment is affected by many factors, the most important of which are protein concentration, ionic strength, pH, and temperature (Schulte et al., 2020). Specifically, the critical micelle concentration (CMC) of β-CN can range between 0.05% and 0.2% (w/v), while the critical micelle temperature (CMT) is normally above ~20 ℃ at a neutral pH

(Perinelli et al., 2019; Portnaya et al., 2006). Therefore, β-CN exists mainly as monomers under CMC and CMT, while it starts to self-assemble through the formation of hydrophobic interactions as concentration and temperature increase, giving rise to micellar aggregates characterized by a hydrophobic core and a less dense hydrophilic outer layer (Dauphas et al., 2005).

The unique structural organization of β-CN micelles makes them suitable for encapsulation, stabilization, and protection of several hydrophobic bioactive molecules, such as polyphenols, fat-soluble vitamins, and oils (Forrest et al., 2005; Li et al., 2019). Recently, several studies have introduced β-CN micelles as natural potential nano vehicles for the entrapment and oral delivery of hydrophobic drugs as anticancer chemotherapeutics including mitoxantrone (MX) (Shapira et al., 2010).

In the literature, several studies have presented the chemical-physical characterization and applications of β-CN proteins, but all of them concern the protein of bovine origin. Indeed, structural information about donkey milk β-casein are very few and only regarding the primary structure. Donkey milk β-casein consists of a full-length form A (226 amino acids) and a spliced form named B (218 amino acids) characterized by the lack of the peptide $_{27}$ESITHINK$_{34}$ in the exon 5. These two A and B forms are in turn phosphorylated carrying 5, 6 and 7 phosphate groups (Licitra, et al., 2019). Other authors described another β-casein variant characterized by higher molecular weight and the presence of 5, 6 and 7 phosphate groups (Chianese, et al., 2010).

The interest of the food industry in donkey milk is mainly due to its hypoallergenic properties; several authors have demonstrated that serum of patients affected by Cow's Milk Protein Allergy (CMPA) does not cross-react with caseins and whey proteins isolated by donkey milk (Monti et al., 2007; Vincenzetti et al., 2014).

Furthermore, in a previous work, it was demonstrated that donkey β-CN was not recognized by bovine anti-β-CN antibodies and this could determine the low immunogenicity potential of the protein from donkey source (Perinelli et al., 2019). This may be due to that fact that the IgE and IgG allergenic epitopes of bovine β-CN found in CMPA patients lies in an amino acid sequence that is

different in the donkey β-CN (Perinelli et al, 2019; Vincenzetti et al., 2022).

Considering the emerging interest of the food field in donkey milk, it is worth elucidating the self-assembling behavior of donkey β-CN in comparison to the protein of bovine origin with the aim to acquire basic knowledge to exploit donkey β-CN as a potential biomaterial for the encapsulation and delivery of active compounds and drugs. Specifically, this research focuses on the characterization of self-assembling properties and structural changes of purified β-CN (obtained from donkey milk) at different conditions of pH (from 5.5 to 9.0), temperature (from 20 ℃ to 50 ℃) and buffer concentration (50 mM and 250 mM) using fluorescence spectroscopy, dynamic light scattering, and far-UV circular dichroism. The obtained results were then compared to those from commercial bovine β-CN and analyzed under the same experimental conditions.

2.2. Materials and methods

2.2.1 Materials

The donkey milk used in this study (from animals at the mid-stage of lactation), was purchased from a local farm (Azienda Agricola Mamma Asina, Colmurano, MC), located in the Marche region and immediately stored at 4 ℃. The β-CN proteins of donkey's milk were obtained according to the method described below (section 2.2). Lyophilized bovine β-CN, used as reference, was purchased from Sigma Aldrich (St. Louis, MO).

Ultrapure water was produced using an Adrona Crystal EX Trace/HPLC/Bio water purification system (Adrona SIA, Riga, Latvia). The reagent-grade chemicals used in this study were purchased from Sigma-Aldrich (St. Louis, MO).

2.2.2 Methods

2.2.2.1. Purification of β-CN from donkey milk

Native β-CN was extracted and purified from donkey milk as previously described (Perinelli et al., 2019) with some modifications. After separation from the whey proteins by isoelectric precipitation at pH 4.6, the donkey casein fraction (obtained from 10 mL of milk) was resuspended in 10 mL of buffer A (50 mM ammonium acetate, 8 M urea; pH 5.5) and subsequently subjected to cationic exchange chromatography by using Carboxymethyl cellulose (CM52, Whatman, Merck, Darmstadt, Germany). The column was equilibrated in buffer A (flow rate 0.5 mL/min) and eluted by a linear gradient between buffer A and buffer B (1 M ammonium acetate, 8 M urea; pH 5.5). The chromatographic peak corresponding to β-CN was identified by a 15% SDS-PAGE followed by mass spectrometry analysis, performed as already described (Perinelli et al., 2019). The peak corresponding to β-CN was dialyzed against 50 mM and 20 mM phosphate buffer using dialysis membranes (Spectra/Por ®, MWCO = 3000 Da, Spectrum Lab. Inc., Phoenix, AZ). After protein concentration determination (Bradford, 1976), the dialyzed β-CN was divided into 2.0 mg aliquots, dried by a Speed Vacuum concentrator (Savant SpeedVac™ Thermo Fischer Scientific, Waltham, MA, USA), and stored at -20 ℃ until use.

2.2.2.2. Critical micelle concentration (CMC) determination by pyrene fluorescence emission

Steady-state fluorescence spectra of pyrene in the presence of various concentrations (from 0.0125 mg/mL to 5.0 mg/mL) of donkey and bovine milk β-CNs as a function of pH (6.0, 7.0, 8.0 and 9.0) and buffer concentrations (50 mM and 250 mM) were recorded at 25 ℃ using a spectrofluorimeter (LS-55, PerkinElmer, equipped with a HAAKE C25 P thermostat). The fluorescence emission spectra (200-700 nm) were measured using an excitation wavelength λ_{exc} = 334 nm and 5.0/3.0 nm slits. The ratio between the first (I) and third (III) vibronic bands' intensity of

pyrene emission, respectively at 372 nm and 382 nm, was plotted against the β-CN concentration. The critical micelle concentration (CMC) of β-CNs was determined by fitting the experimental data using the following equation (GraphPad Prism 9.2; Equation 1):

$$Y = \frac{Bottom+(Top-Bottom)}{1+10\hat{}[(LogCMC-x)*Hill\ slope]} \quad (1)$$

where the Top and Bottom are two plateaus of the curve in the unit of Y axis, and the Hill slope is the steepness of the curve. Data were collected in triplicate.

The composition of the buffers was 50 and 250 mM phosphate buffer (KH_2PO_4/Na_2HPO_4), pH 6.0; 50 and 250 mM Tris buffer (Tris/HCl), pH 7.0, 8.0, 9.0.

2.2.2.3. Critical micelle temperature (CMT) determination by dynamic light scattering (DLS)

β-CN proteins from donkey and bovine milk were dissolved at the concentration of 5 mg/mL in the previously prepared buffers (50 mM and 250 mM) at various pH values (from 6.0 to 9.0) as for CMC determination. Then, protein solutions were analyzed in the range of temperature 10.0-40.0 ℃ with a stepwise increase of 2.5 ℃ using a Malvern Zetasizer NanoS (Malvern Instrument Worcestershire, UK), equipped with a backscattering detector at 173 °. The mean average size of hydrodynamic diameter (according to volume % distribution) was recorded at the fixed position of 4.65 mm, after an equilibration time of 300 s for each measurement. Critical micelle temperature (CMT) values were determined by fitting the experimental data using sigmoidal model in Eq.1 modified for temperature dependence.

2.2.2.4. Hydrophobicity determination by fluorescence spectroscopy

Fluorescence spectra of β-CN proteins from donkey and bovine milk at the concentration of 0.2 mg/mL were recorded using a spectrofluorimeter in a 1cm quartz cell. The slit widths were set at 5/3.5 nm respectively in emission and excitation pathways. Each sample was measured in triplicate at various temperatures (from 20.0 to 50.0 ℃), pH (from 6.0 to 9.0), and buffer concentrations (50

mM and 250 mM, respectively). Emission spectra were recorded between 300 and 450 nm with an excitation wavelength of 295 nm. The scan speed was set at 60 nm/min.

8-Anilinonaphthalene-1-sulfonate (ANS) binding to donkey and bovine β-CN at various temperatures (from 20.0 °C to 50.0 °C), pH (from 6.0 to 9.0) and buffer concentrations (50 mM and 250 mM, respectively) was assessed after 10 min incubation (in dark) of 0.2 mg/mL β-CN with different ANS concentration (from 0 μM to 600 μM). Fluorescence emission spectra were measured using excitation at 370 nm and bandwidths of 5.0/3.5 nm in excitation/emission channel. All measurements were done in triplicate. The hydrophobic parameters (expressed as hydrophobic surface and affinity index) were calculated according to this formula (Equation 2, adapted from (Möller & Denicola, 2002)):

$$F = Fmax * \frac{Ka*[ANS]^n}{n+Ka*[ANS]^n} \quad (2)$$

where F is the Fluorescence intensity, K_a is the affinity constant (corresponding to the affinity index), n is the binding sites (corresponding to the hydrophobic surface).

2.2.2.5. Circular dichroism (CD)

Far-UV CD spectra were recorded by Jasco J-810 Spectropolarimeter (Jasco Incorporated) in 0.02 cm-quartz cuvette Hellma 106-QS at donkey and bovine β-CN concentration of 0.3 mg/mL in 50 mM phosphate buffer. CD spectra were obtained at controlled temperature (from 10.0 to 40.0 °C) and pH (from 6.0 to 9.0). Each spectrum represents the average of three scans, acquired with a scan rate of 50 nm/min in the spectral range from 180 to 260 nm with a 1 nm data collection. Protein spectra were corrected by buffer subtraction and expressed as mean residue ellipticity (degrees cm^2/dmol). For the estimation of protein secondary structure content data were processed using the software CONTIN (http://dichroweb.cryst.bbk.ac.uk) and compared with CD spectra measured from the basic set of proteins (Set 7) for which X-ray diffraction data are available (Whitmore & Wallace, 2008). Given the high degree of unordered structure of β-caseins, the deconvolution of CD spectra obtained in this spectral region can only provide semi-quantitative estimation of the protein

secondary structure's changes.

2.3. Results and Discussion

2.3.1. Purification of β-CN

The mass spectrometry analysis of the peak eluted from cation exchange chromatography gave as a result donkey β-CN (CASB_EQUAS, Beta-casein *Equus asinus*, Mascot score 266, sequence: VMPFLKSPIVPFSERQILNPTNGENLR. The purified donkey milk β-CN shows a purification grade > 95% according to the 15% SDS-PAGE (Fig. SF1). The electrophoretic behaviour of donkey milk β-CN has been compared with that of a commercial bovine beta-casein (Sigma Aldrich, St. Louis, MO). The calculated molecular weight for both caseins (donkey and bovine) after the 15% SDS-PAGE is around 35-33 kDa, higher than the molecular weight of about 24 kDa expected from the protein sequence (around 24 kDa). This anomalous behavior of caseins has been described by several authors and could be due to a slower migration of caseins in SDS-PAGE because of the formation of a casein-SDS complex that could influence the shape of the protein (Raak, N. et al. 2018; Chakraborty and Basak, 2008). In addition, the molecular weight of donkey β-CN of about 2 kDa higher than bovine one is justified by the extra 20 amino acids in its primary sequence (Perinelli et al., 2019).

2.3.2 Characterization of the self-assembling behavior of bovine and donkey β-CNs

The amphiphilic properties of β-CNs are responsible for their self-assembling behavior into spheroidal micelles, which are strongly influenced by physicochemical factors such as pH, temperature and ionic strength (Zhou et al 2019). In order to assess the role played by these factors on the micellization phenomenon we have investigated their effect on CMC and CMT, which macroscopically define the behavior of self-assembling amphiphiles, including biopolymers. In the following sub-paragraphs the results obtained by pyrene fluorescence spectroscopy, and dynamic

light scattering (DLS) are reported to investigate the effects of pH, temperature and buffer concentration on these parameters.

2.3.2.1. Effect of pH, temperature, and buffer concentration on CMC of donkey and bovine β-CN by pyrene fluorescence emission

Pyrene as a fluorescence extrinsic probe was used for the CMC determination of β-CN in this study. This method is based on the nonlinear relationship between protein concentration and the ratio of its fluorescence intensities at peaks I and III. The concentration corresponding to the sudden decrease of the curve (as determined from Eq. 1) is recognized as the CMC value, which is the minimum concentration at which micelles begin to form.

It is well-known that CMC values of bovine β-CN are drastically affected by a variety of factors that can change the hydration state of the protein, thereby favoring hydrophobic intermolecular interactions between protein monomers (Portnaya et al., 2006). To verify such effects also on the self-assembling of donkey β-CN, we performed experiments at different experimental conditions such as four different pH values (6.0, 7.0, 8.0 and 9.0), two different buffer concentrations (50 mM and 250 mM), and two different temperatures (25 and 50 ℃). The obtained results were compared with those from bovine β-CN.

The changes of I/III pyrene fluorescence intensity ratio as a function of β-CN concentration (from 0.0125 mg/mL to 5 mg/mL) have been shown in Fig. SF2. All the obtained profiles have a sigmoidal shape (from pH 6 to 8) in which two plateau regions can be observed, indicating a similar self-assembling behavior as a function of protein concentration for both β-CNs. The first plateau corresponds to the concentrations of protein when only monomers of β-CN are present in the solution, while the other one refers to the concentrations at which micelles have been formed. The intermediate region of the curve, instead, represents the range of concentrations in which the self-assembling transition occurs. CMC values at pH of 6.0-8.0 have been calculated from these profiles by fitting the experimental data with a sigmoidal model as shown in Table 1. On the contrary, the

obtained profiles at pH 9.0 did not show a sigmoidal shape, making it impossible to calculate a CMC value by fitting these data at this pH, suggesting that no micellization occurs.

Table 1 Critical micelle concentration (CMC) values calculated by spectrofluorimetry using pyrene as fluorescent probe as a function of pH (6.0, 7.0, 8.0, and 9.0), temperature (25 and 50 ℃) and buffer concentrations (50 mM, 250 mM, respectively). Number of repeats, n =3.

CMC (mg/mL) determination (pyrene fluorescence)									
		25 ℃				**50 ℃**			
		50 mM buffer		**250 mM buffer**		**50 mM buffer**		**250 mM buffer**	
		mg/mL	R^2	mg/mL	R^2	mg/mL	R^2	mg/mL	R^2
Donkey	pH 6.0	0.32±0.04	0.97±0.00	0.31±0.01	0.80±0.00	0.27±0.01	0.96±0.00	0.24±0.01	0.97±0.00
	pH 7.0	0.74±0.01	0.99±0.00	0.80±0.18	0.82±0.01	0.66±0.03	0.98±0.00	0.63±0.01	0.98±0.00
	pH 8.0	0.94±0.04	0.91±0.01	0.91±0.10	0.95±0.00	0.84±0.01	0.98±0.00	0.81±0.01	0.98±0.01
	pH 9.0	n.d.	--	n.d.	--	n.d.	--	n.d.	--
Bovine	pH 6.0	0.51±0.01	0.99±0.00	0.43±0.14	0.93±0.01	0.42±0.01	0.98±0.00	0.34±0.01	0.99±0.00
	pH 7.0	0.91±0.03	0.97±0.00	0.96±0.09	0.71±0.02	0.73±0.01	0.94±0.00	0.70±0.00	0.96±0.00
	pH 8.0	1.27±0.05	0.98±0.01	1.15±0.26	0.78±0.01	1.10±0.00	0.94±0.01	0.97±0.01	0.96±0.00
	pH 9.0	n.d.	--	n.d.	--	n.d.	--	n.d.	--

The CMC values for both donkey and bovine β-CNs showed an increasing trend within the investigated pH range (from pH 6.0 to 8.0) regardless of the buffer concentration and temperature. At 25 ℃, the CMC value of donkey β-CN is around 0.30 mg/mL at pH 6.0, much lower than at pH 7.0 (～0.80 mg/mL) and pH 8.0 (～0.90 mg/mL). Similarly, the CMC value of bovine β-CN is around 0.45 mg/mL at pH 6.0, much lower than that at pH 7.0 (～0.90 mg/mL) and pH 8.0 (～1.20 mg/mL). At pH 9.0, the CMC values of both β-CN proteins cannot be determined. These results indicate that the self-assembly behavior of β-CN is strongly pH-dependent. In previous studies, the reported CMC values for bovine β-CN were usually in the range of 0.05-0.2% (w/v) depending on different conditions (pH, temperature and concentration, etc.) (Portnaya et al., 2006), which are in agreement with those detected in our research (0.34~1.27 mg/mL). The CMC values of bovine β-CN proteins in the present study at pH 7.0, were slightly larger than those (～0.5 mg/mL) obtained by using DLS at pH 6.5 in 50 mM isotonic HEPES buffer (O'Connell et al., 2003), but nearly similar to

those reported (~0.7 mg/mL) by using fluorescence spectroscopy in 100 mM isotonic phosphate buffer (Zhang et al., 2004). According to Perinelli et al. (2019), the CMC values of donkey β-CN and bovine β-CNs were 0.44 mg/mL and 0.57 mg/mL in 50 mM HEPES buffer (pH 7.3, 37 ℃), respectively (Perinelli et al., 2019). The small differences in CMC values can be explained by the variability due to the buffer type and operating temperature. Overall, the changes in CMC in response to increasing pH can reflect the contribution of electrostatic interactions and hydrogen bonding in the micellization process: the decrease in amino acid protonation occurring at high pH might neutralize positively charged side chains, which could be engaged in salt bridges and/or hydrogen bonds established in the micellar structure. The increase of pH above the isoelectric point can gradually induce the denaturation of β-CN or neutralize its positively charged side chains, causing a more difficult self-association process for the protein (Qi et al., 2004). As regards the effect of temperature, the CMC values decreased with the temperature from 25 ℃ to 50 ℃. Ellouze et al. (2021) found that the CMC of bovine β-CN decreased from around 0.5 wt % at 4 ℃ (pH 2.6) to 0.1 wt % at 24 ℃, which was consistent with our study (Ellouze et al., 2021). The decrease in the CMC upon the raising temperature may be due to more hydrophobic groups being exposed at the higher temperature, which drives the formation of β-CN micelles at lower concentrations (Anema, 2021).

The effect of buffer concentration on CMC for both donkey and bovine β-CNs appears to be less pronounced than observed by pH changes. The CMC values of β-CN proteins were a little bit larger in 50 mM than in 250 mM buffer concentration, but no marked differences were observed, indicating a moderate impact of ionic strength on the self-assembling properties of both β-CN proteins, at these three pH values. Mikheeva et al. (2003) observed that Tris had less effect on the micellization behavior of β-CN, in comparison with other co-solutes including inorganic salts, urea, and ethanol, which was in close agreement with the results reported by our research (Mikheeva et al., 2003).

2.3.2.2. Effect of pH and buffer concentration on CMT of bovine and donkey β-CNs by DLS

Critical micelle temperature (CMT), defined as the temperature at which proteins start to reversibly interact and form micelles, is another fundamental parameter to describe the self-assembly behavior of proteins with amphiphilic properties. In the present study, dynamic light scattering (DLS) was applied to investigate the changes in particle size distribution of both donkey

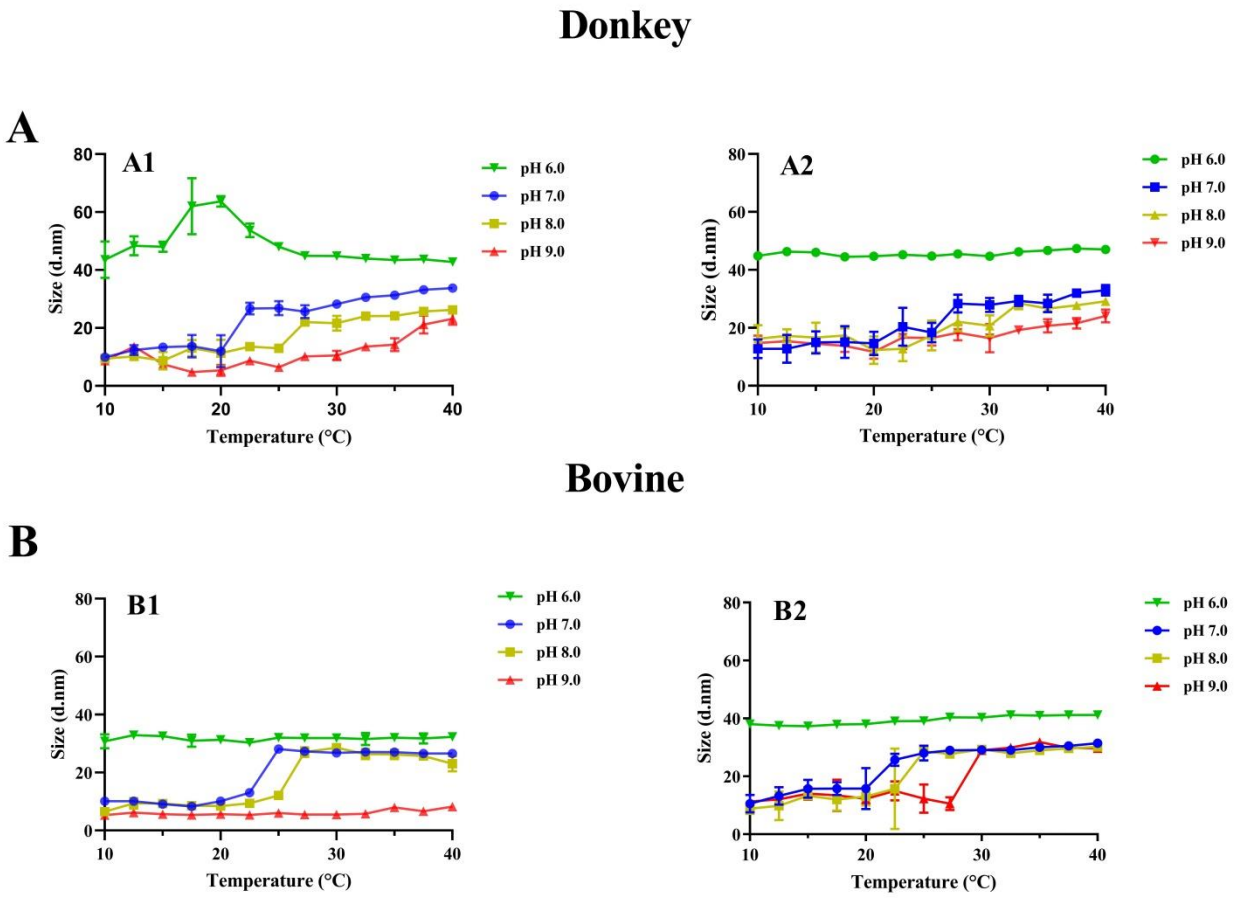

Fig. 1. Variation of the hydrodynamic diameter (nm) over temperature for donkey and bovine β-CN as a function of pH value (6.0, 7.0, 8.0, and 9.0) at concentration of 5 mg/mL, buffer concentration is 50 mM (A1) and (B1), buffer concentration is 250 mM (A2) and (B2).

and bovine β-CNs as a function of pH (from 6.0 to 9.0) and buffer concentrations (50 mM and 250 mM). The analyses were performed in the temperature range from 10 ℃ to 40 ℃, in which CMT values are supposed to be found according to our previous investigation (Perinelli et al., 2019). Fig. 1. shows the average particle size values, expressed as hydrodynamic diameter, plotted versus

temperature for donkey and bovine β-CN's solutions at different pH and buffer concentrations.

The measured particle size displayed a pH-dependent behavior over temperatures. At pH 7.0 and 8.0, all the obtained data have a sigmoidal trend in which two plateau regions can be observed, as occurs for a micellization process. The first one refers to the range of temperatures in which protein in the monomeric state is predominant. The second one, instead, indicates the range of temperature at which micelles populate and coexist with unimers. The middle region, since micellization is a dynamic process, represents an intermediate state in which unimers start to aggregate into micelles. From these plots, the CMT values were calculated and reported in Table 2.

Table 2 Critical micelle temperature (CMT) values calculated by spectrofluorimetry using dynamic light scattering (DLS) as a function of pH at room temperature in different buffer concentrations (50 mM, 250 mM, respectively). Number of repeats, n =3.

	CMT (℃) determination (DLS)							
	Donkey				**Bovine**			
	50 mM buffer		**250 mM buffer**		**50 mM buffer**		**250 mM buffer**	
	℃	**R^2**	**℃**	**R^2**	**℃**	**R^2**	**℃**	**R^2**
pH 6.0	n.d.	--	n.d.	--	n.d.	--	n.d.	--
pH 7.0	22.6±1.5	0.89±0.00	25.7±1.5	0.81±0.00	22.7±0.53	0.99±0.00	21.6±1.7	0.81±0.01
pH 8.0	26.5±1.2	0.89±0.00	29.0±5.7	0.81±0.01	25.2±0.59	0.96±0.00	23.1±3.5	0.81±0.01
pH 9.0	n.d.	--	n.d.	--	n.d.	--	n.d.	--

With the increase in pH from 7.0 to 8.0, the CMT of donkey β-CN increased from 22.6 ℃ to 26.5 ℃ in 50 mM buffer, while that of bovine β-CN increased from 22.7 ℃ to 25.2 ℃. In 250 mM buffer, the CMT of donkey β-CN increased from 25.68 °C to 28.99 °C, while that of bovine β-CN increased from 21.6 ℃ to 23.1 °C. As a result, the CMT values of donkey and bovine β-CN do not have marked differences as a function of buffer concentration. In fact, micelles can form at pH 7.0 and pH 8.0 for both β-CNs. Compared to pH 8.0, the inflection point (CMT) of the curve at pH 7.0 appears at a lower temperature, indicating that micellization is favored at this pH for both β-CNs. The hydrodynamic diameter of protein monomers is of about 8-14 nm, while the micelles have a

measured diameter of around 24-30 nm. Such values are in agreement with those from previous studies (Perinelli et al., 2019). Perinelli et al. (2019) found that the hydrodynamic diameter of β-CN as monomers was in the range of 6-10 nm and around 26-27 nm for the micellar aggregates (Perinelli et al., 2019). More recently, Wu et al. (2021) reported that the particle size distribution of buffalo β-CN monomer was about 10 nm, and protein gradually aggregated with the decrease in pH values (Wu et al., 2021). The pH effect on CMT of the protein was explained by altering the ionization of protein functional groups and double-layer thickness to lead to more exposure of hydrophobic groups (Boulet et al., 2001).

On the contrary, both donkey and bovine β-CNs are more aggregated at pH 6.0 with a particle size of ~40 nm, larger than that measured for micelles. This marked increase in size can be explained by taking into account that pH 6.0 is closer to the isoelectric point of β-CN (around pH 5.2) (Wüstneck et al., 2012). The formation of these aggregates can be driven by the tendency of the protein to reduce its electrical charge, thereby affecting solubility.

Increasing the pH up to 9.0 had a negative effect on the micellization process of both β-CNs. This resulted in a non-complete micellization process, in most cases, in the range of the experimental temperatures (10-40 ℃). This behavior could be related to the deprotonation of some basic amino acids, involved in hydrogen bonding. Therefore, the micellar structure of both β-CNs seems to be destabilized by alkaline pH and require a higher temperature to form, and eventually relax at pH 9.0, as reported elsewhere (Ellouze et al., 2021).

Noticeably, the CMT values of bovine β-CN obtained by DLS in this study were also comparable to those calculated from other techniques, such as high-sensitivity differential scanning calorimetry and isothermal titration calorimetry (Mikheeva et al., 2003; Portnaya et al., 2006).

2.3.4. Characterization of the hydrophobic property's dependence on pH, temperature and buffer concentration of bovine and donkey β-CNs

Hydrophobic effect is one of the most important non-covalent interactions involved in micelles self-assembling. β-caseins amphiphilic properties rely on an N-terminal polar region and an apolar C-terminal tail (residues 136–209) that drives the micelle formation by hydrophobic effect. A tryptophan residue is present in the β-CNs hydrophobic region allowing the measurement of intrinsic Trp fluorescence measurements to explore conformational modifications involving the hydrophobic tail, and that can affect micelle formation. In addition, being intrinsically disordered proteins (IDP), β-CNs present an extended structure offering a wide binding surface area available for ligands, which can be used as extrinsic fluorescent probes, such as ANS. All the experiments reported below have been performed at a concentration lower than CMC; this choice has been determined not only by technical reasons but also to investigate the effect of pH, temperature and ionic strength on the structural properties of the unimeric β-CNs leading to the micellization phenomenon.

2.3.4.1. Hydrophobic properties of β-CNs examined by Trp fluorescence spectroscopy.

The single Trp143 residue located in the hydrophobic domain of β-CN primary structure has a high absorption and fluorescence yield, which can be used as an intrinsic fluorescent probe to study the protein's hydrophobic properties (Moeiniafshari et al., 2015). Moreover, the fluorescence intensity of tryptophan fluorophore was strongly influenced by its microenvironment. In the present study, the intrinsic Trp fluorescence of donkey and bovine β-CNs was measured to evaluate their structural changes induced by changes of pH (from 6.0 to 9.0), temperature (from 20 ℃ to 50 ℃) and buffer concentrations (50 mM and 250 mM), respectively. The presence of a tryptophan residue in the β-CN from donkey milk has been confirmed by a search carried out in a protein database (https://www.expasy.org/resources/uniprotkb-swiss-prot) where it is possible to find an isoform of this protein showing a tryptophan residue in the third position of the amino acid sequence (accession

number: A0A8C4ME87 · A0A8C4ME87_EQUAS). Fig. 2A shows the changes in the relative fluorescence intensity of donkey and bovine β-CN at various pH values. As the pH decreased from 9.0 to 6.0, a gradual increase in the fluorescence intensity coupled with a blue shift to its maximum fluorescence (from ~350 to ~340 nm) was observed, reflecting the transfer of Trp to a more apolar environment. The temperature effect of both β-CN proteins on the Trp fluorescence intensity was presented in Fig. 2B.

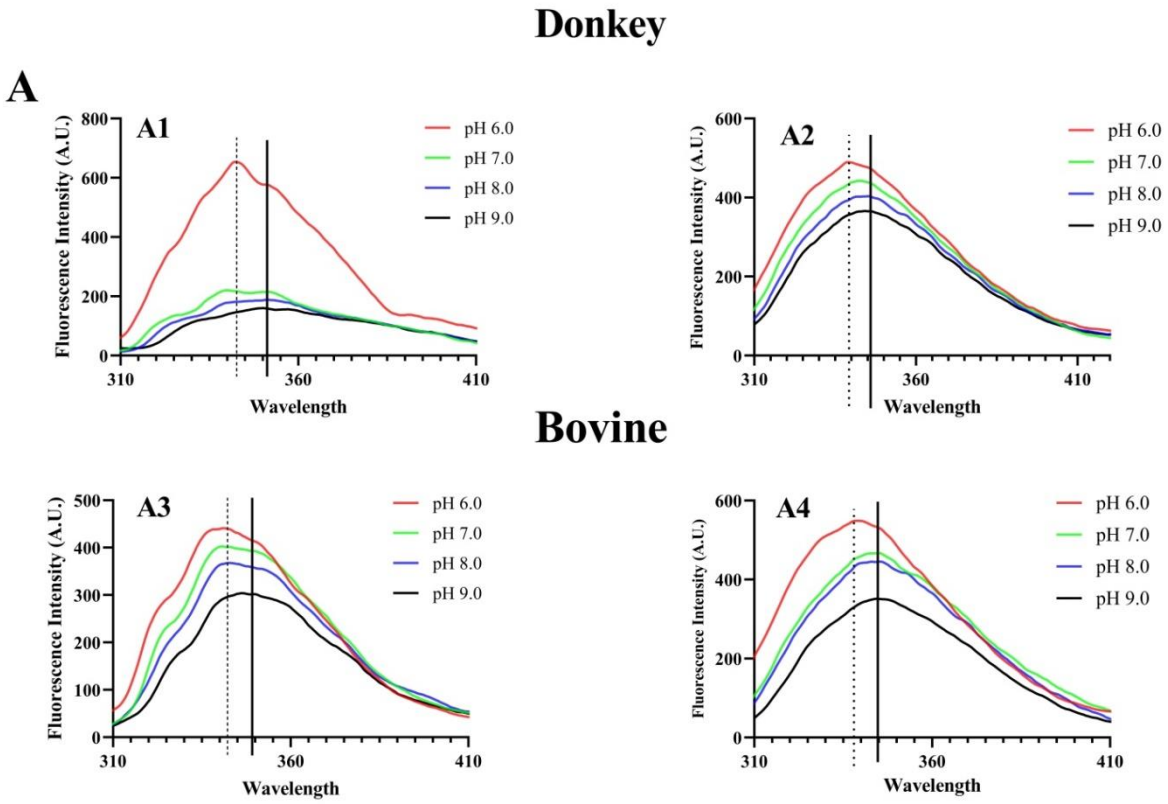

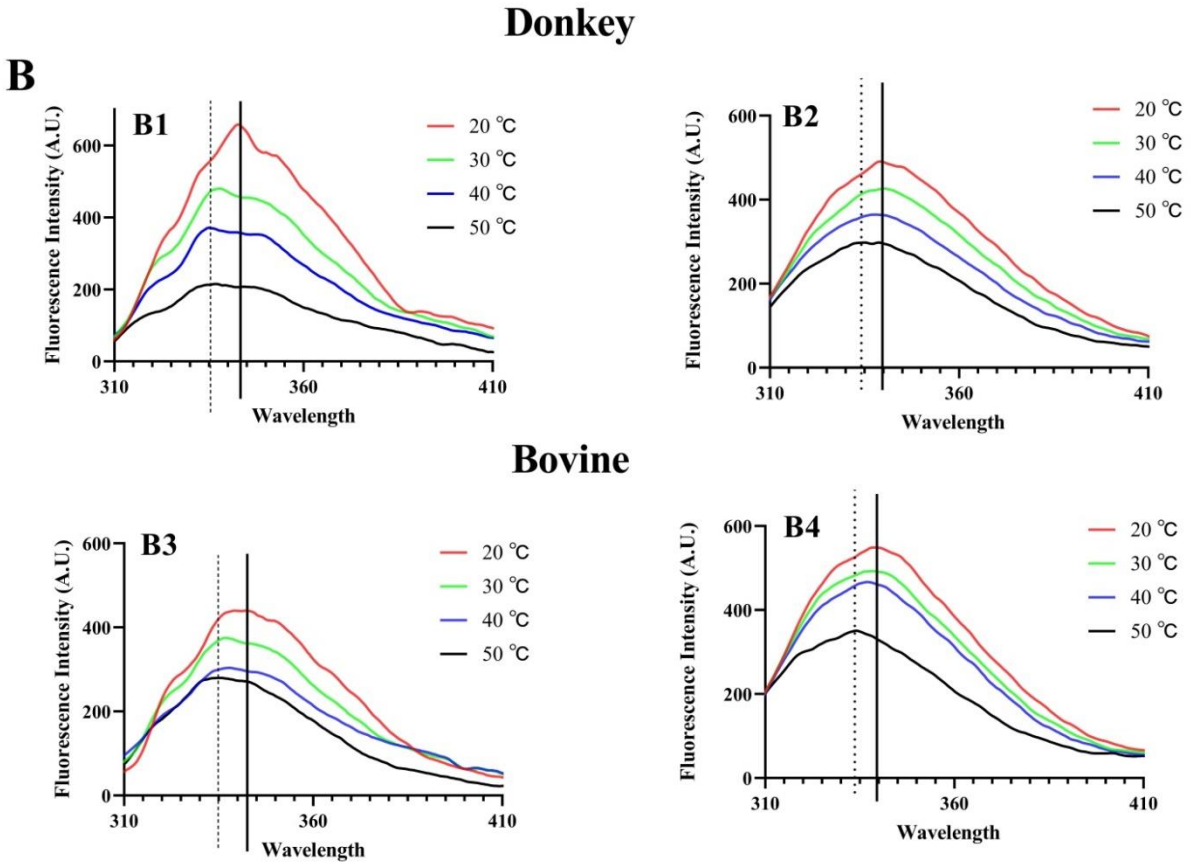

Fig. 2. (A) Tryptophan intrinsic fluorescence spectra of β-casein from donkey and bovine as a function of pH value (6.0, 7.0, 8.0, and 9.0) at concentration of 0.2 mg/mL (lower than CMC); buffer concentration is 50 mM (A1) and (A3), and 250 mM (A2) and (A4). The dotted line represents maximum fluorescence at around 340 nm at pH 6.0 and the solid line represents maximum fluorescence at around 350 nm at pH 9.0.

(B) Tryptophan intrinsic fluorescence spectra of β-casein from donkey and bovine as a function of temperature (20 ℃, 30 ℃, 40 ℃, and 50 ℃) at concentration of 0.2 mg/mL (lower than CMC); buffer concentration is 50 mM (B1) and (B3), and 250 mM (B2) and (B4). The dotted line represents maximum fluorescence at around 335 nm at temperature 50 ℃ and the solid line represents maximum fluorescence at around 340 nm at temperature 20 ℃.

It was interesting to find out that, the fluorescence intensity was decreased accompanied by a blue shift to its maximum fluorescence (from ~342 to ~333 nm) when temperature shifted from 20 ℃ to 50 ℃. The fluorescence blue shift can be interpreted as a change in Trp environment's polarity, due to the self-association of β-CN via hydrophobic interactions, burying Trp residues from water molecules. These results are in agreement with Yousefi's et al (2009) research, which

reported that the polarity of Trp environment of bovine β-CN undergoes a change in polarity and its emission intensity decreases by increasing temperature (Yousefi et al., 2009). The main reason for this phenomenon is the quenching of protein fluorescence intensity at high temperatures, showing a temperature-induced compaction of β-CN structure. In addition, a change in the geometry of β-CNs micelle induced by temperature could decrease its compaction as previously studied (O'Connell et al., 2003).

Furthermore, the buffer concentration has a greater effect on the fluorescence intensity of donkey β-CN than that of bovine (Fig. 2A and B); focusing on donkey β-CN under the same pH condition, the fluorescence intensity at a high buffer concentration (250 mM) was significantly higher compared with that measured at a low concentration (50 mM).

Therefore, the low pH, high temperature, and high buffer concentration appear to induce a structural change of both β-CN from donkey and bovine milk resulting in the hydrophobic tail intra- or inter-molecular self-association protecting the tryptophan residues from the aqueous environment and promoting the more favorable micelle formation (Yousefi et al., 2009).

Wu et al. (2021) have found that the Trp fluorescence of β-CN was enhanced with a blue shift to its maximum value over the decrease in pH (from 7.5 to 5.0) and the increase in NaCl concentration (from 0.01M to 0.30M), which is consistent with our research (Wu et al., 2021).

2.3.4.2. Hydrophobic properties of β-CNs examined by 8-anilino-1-naphtalene-sulfonic acid (ANS) binding fluorescence analysis.

The use of ANS as an anionic fluorescent probe is one of the most common methods for the determination of protein hydrophobicity. Such a method is based on the binding of ANS with hydrophobic (nonpolar) surfaces of proteins, resulting in increased fluorescence intensity and a blue shift of its fluorescence maximum (Helmick et al., 2023). To further explore the hydrophobicity of β-CN, the binding of ANS was monitored at concentrations ranging from 10 μM to 600 μM, as a function of pH (from 6.0 to 9.0), temperature (from 20.0 ℃ to 50.0 ℃) and buffer concentration (50

mM and 250 mM), respectively. Fig. SF3 and Fig. SF4 showed that the studied β-CN proteins had different abilities to enhance ANS fluorescence intensity. The formula in Equation 2 can be used to determine the number of ANS binding sites (n) per protein molecule and the dissociation constant (Kd). After fitting the data, the influence of pH on the surface hydrophobic parameters (n, Ka and Kd) of β-CN proteins were summarized in Table ST1. The results indicated that both β-CN proteins had a high number of binding sites ($n \geq 1$) with low affinity at pH 6.0. As the pH values increased from 6.0 to 9.0, an increase in the number of hydrophobic binding sites (protein-bound ANS) and a decrease in the affinity constant were observed. Furthermore, the relative fluorescence intensity of ANS bound to β-CN decreased and the fluorescence maximum had a red shift from pH 6.0 to pH 9.0 (Fig. SF5).

In particular, as reported in Table ST1, we could observe a higher affinity for ANS to donkey β-CN at 20 ℃ in the entire pH range 6-9, and that high alkaline pH caused the reduction of the number of the hydrophobic binding sites for ANS, with increased affinity, on both β-CNs. The titration of protein solutions with increasing concentrations of the fluorescent probe (ANS) can provide information on the surface hydrophobicity and affinity index of binding sites as a function of pH (Figure 3A) (Annan et al., 2006).

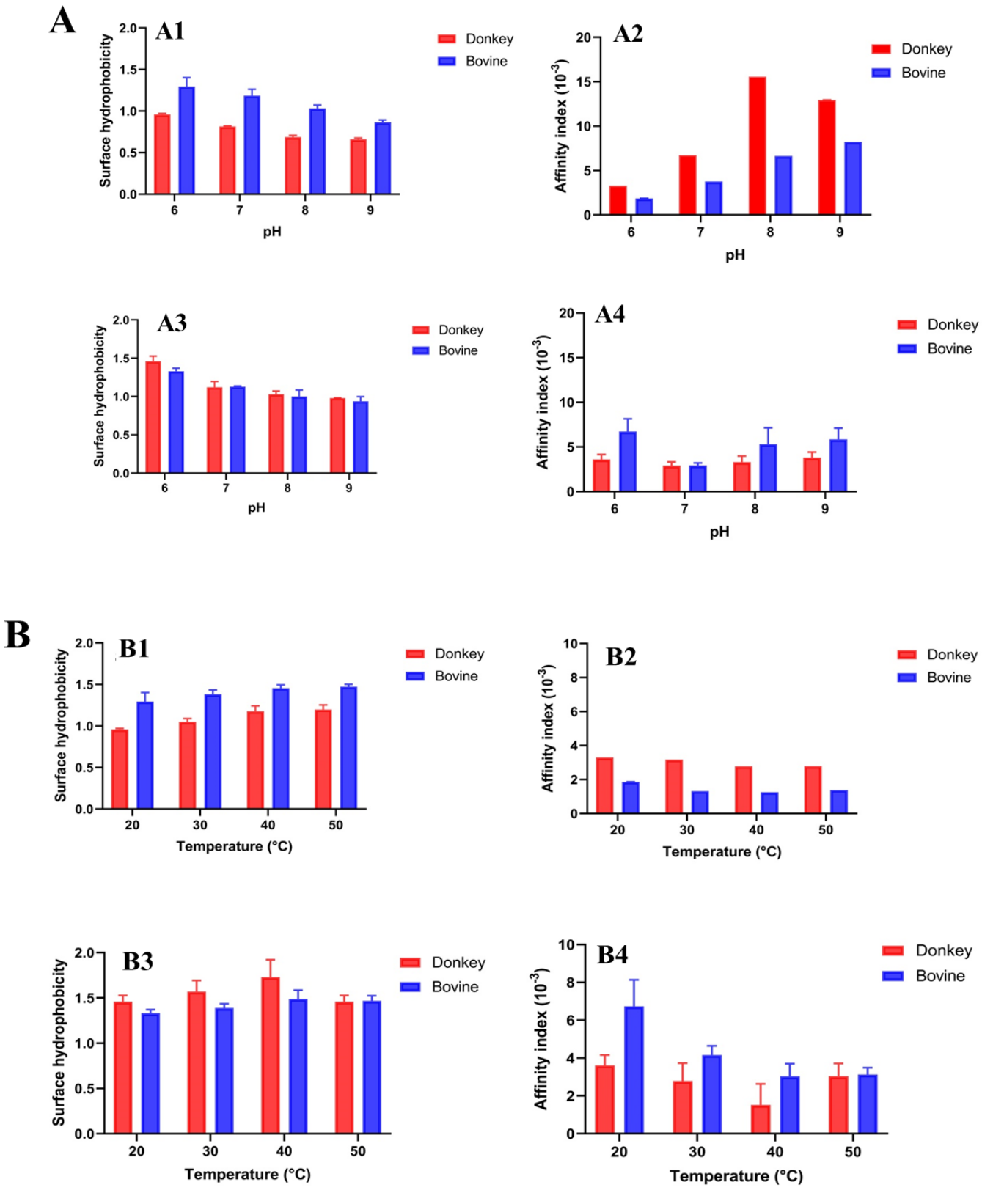

Fig. 3. (A) Hydrophobicity variation of donkey and bovine β-CNs as a function of pH value (6.0, 7.0, 8.0, and 9.0), surface hydrophobicity index in 50 mM buffer concentration (A1), affinity index in 50 mM buffer concentration (A2), surface hydrophobicity index in 250 mM buffer concentration (A3), affinity index in 250 mM buffer concentration (A4).

(B) Hydrophobicity variation of donkey and bovine β-CNs as a function of temperature (20 ℃ , 30 ℃, 40 ℃, and 50 ℃), surface hydrophobicity index in 50 mM buffer concentration (B1), affinity index in 50 mM buffer concentration (B2), surface hydrophobicity index in 250 mM buffer concentration (B3), affinity index in 50 mM buffer concentration (B4).

In Table ST2, the calculated surface hydrophobic parameters (n, Ka, and Kd) of two β-CN proteins at pH 6.0 in terms of temperature effect (from 20 ℃ to 50 ℃) were reported. These data indicated that both donkey and bovine β-CNs had a low number of binding sites ($n \leq 1$) with high affinity at low temperature of 20 ℃. Generally, with the increase in temperature from 20 ℃ to 50 ℃, the number of binding sites of protein for ANS was increased and their affinity was gradually reduced (Fig. 3B). Meanwhile, with increasing temperature, there was a blueshift of the fluorescence maximum value. However, a gradual decrease in the relative fluorescence intensity was observed (Fig. SF6), suggesting that the fluorescence quenching has occurred, which was the same phenomenon as the intrinsic Trp fluorescence described before. Changes in surface hydrophobicity of β-CN confirmed that the heating process loosens the protein structure, and then more hydrophobic binding sites were exposed to the solvent. This can explain the temperature-induced and concentration-dependent micellization process of β-CN. O'Connell et al. (2003) reported the number of surface or accessible hydrophobic sites in β-CN progressively increased with the increasing temperature, in agreement with our results (O'Connell et al., 2003).

It should also be mentioned that the buffer concentration effect on the hydrophobic surface exposure of donkey β-CN was slightly more pronounced than in bovine protein. At each pH or temperature, the number of hydrophobic binding sites of donkey β-CN in 250 mM buffer was significantly higher than that in 50 mM buffer, while there was no evident difference in the hydrophobic surface exposure of bovine β-CN as a function of the two buffer concentrations. This may be due to the small differences in the amino acid sequence between donkey β-CN and bovine β-CN. In addition, the result was consistent with our previous description using Trp as the intrinsic fluorescent probe.

Thus, it can be seen that the fluorescence intensity of both donkey and bovine β-CNs bound to

ANS was influenced by pH, temperature, and buffer concentration. The increase in surface hydrophobicity of β-CN suggested that a rearrangement of its structure led to the larger exposure of hydrophobic regions, especially at a lower pH (pH 6.0), a higher temperature (50 ℃) and a higher buffer concentration (250 mM).

2.3.5. Analysis of secondary structure of β-CNs by far-UV circular dichroism (CD)

The self-assembly phenomenon involved in β-CN micellization is thermodynamically controlled by supramolecular interactions, according to three-dimensional constraints that are encoded in the structural motifs of individual proteins (Mendes et al. 2013). Circular dichroism can thus provide helpful information in the secondary structure involvement in the micellar organization.

The conformational changes of the secondary structure in donkey and bovine β-CN in terms of different pH and temperature were detected by monitoring the alterations in the far-UV CD spectra (Fig. 4A and Fig. 4B).

The CD spectra of both donkey and bovine β-CNs at various pH values (pH 6.0, 7.0, 8.0, and 9.0) in 50 mM phosphate buffer at temperatures of 10.0 ℃, 20.0 ℃, 30.0 ℃, and 40.0 ℃, are shown in Fig. 4A. With the decreasing pH values from 9.0 to 6.0, there was a slight shift of the wavelength from about 198 to 202 nm with an increase in the negative value of ellipticity at the observed λmax (θ_R-200 nm). Meanwhile, the negative peak intensity between the shoulders in the region between 215 and 230 nm was decreased. The obtained CD spectra changes of β-CN from both donkey and bovine as a function of pH values were close to those previously reported (Wu et al., 2021). CD spectra of both donkey and bovine β-CNs recorded at different pH values did not display isodichroic points, showing a monotonic change in the secondary structure (Faizullin et al., 2017).

Fig. 4B. shows the temperature dependence of CD spectra of both donkey and bovine β-CNs at all detected pH values. All these spectra have a minimum ellipticity around 200 nm and a secondary

negative trough between 210 and 230 nm, which has been observed by Farrell et al. (2001) in the case of native β-CN (Farrell et al., 2001). With the increase in temperature from 10.0 ℃ to 40.0 ℃,

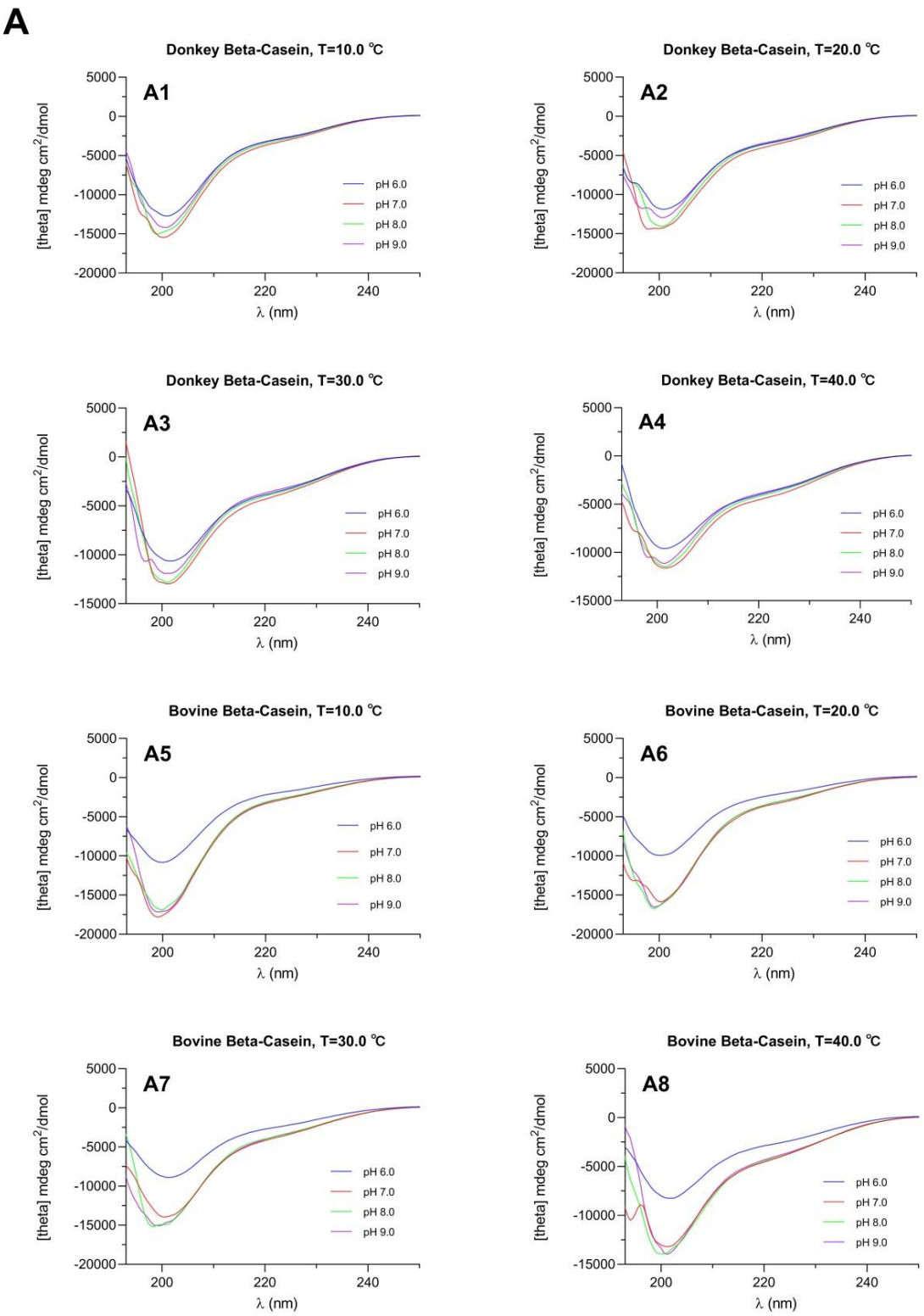

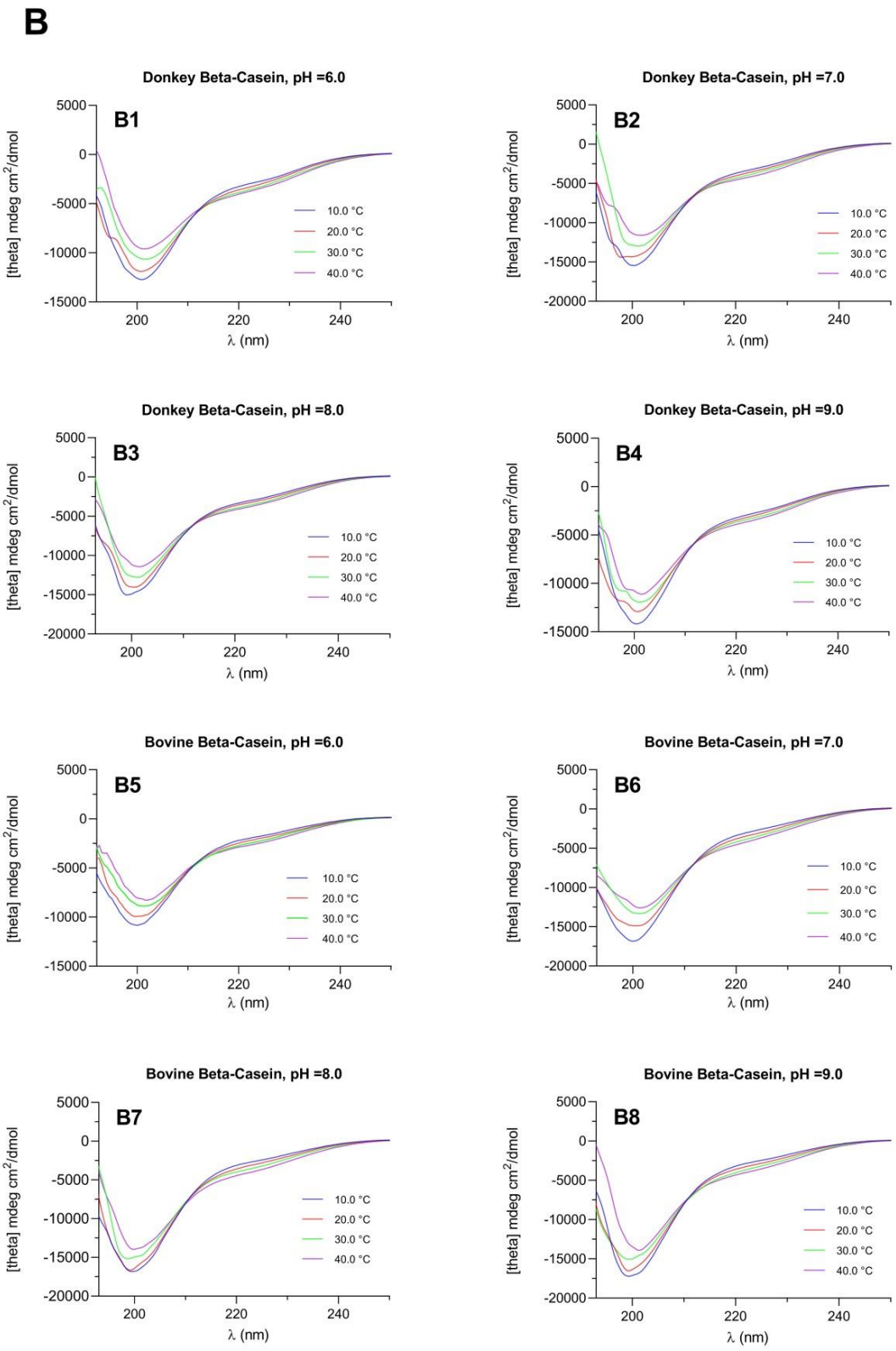

Fig. 4. (A) Circular dichroism spectra of donkey β-CN (0.3 mg/mL) as a function of pH value (6.0, 7.0, 8.0, and 9.0) at 10.0 ℃ (A1), 20.0 ℃ (A2), 30.0 ℃ (A3), 40.0 ℃ (A4); Circular dichroism spectra of bovine β-CN (0.3 mg/mL) as a function of pH value (6.0, 7.0, 8.0, and 9.0) at 10 ℃ (A5); 20 ℃ (A6); 30 ℃ (A7); 40 ℃ (A8).

(B) Circular dichroism spectra of donkey β-CN (0.3 mg/mL) as a function of temperature (10 ℃, 20 ℃, 30 ℃, 40 ℃) at pH 6.0 (B1), 7.0 (B2), 8.0 (B3), 9.0 (B4); Circular dichroism spectra of bovine β-CN (0.3 mg/mL) as a function of temperature (10.4 ℃, 20 ℃, 29.6 ℃, 40 ℃) at pH 6.0 (B5), 7.0 (B6), 8.0 (B7), 9.0 (B8);

the maximum negative CD peak at 200 nm was reduced along with a small shift of the negative peak from about 198 to 202 nm in both donkey and bovine β-CNs. Meanwhile, the negative peak between the shoulders of 215-230 nm gradually increased.

Taking into account that the optical activity observed in the region between 215-230 nm is dominated by electronic transitions $n > \pi^*$ of the non-bonding carboxylic oxygen in the polypeptide backbone, it suggested that the α-helix content was increased with the increasing temperature. This behavior is quite different from that of a typical globular protein that displays temperature-induced reduction of α-helical content, and it may be due to an increase in polyproline II helix structure and self-association beginning to take place with increased temperature, as noted above (Qi et al., 2004; Kuemin et al., 2010). Gangnard et al. (2007) also demonstrated that the CD spectra showed an upward shift of ellipticity at 200 nm and a downward shift in the 210-230 nm with the increasing temperature, as observed in our study (Gangnard et al., 2007).

The composition of β-CN secondary structure of donkey and bovine is given in Table ST3, and we found that there was little change in the calculated amounts of unordered, helix, turns, or sheet structure. Generally, the content of α-helix was increased and the unordered structure was decreased at pH values from 9.0 to 6.0 at all temperatures. With the increase in the temperature from 10.0 ℃ to 40.0 ℃, at all pH values, the composition in α-helix increased, while unordered structure decreased. However, compared with α-helix and unordered structure, the composition in β-strands and turns did not display significant changes in terms of pH and temperature. Faizullin et al (2017) reported that at 10 ℃ in the buffer solution, β-CN possesses 10% of helical, 12% extended, 14% turns, and 64% unordered structural content, in close agreement with our results on secondary structure of donkey and bovine β-CNs (Faizullin et al., 2017).

2.4. Conclusions

Similar self-assembling behavior as a function of protein concentration, temperature, and pH was found for donkey and bovine β-CNs. pH exerted a strong effect on both CMC and CMT, suggesting a strong contribution of electrostatic interactions and hydrogen bonding in the micellization process. Micelles formation of both β-CNs was therefore favored by increasing protein concentration, increasing temperature and decreasing pH (as long as above the isoelectric point). β-CNs eventually populate a relaxed conformation at pH 9.0, less prone to micellization, in particular at low ionic strength (50 mM buffer).

Furthermore, the data obtained by Trp and ANS spectrofluorometric analysis of both donkey and bovine β-CNs have shown that the hydrophobic surface exposure properties were noticeably influenced by pH, temperature, and buffer concentration. In particular, a structural rearrangement leading to an increase in surface hydrophobicity of β-CNs has been mainly observed at the lower pH (pH 6.0), the higher temperature (50.0 °C), and at the higher buffer concentration (250 mM).

Based on these results it is possible to assess that pH, by modifying the net charge of the protein, can strongly affect the propensity of both β-CNs to undergo the temperature-dependent transition involved in the micellization process. Both hydrophobic interactions and electrostatic repulsions are considered to play a role in the micellization of β-CN. The protonation of the acidic residues at a low pH can reduce the occurrence of charges of the phosphoserine residues in the N-terminal portion of the protein, thus minimizing electrostatic repulsion and favoring micellar self-assembly (Lajnaf et al., 2021).

Moreover, CD data have shown a temperature-induced increase in the degree of ordered structure at all pH values and in the range of temperature 10-40 °C, in which micellization occurs, as reflected by the slight increase in the ellipticity at 222 nm. Therefore, it can be assessed that under a pH-controlled favorable environment, the conditions for micellization upon heating are accompanied by an increase in the ordered secondary structure, predominantly represented by α-

helix and poly (Pro)II helix-like conformations. This behavior has been observed for both donkey and bovine β-CNs, and confirms the importance of the structural motifs organization of the C-terminal hydrophobic tail in the micellization process. Our results demonstrate that polyproline II helical structure favoring protein-protein interactions together with the promotion of a hydrophobic α-helix in the C-terminal domain play a major role as structural determinants also for donkey β-CN self-association and micellization.

In conclusion, the temperature-induced, pH-dependent, hydrophobic surface exposure of both bovine and donkey's β-CNs, responsible for micelle formation, and observed by fluorescence spectroscopy, does collimate with the promotion of the α-helical secondary structure of the hydrophobic C-terminal tail observed by CD spectroscopy. Together, these structural features are responsible for the CMC and CMT dependence on pH, temperature and ionic strength.

A biophysical characterization of the self-assembly of proteins is attracting more and more attention aimed at discovering new functions of liquid-liquid condensate states, by intrinsically disordered proteins (Fuxreiter & Vendruscolo, 2021). The results of this work can provide structural information and insight on critical parameters promoting intra and inter-molecular interactions involved in micellization for the development of β-CNs based nanocarriers useful to encapsulate bioactive compounds for pharmaceutical and nutraceutical applications.

References

Annan, W. S., Fairhead, M., Pereira, P., & Walle, C. F. v. d. (2006). Emulsifying performance of modular β-sandwich proteins: the hydrophobic moment and conformational stability. *Protein Engineering, Design and Selection*, *19*(12), 537-545. https://doi.org/ https://doi.org/10.1093/protein/gzl041

Anema, S. G.(2021). Heat-induced changes in caseins and casein micelles, including interactions with denatured whey proteins. *International Dairy Journal*, *122*:105136. https://doi.org/10.1016/ j .idairyj .2021.105136.

Bradford, M. M. (1976). A rapid and sensitive method for the quantitation of microgram quantities of protein utilizing the principle of protein-dye binding. *Analytical biochemistry*, *72*(1-2), 248-254. https://doi.org/10.1016/0003-2697(76)90527-3

Boulet, M., Britten, M., & Lamarche, F. (2001). Dispersion of food proteins in water-alcohol mixed dispersants. *Food Chemistry*, *74*(1), 69-74. https://doi.org/https://doi.org/10.1016/S0308-8146(01)00099-1

Chakraborty A, Basak S. (2008). Effect of surfactants on casein structure: a spectroscopic study. *Colloids and Surfaces B: Biointerfaces*. 263, 83-90. https://doi.org/10.1016/j.colsurfb.2007.11.005.

Chia, J., McRae, J., Kukuljan, S., Woodford, K., Elliott, R., Swinburn, B., & Dwyer, K. (2017). A1 beta-casein milk protein and other environmental pre-disposing factors for type 1 diabetes. *Nutrition & Diabetes*, *7*(5), e274-e274. https://doi.org/https://doi.org/10.1038/nutd.2017.16

Chianese, L., Calabrese, M.G., Ferranti, P., Mauriello, R., Garro, G., De Simone, C., Ramunno, L., (2010). Proteomic characterization of donkey milk "caseome". *Journal of Chromatography A.* 1217, 4834–4840. https://doi.org/10.1016/j.chroma.2010.05.017

Criscione, A., Cunsolo, V., Bordonaro, S., Guastella, A. M., Saletti, R., Zuccaro, A., D'Urso, G., & Marletta, D. (2009). Donkeys' milk protein fraction investigated by electrophoretic methods and mass spectrometric analysis. *International Dairy Journal*, *19*(4), 190-197.

https://doi.org/https://doi.org/10.1016/j.idairyj.2008.10.015

Dauphas, S., Mouhous-Riou, N., Metro, B., Mackie, A., Wilde, P. J., Anton, M., & Riaublanc, A. (2005). The supramolecular organisation of β-casein: Effect on interfacial properties. *Food Hydrocolloids*, *19*(3), 387-393. https://doi.org/https://doi.org/10.1016/j.foodhyd.2004.10.005

Ellouze, M., Vial, C., Attia, H., & Ayadi, M. A. (2021). Effect of pH and heat treatment on structure, surface characteristics and emulsifying properties of purified camel β-casein. *Food Chemistry*, 365, 130421. https://doi.org/https://doi.org/10.1016/j.foodchem.2021.130421

Faizullin, D. A., Konnova, T. A., Haertlé, T., & Zuev, Y. F. (2017). Secondary structure and colloidal stability of beta-casein in microheterogeneous water-ethanol solutions. *Food Hydrocolloids*, *63*, 349-355. https://doi.org/https://doi.org/10.1016/j.foodhyd.2016.09.011

Farrell, H. M., Wickham, E. D., Unruh, J. J., Qi, P. X., & Hoagland, P. D. (2001). Secondary structural studies of bovine caseins: temperature dependence of β-casein structure as analyzed by circular dichroism and FTIR spectroscopy and correlation with micellization. *Food Hydrocolloids*, *15*(4), 341-354. https://doi.org/https://doi.org/10.1016/S0268-005X(01)00080-7

Forrest, S. A., Yada, R. Y., & Rousseau, D. (2005). Interactions of vitamin D3 with bovine β-lactoglobulin A and β-casein. *Journal of agricultural and food chemistry*, *53*(20), 8003-8009. https://doi.org/https://doi.org/10.1021/jf050661l

Fuxreiter, M., & Vendruscolo, M. (2021). Generic nature of the condensed states of proteins. *Nature cell biology*, *23*(6), 587-594. https://doi.org/10.1038/s41556-021-00697-8

Gangnard, S., Zuev, Y., Gaudin, J.-C., Fedotov, V., Choiset, Y., Axelos, M. A., Chobert, J.-M., & Haertlé, T. (2007). Modifications of the charges at the N-terminus of bovine β-casein: Consequences on its structure and its micellisation. *Food Hydrocolloids*, *21*(2), 180-190. https://doi.org/https://doi.org/10.1016/j.foodhyd.2006.03.007

Hasni, I., Bourassa, P., Hamdani, S., Samson, G., Carpentier, R., & Tajmir-Riahi, H.-A. (2011). Interaction of milk α-and β-caseins with tea polyphenols. *Food Chemistry*, *126*(2), 630-639.

https://doi.org/https://doi.org/10.1016/j.foodchem.2010.11.087

He, F. (2011). Laemmli-sds-page. *Bio-protocol*, e80-e80.

Helmick, H., Tonner, T., Hauersperger, D., Ettestad, S., Hartanto, C., Okos, M., ... & Kokini, J. L. (2023). Physicochemical characterization of changes in pea protein as the result of cold extrusion. *Food Chemistry*, *423*, 136240. https://doi.org/10.1016/j.foodchem.2023.136240.

Holt, C. (2013). Unfolded phosphopolypeptides enable soft and hard tissues to coexist in the same organism with relative ease. *Current opinion in structural biology*, *23*(3), 420-425. https://doi.org/https://doi.org/10.1016/j.sbi.2013.02.010

Kuemin, M., Engel, J., & Wennemers, H. (2010). Temperature-induced transition between polyproline I and II helices: quantitative fitting of hysteresis effects. *Journal of Peptide Science*, *16*(10), 596-600. https://doi.org/10.1002/psc.1245.

Kumosinski, T., Brown, E., & Farrell Jr, H. (1993). Three-dimensional molecular modeling of bovine caseins: an energy-minimized β-casein structure. *Journal of dairy science*, *76*(4), 931-945. https://doi.org/https://doi.org/10.3168/jds.S0022-0302(93)77420-2

Lajnaf, R., Gharsallah, H., Attia, H., & Ayadi, M. A. (2021). Comparative study on antioxidant, antimicrobial, emulsifying and physico-chemical properties of purified bovine and camel β-casein. *LWT*, *140*, 110842. https://doi.org/10.1016/j.lwt.2020.110842.

Li, M., Fokkink, R., Ni, Y., & Kleijn, J. M. (2019). Bovine beta-casein micelles as delivery systems for hydrophobic flavonoids. *Food Hydrocolloids*, *96*, 653-662. https://doi.org/https://doi.org/10.1016/j.foodhyd.2019.06.005

Licitra, R., Chessa, S., Salari, F., Gattolin, S., Bulgari, O., Altomonte, I., Martini, M. (2019). Milk protein polymorphism in Amiata donkey. *Livestock Science*, 230, 103845. https://doi.org/10.1016/j.livsci.2019.103845

Mendes, A. C. Baran, E. T., Reis, R. L. & Azevedo, H. S. (2013) Self-assembly in nature: using the principles of nature to create complex nanobiomaterials. *WIREs Nanomed Nanobiotechnol.*, 5, 582–612. doi: 10.1002/wnan.1238

Mikheeva, L. M., Grinberg, N. V., Grinberg, V. Y., Khokhlov, A. R., & de Kruif, C. G. (2003). Thermodynamics of micellization of bovine β-casein studied by high-sensitivity differential scanning calorimetry. *Langmuir*, *19*(7), 2913-2921. https://doi.org/https://doi.org/10.1021/la026702e

Moeiniafshari, A.-A., Zarrabi, A., & Bordbar, A.-K. (2015). Exploring the interaction of naringenin with bovine beta-casein nanoparticles using spectroscopy. *Food Hydrocolloids*, *51*, 1-6. https://doi.org/https://doi.org/10.1016/j.foodhyd.2015.04.036

Möller, M., & Denicola, A. (2002). Study of protein-ligand binding by fluorescence. *Biochemistry and Molecular Biology Education*, *30*(5), 309-312. https://doi.org/https://doi.org/10.1002/bmb.2002.494030050089

Monti, G., Bertino, E., Muratore, M.C., Coscia, A., Cresi, F., Silvestro, L., Fabris, C., Fortunato, D., Giuffrida, M.G., Conti, A. (2007). Efficacy of donkey's milk in treating highly problematic cow's milk allergic children: an in vivo and in vitro study. *Pediatric Allergy and Immunology*. 18, 258–64. https://doi.org/10.1111/j.1399-3038.2007.00521.x

O'Connell, J., Grinberg, V. Y., & De Kruif, C. (2003). Association behavior of β-casein. *Journal of Colloid and Interface Science*, *258*(1), 33-39. https://doi.org/https://doi.org/10.1016/S0021-9797(02)00066-8

Perinelli, D. R., Bonacucina, G., Cespi, M., Bonazza, F., Palmieri, G. F., Pucciarelli, S., Polzonetti, V., Attarian, L., Polidori, P., & Vincenzetti, S. (2019). A comparison among β-caseins purified from milk of different species: Self-assembling behaviour and immunogenicity potential. *Colloids and Surfaces B: Biointerfaces*, *173*, 210-216.

Portnaya, I., Cogan, U., Livney, Y. D., Ramon, O., Shimoni, K., Rosenberg, M., & Danino, D. (2006). Micellization of bovine β-casein studied by isothermal titration microcalorimetry and cryogenic transmission electron microscopy. *Journal of agricultural and food chemistry*, *54*(15), 5555-5561. https://doi.org/https://doi.org/10.1021/jf060119c

Qi, P. X., Wickham, E. D., & Farrell, H. M. (2004). Thermal and alkaline denaturation of bovine β-

casein. *The protein journal*, *23*(6), 389-402. https://doi.org/https://doi.org/10.1023/B:JOPC.0000039553.66233.3f

Raak, N., Abbate, R.A., Lederer, A., Rohm, H., Jaros, D. (2018). Size Separation Techniques for the Characterisation of Cross-Linked Casein: A Review of Methods and Their Applications. *Separations*. 5, 14. https://doi.org/10.3390/separations5010014

Ranadheera, C., Liyanaarachchi, W., Chandrapala, J., Dissanayake, M., & Vasiljevic, T. (2016). Utilizing unique properties of caseins and the casein micelle for delivery of sensitive food ingredients and bioactives. *Trends in Food Science & Technology*, *57*, 178-187. https://doi.org/https://doi.org/10.1016/j.tifs.2016.10.005

Raynes, J., Day, L., Augustin, M. A., & Carver, J. (2015). Structural differences between bovine A1 and A2 β-casein alter micelle self-assembly and influence molecular chaperone activity. *Journal of dairy science*, *98*(4), 2172-2182. https://doi.org/https://doi.org/10.3168/jds.2014-8800

Schulte, J., Stöckermann, M., & Gebhardt, R. (2020). Influence of pH on the stability and structure of single casein microparticles. *Food Hydrocolloids*, *105*, 105741. https://doi.org/https://doi.org/10.1016/j.foodhyd.2020.105741

Shapira, A., Markman, G., Assaraf, Y. G., & Livney, Y. D. (2010). β-casein-based nanovehicles for oral delivery of chemotherapeutic drugs: drug-protein interactions and mitoxantrone loading capacity. *Nanomedicine: Nanotechnology, Biology and Medicine*, *6*(4), 547-555. https://doi.org/https://doi.org/10.1016/j.nano.2010.01.003

Shevchenko, A., Tomas, H., Havli, J., Olsen, J. V., & Mann, M. (2006). In-gel digestion for mass spectrometric characterization of proteins and proteomes. *Nature protocols*, *1*(6), 2856-2860. https://doi.org/https://doi.org/10.1038/nprot.2006.468

Swaisgood, H. E. (2003). Chemistry of the caseins. In *Advanced dairy chemistry—1 Proteins* (pp. 139-201). Springer. https://doi.org/10.1007/978-1-4419-8602-3_3

Tidona, F., Criscione, A., Devold, T. G., Bordonaro, S., Marletta, D., & Vegarud, G. E. (2014).

Protein composition and micelle size of donkey milk with different protein patterns: Effects on digestibility. *International Dairy Journal*, *35*([1]), 57-62. https://doi.org/10.1016/j.idairyj.2013.10.018

Vincenzetti, S., Foghini, L., Pucciarelli, S., Polzonetti, V., Cammertoni, N., Beghelli, D., Polidori, P. (2014). Hypoallergenic properties of donkey's milk: a preliminary study. *Veterinaria Italiana*. 50, 99-107. https://doi.org/10.12834/VetIt.219.125.5.

Vincenzetti, S., Pucciarelli, S., Huang, Y., Ricciutelli, M., Lambertucci, C., Volpini, R., Scuppa, G., Soverchia, L., Ubaldi, M., & Polzonetti, V. (2019). Biomarkers mapping of neuropathic pain in a nerve chronic constriction injury mice model. *Biochimie*, *158*, 172-179.

Vincenzetti, S., Cammertoni, N., Rapaccetti, R., Santini, G., Klimanova, Y., Zhang, J.-J., Polidori, P. (2022). Nutraceutical and Functional Properties of Camelids' Milk. *Beverages*. 8, 12. https://doi.org/10.3390/beverages8010012

Whitmore, L., & Wallace, B. A. (2008). Protein secondary structure analyses from circular dichroism spectroscopy: methods and reference databases. *Biopolymers: Original Research on Biomolecules*, *89*(5), 392-400. https://doi.org/https://doi.org/10.1002/bip.20853

Wu, K. Y., Yang, T. X., & Li, Q. Y. (2021). The effects of pH and NaCl concentration on the structure of β-casein from buffalo milk. *Food Science & Nutrition*, *9*(5), 2436-2445. https://doi.org/ https://doi.org/10.1002/fsn3.2157

Wüstneck, R., Fainerman, V. B., Aksenenko, E. V., Kotsmar, C., Pradines, V., Krägel, J., & Miller, R. (2012). Surface dilatational behavior of β-casein at the solution/air interface at different pH values. *Colloids and Surfaces A: Physicochemical and Engineering Aspects*, *404*, 17-24. https://doi.org/https://doi.org/10.1016/j.colsurfa.2012.03.050

Yousefi, R., Gaudin, J.-C., Chobert, J.-M., Pourpak, Z., Moin, M., Moosavi-Movahedi, A. A., & Haertle, T. (2009). Micellisation and immunoreactivities of dimeric β-caseins. *Biochimica et Biophysica Acta (BBA)-Proteins and Proteomics*, *1794*(12), 1775-1783. https://doi.org/https://doi.org/10.1016/j.bbapap.2009.08.015

Zhou, M., Xia, Y., Cao, F., Li, N., Hemar, Y., Tang, S. & Sun, Y. (2019). A theoretical and experimental investigation of the effect of sodium dodecyl sulfate on the structural and conformational properties of bovine β-casein. *Soft Matter*, 15, 1551-1561

Zhang, Z., Dalgleish, D., & Goff, H. (2004). Effect of pH and ionic strength on competitive protein adsorption to air/water interfaces in aqueous foams made with mixed milk proteins. *Colloids and Surfaces B: Biointerfaces*, *34*(2), 113-121. https://doi.org/https://doi.org/10.1016/j.colsurfb.2003.11.009

CHAPTER 3 - Interaction of vitamin D2 with donkey and bovine β-casein: Binding analysis, Surface hydrophobicity, and particle size of β-casein

Abstract

Interaction mechanisms between donkey β-casein (β-CN) with vitamin D2 (VD2) were studied at high vitamin/protein ratios using fluorescence and Dynamic Light Scattering (DLS) techniques and were compared with commercial bovine β-CN. Fluorescence results showed that VD2 effectively quenched the intrinsic fluorescence of both donkey and bovine β-CNs through static quenching, while the number of binding sites with proteins was approximately equal to one. The binding constants for donkey and bovine β-CNs ranged from 0.15 to 2.37 $\times 10^4$ M^{-1}, and from 0.12 to 1.14 M^{-1}, respectively, suggesting that the binding affinity of donkey β-CN-VD2 complex was slightly stronger than that of bovine β-CN-VD2 complex. Thermodynamic parameters revealed that the binding of VD2 to donkey and bovine β-CN was spontaneous ($\Delta G < 0$), and mainly driven by the hydrophobic effect with an endothermic process ($\Delta S > 0$, $\Delta H > 0$). Meanwhile, synchronous fluorescence spectra demonstrated the conformational changes of both β-CNs induced by the addition of VD2 that increased surface hydrophobicity of these proteins. Furthermore, the particle size determinations indicated that for both donkey and bovine β-CN-VD2 complexes with protein concentrations of 0.1, 1, and 2 mg/mL, the mean hydrodynamic diameters were around 10 nm at lower molar ratios (VD2-to-β-CN) from 0.25 to 0.75 but increased to at least 100 nm at higher molar ratios from 2 to 16. These findings can provide valuable references for utilizing hypoallergenic donkey β-CN as a potential delivery vehicle for hydrophobic vitamins, facilitating the enrichment of non-fat foods.

Keywords: Donkey β-CN; Vitamin D2; Binding site; Conformational change; Surface

hydrophobicity; Nanoparticle size

3.1. Introduction

Donkey milk is generating a growing interest in human nutrition owing to its peculiar composition and attractive functional properties, which has been found to be more similar to human milk when compared to bovine milk (Malissiova et al., 2016; Vincenzetti et al., 2008). Due to its hypoallergenic properties, donkey milk is considered a good substitute for dairy cow's milk derivatives in feeding infants suffering from severe Ig-E mediated cow's milk protein allergy (CMPA), as reported by Businco and Malissiova (Businco et al., 2000; Malissiova et al., 2016). Casein is the major protein component in mammalian milk, with four different protein species: αs1-CN, αs2-CN, β-CN, and κ-CN (Buitenhuis et al., 2016). Beta-casein (β-CN) is one of the main casein proteins in donkey milk and represents a key factor in the allergenicity of milk proteins. Furthermore, β-CN in donkey milk has also been demonstrated do not cross-react with bovine anti-β-CN antibodies due to its amino acid sequence, which is similar to the one determined in human milk (Perinelli et al., 2019).

Bovine β-CN, has a well-defined hydrophilic N-terminal domain and a hydrophobic C-terminal domain, which embed a 209 amino acid residues long polypeptide chain with a molecular mass of about 24 kDa. (Pinto et al., 2014). The prominent amphiphilic structure of β-CN has great advantages for their use in the development of natural nano-delivery carriers for bioactive compounds such as vitamins (Poiffait & Adrian, 1991), polyphenols (Moeiniafshari et al., 2015), oils (Zimet et al., 2011), fatty acids (Ghasemi & Abbasi, 2014), probiotics (Heidebach et al., 2010), and hydrophobic drugs including anticancer chemotherapeutics (as mitoxantrone) (Shapira et al., 2010). In particular, these bioactive compounds and drugs could be encapsulated inside the core of β-CN micelles or to form complexes via intermolecular interactions involving protein sequences in order to be stabilized and protected by this protein, together with improving their delivery efficiency (Horne, 2002). To date, most of the studies on the physicochemical properties and applications of β-

CN have employed the protein of bovine origin. However, it is noteworthy that a recent study has been preliminarily confirmed that donkey β-CN has similar self-assembling property as bovine β-CN in terms of critical micelle concentration and temperature. Thus, the use of β-CN from donkey milk for their potential encapsulation ability as a novel delivery system will be interesting to develop (Perinelli et al., 2019).

Vitamin D, as a fat-soluble vitamin, plays a crucial role in calcium and phosphate metabolism (Pludowski et al., 2013). Vitamin D2 (VD2), also known as ergocalciferol, is available in nature of vitamin D and mainly present in plants or fungi, such as yeast and mushrooms, which could produce VD2 through ultraviolet B irradiation of ergosterol (Barvencik & Amling, 2015).The main functions of VD2 were to promote the absorption of calcium and phosphate in the body, participate in the formation of osteoblasts, and maintain the normal function of the nervous system and immune system (Semo et al., 2007). Attributed to the poor sun exposure and the lack of nutrient absorption, VD2 deficiency occurs in approximately one billion people in all age groups worldwide (Holick et al., 2007), and may contribute to the development of certain diseases including cancers, autoimmune diseases, osteoporosis, high blood pressure, and depression (Autier et al., 2014; Pludowski et al., 2013). Therefore, supplementing the dairy food with VD2 is a common practice and helps to meet daily nutritional requirements (Polzonetti et al., 2020).

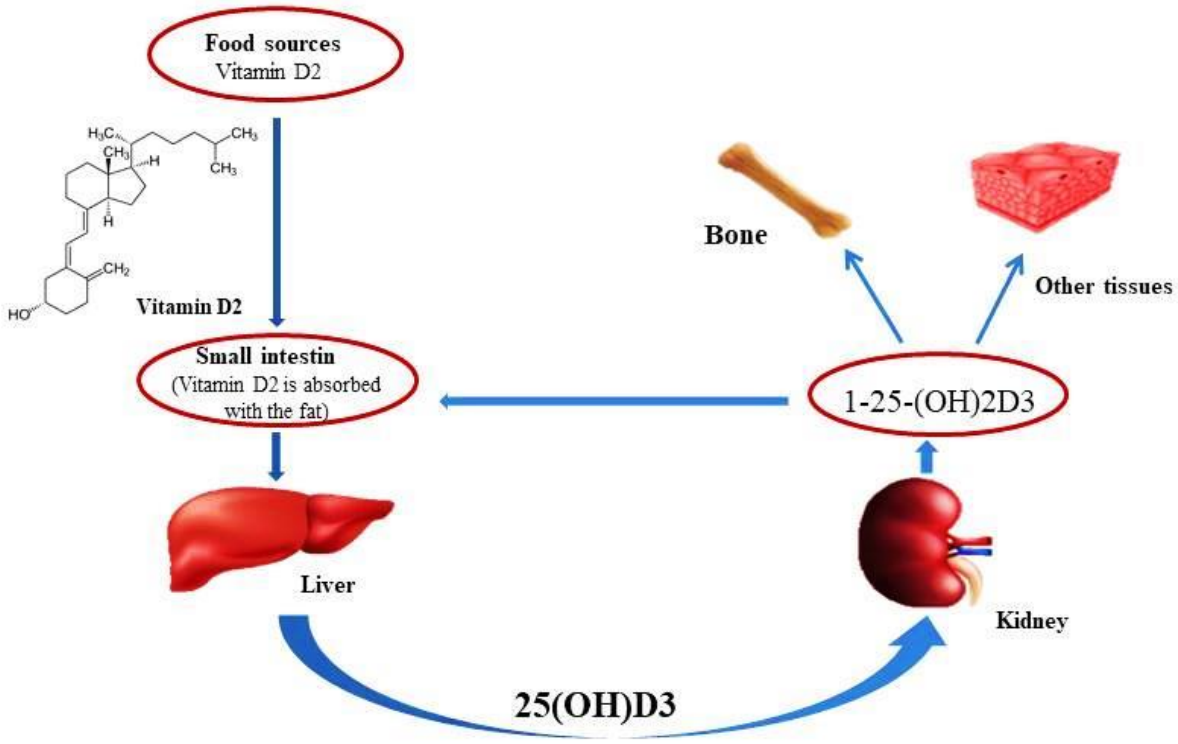

Fig.1. Schematic representation of vitamin D2 sources and metabolism.

VD2 is considered as a highly hydrophobic molecule that shows a low solubility in gastrointestinal fluids, resulting in relatively poor absorption in the body. After being absorbed by the human body, VD2 was primarily catalyzed by the 25-hydroxylase system to produce 25-hydroxyvitamin D (25OHD3) in the cellular microsomes of the liver, which was then transferred to the kidney with the help of the 1-hydroxylase system of the proximal curved tubular cells to produce the biologically active calcitriol (1-25-(OH)2D3) (Fig. 1). Additionally, VD2 is unstable since can be easily damaged by light, stress or oxidation (Grossmann & Tangpricha, 2010). Thus, it is necessary to adopt protective vehicles for VD2 to improve its stability and bioavailability. In previous studies, milk proteins have been employed for the preparation of nanocarriers to deliver vitamins by co-assembling or self-assembling into supra-molecular structures. Semo et al, (2007) demonstrated that VD2 can be loaded into bovine casein micelles that can protect this vitamin from UV-light-induced degradation. In addition, the re-assembled micelles have the similar morphology and particle size to that of CM alone, and the concentration of VD2 encapsulated inside the micelles was 4.5 times

greater than that in the serum (Semo et al., 2007a). Moreover, recent study working on loading of VD2 in native and modified sodium caseinate have shown significant improvement in the in-vitro bioavailability of VD2 (Semo et al., 2007). Meanwhile, it has also been confirmed that the binding of vitamin D3 with bovine β-CN may have a strong effect on its stability, thereby increasing the bioavailability of this vitamin in processed dairy products (Forrest et al., 2005).

However, all these previous studies were focused on the encapsulation of VD2 into bovine casein micelles, and the interaction mechanism between bovine β-CN (β-CNB) and VD2. Considering the properties of donkey β-casein (β-CND) described above, the present work aims to study the interactions between β-CND and VD2 in comparison to the protein of bovine origin to explore the applicability of β-CND as a new carrier of VD2. The emphasis was to elucidate the effect of VD2 addition on β-CN with a large range molar ratio of β-CN to VD2 by adopting various analysis methods. For example, the UV-Vis absorption and fluorescence quenching spectroscopy was used to investigate the interaction and binding mechanism of β-CN with VD2, fluorescence spectroscopy with the extrinsic probe ANS (8-Anilinonaphthalene-1-sulfonate) was used to detect the surface hydrophobicity of both β-CNs, synchronous fluorescence was used to evaluate the conformation change of the proteins, and dynamic light scattering (DLS) was utilized to measure the particle size of β-CN-VD2 complexes.

3.2. Materials and methods

3.2.1 Chemicals and reagents

VD2 (purity ≥ 98%, PubChem CID: 66577029), 1-Anilinonaphthalene-8-sulfonic acid (ANS, purity ≥ 95%), Carboxymethyl cellulose (CM52, Whatman, Merck, Darmstadt, Germany), and bovine β-CN (purity ≥ 98%, Molecular weight: 24 kDa) was acquired from Sigma Aldrich (St. Louis, MO). Donkey milk was produced from donkeys at the middle-stage lactation in a local farm (Azienda Agricola Mamma Asina, Colmurano, Marche region), and immediately stored at 4 °C. The

β-CN proteins from donkey's milk were purified according to the method previously described (see Chapter2, Zhang et al., 2023). Ultrapure water used in this study was produced using a Milli-Q water purification system (Millipore Corp., Milford, MA, USA). All other chemical reagents are of analytical reagent grade and bought from Sigma-Aldrich (St. Louis, MO).

3.2.2. Preparation of β-CN and vitamin D2 solution

Both donkey and bovine β-CNs were dissolved in buffer (50 mM sodium phosphate, pH 7.0) with a final concentration of 5 mg/mL. VD2 stock solution was prepared in absolute ethanol at a final concentration of 8 mM. Mixtures of different compositions of β-CN and VD2 were obtained by adding an aliquot of VD2 stock solution to β-CN solutions, and the final vitamin/protein molar ratios (VD2-to-β-CN) were 0, 2, 4, 6, 8, 10, 12, 14, 16, 18 and 20. All the solutions were prepared under continuous slightly stirring in dark at room temperature. The ethanol concentration does not exceed 2% v/v in the final solution.

3.2.3. UV-VIS absorption spectroscopy experiments

The absorption spectra of β-CN-VD2 systems in the range of 200-600 nm were measured using a UV-2450 spectrophotometer (Shimadzu, Japan) at temperatures of 290 K, 297 K, 304 K, 311 K, and 318 K according to Zhu and co-workers (Zhu et al., 2018). The final concentration of bovine and donkey β-CN in the solution of β-CN-VD2 complexes was 4.2 μM (0.1 mg/mL). All VD2-to-β-CN ratios (from 0 to 20) were investigated. The absorption spectra of the samples were recorded after subtracting the absorption spectra of the phosphate buffer blank.

3.2.4. Fluorescence emission spectroscopy measurements

The fluorescence spectra of β-CN-VD2 complexes were measured using a fluorescence spectrophotometer (LS-55, Perkin-Elmer, MA, USA) equipped with a temperature controller device at five measurement temperatures (290, 297, 304, 311 and 318 K) (Moeiniafshari et al., 2015). Briefly, the detected samples were β-CN (4.2 μM) solutions containing different concentrations of

VD2 with the molar ratios of VD2-to-β-CN varied from 0 to 20. The excitation wavelength was fixed at 295 nm, the emission wavelength was recorded from 300 to 500 nm, and the slit widths of excitation and emission were set at 5.0 and 4.0 nm, respectively.

To investigate the effects of the absence or the presence of VD2 on the microenvironment of tyrosine (Tyr) and tryptophan (Trp) residues in bovine and donkey β-CN, the synchronous fluorescence spectrum was scanned when the wavelength interval (Δλ) between the emission and excitation wavelength was fixed as Δλ = 15 nm or Δλ = 60 nm. The original fluorescence intensity was corrected by removing the influence of the inner effect of the VD2 using the following equation (Zeng et al., 2019):

$$F_c = F_m \times e^{(A1+A2)/2} \quad (1)$$

Here, Fc and F_m represent the fluorescence intensity after correction and the actual measured fluorescence intensity, respectively. A_1 and A_2 are the absorbance values of the VD2 at the excitation and emission wavelengths, respectively.

3.2.5. Surface hydrophobicity of β-CN

On a basis of a previous method (Li et al., 2018), a fluorescence probe ANS was used to confirm the surface hydrophobicity of β-CN proteins from bovine and donkey milk by utilizing the fluorescence spectrophotometer (LS-55, Perkin-Elmer). For these measurements, β-CN concentration in final solutions ranged from 4.2 to 14.7 μM and the molar ratios of VD2-to-β-CN of 0, 2, 4, 6, 8, and 10 were selected. Ten microliters of 8 mM ANS solution were added to 1 mL β-CN-VD2 mixture, shacked gently, and incubated in the dark for at least 20 minutes to ensure a complete reaction. Fluorescence was performed at the temperature of 304 K when the excitation wavelength was set at 380 nm and the emission spectra were collected between 400 nm to 650 nm. The surface hydrophobicity (S_0) of β-CN was obtained from the slope of the linear equation between fluorescence intensity (F) and protein concentration (C):

$$S_0 = \frac{F}{c} \quad (2)$$

3.2.6. Particle size measurement

Particle size of the β-CN-VD2 complex was determined at the temperature of 297 K by using Dynamic Light Scattering (DLS) instrument (Malvern Instrument Worcestershire, UK). Donkey and bovine β-CN solutions with different concentrations (0.1 mg/mL, 1 mg/mL, and 2 mg/mL) were prepared at room temperature. Mixtures at the VD2 to β-CN molar ratio of 0.25, 0.5, 0.75, 1, 2, 3, 4, 5, 8, 10, 12 and 16 solutions were prepared as described in 2.3. The particle size of VD2 dispersions at the same concentration of vitamin were employed to compare with that of the VD2-β-CN mixture. Samples were measured in triplicate at a fixed position of 4.65 mm and the backscattering angle was 173°.

3.3. Results and discussion

3.3.1. UV-Vis absorption spectra

UV-Vis absorption spectroscopy is an effective method to detect the complex formation between proteins and small molecule ligands (Pathak et al., 2016). The conformational change of proteins will lead to changes in microenvironment of amino acid residues and UV-Vis absorption spectra (Bi et al., 2016). The UV-Vis absorption spectra of β-CN from bovine and donkey milk in the absence or presence of various molar ratios of VD2 at the temperature of 304 K were shown in Fig.2A (The spectra of the other temperatures including 290, 297, 311 and 318 K, have the same trend changes, which are not shown).

With increasing concentrations of VD2, the absorption peak intensities of donkey and bovine β-CNs were enhanced at approximately 280 nm, indicating the formation of β-CN-VD2 complexes. Particularly, the addition of VD2 has been shown to induce conformational changes of proteins, resulting in the exposure of aromatic residues to the external environment. (Zhang et al., 2018).

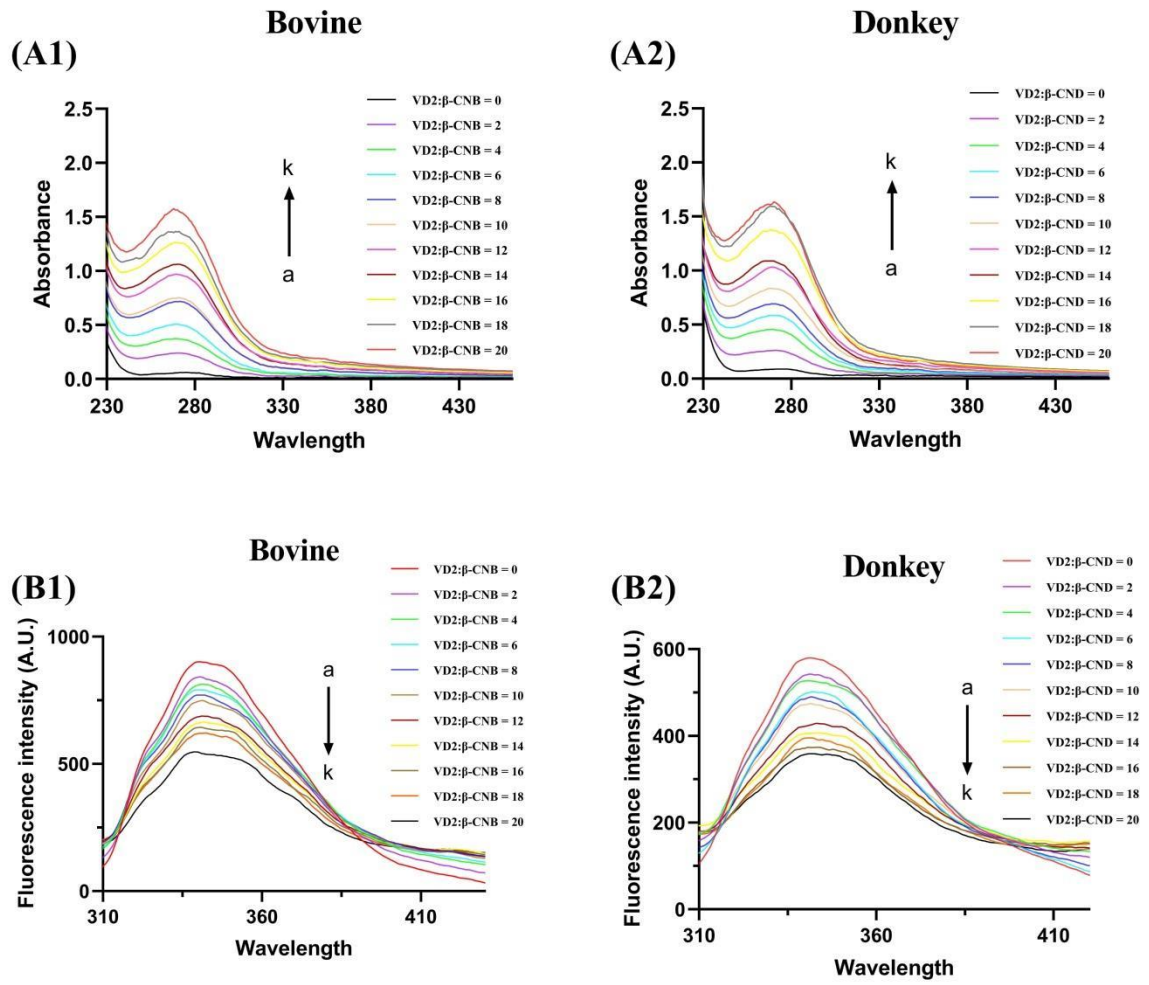

Fig. 2. UV-vis spectra (A1-2) and Fluorescence emission spectra (B1-2) of VD2-β-CN complex at the temperature of 304 K. Concentration of β-CN was 4.2 μM, and the letters a–k represent molar ratios VD2: β-CN = 0, 2, 4, 6, 8, 10, 12, 14, 16, 18 and 20, respectively.

Furthermore, the quenching type could also be determined based on the UV-vis absorption spectra. The quenching process of β-CN-VD2 complexes, as observed in the UV-vis absorption spectra, could be considered as static quenching, since dynamic quenching specifically affects the excited state of the quenching molecule without altering the absorption spectra of the quenching substances (Bi et al., 2016).

3.3.2. Fluorescence spectroscopy analysis

Due to its high sensitivity and convenient accessibility, fluorescence spectroscopy is a valuable

tool for investigating the binding interaction between proteins and small molecules (Raza et al., 2017). In general, the tryptophan and tyrosine residues of β-CN exhibits strong absorption and fluorescence yield at an excitation wavelength of 295 nm, allowing to detect even subtle changes in its surrounding microenvironment (Lou et al., 2017).

Fig. 2B illustrates the spectra obtained from solutions containing bovine (Figure 2B1) and donkey (Figure 2B2) β-CNs at a temperature of 304 K with an excitation wavelength of 295 nm. The maximum fluorescence emission wavelength of both donkey and bovine β-CN was around 340 nm. Moreover, the fluorescence intensity was gradually decreased with the increasing VD2 concentrations, suggesting that the presence of VD2 caused fluorescence quenching in both β-CN proteins. These findings revealed that the β-CN-VD2 complexes have been formed, which was consistent with the study of Mo et al and Arroyo et al., who reported that the fluorescence quenching of β-CN protein was due to their interaction with flavonoid naringenin and pelargonidin (Arroyo-Maya et al., 2016; Li et al., 2019).

3.3.3. Fluorescence quenching mechanism

Fluorescence quenching of protein can provide insights into the complexation of vitamins and proteins. This approach relies on assessing the reduction in fluorescence intensity that occurs when a fluorophore (e.g., a protein) interacts with an external quenching agent (e.g., a vitamin) that facilitates rapid de-excitation of the excited state. Generally, the process of fluorescence quenching was divided into two main mechanisms: dynamic and static quenching (Shaghaghi et al., 2019). Dynamic quenching occurs due to the interaction between two photosensitive compounds, where a donor fluorophore transfers energy to an acceptor, resulting in either self-emission of light or full absorption of the energy, allowing the fluorophore to return from the excited state to the ground state. This process involves electron excitation before quenching. Static quenching, also known as contact quenching, represents another energy transfer mechanism. It can be a predominant mechanism for specific reporter-quencher probes. Unlike dynamic quenching, static quenching takes

place when molecules create a complex in their ground state, prior to excitation. This complex exhibits distinct characteristics, such as non-fluorescence and a unique absorption spectrum. The principle of static quenching is that non-fluorescent or weakly fluorescent compounds are formed between the fluorophore and the quencher in the ground state, leading the decreasing of fluorescence intensity (Fig. 3) (Jahanban-Esfahlan & Panahi-Azar, 2016; Wang et al., 2016). The temperature

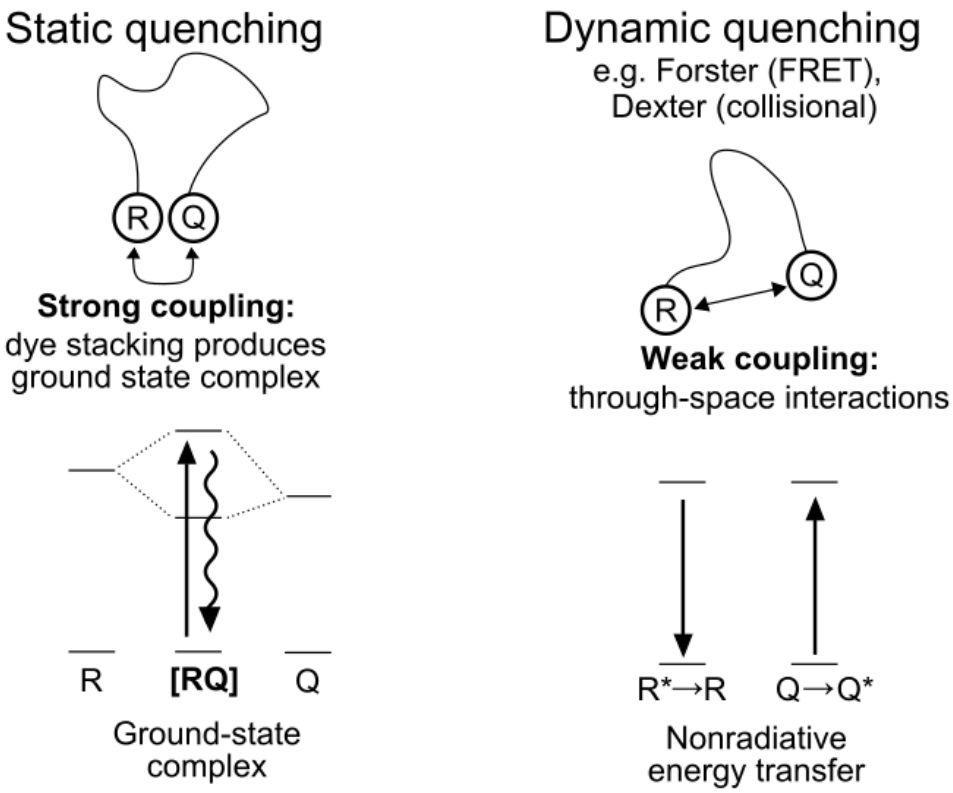

Fig.3. Schematic representation of the mechanism of dynamic and static quenching.

dependence of the formed protein-molecule complexes can be used primarily to distinguish these two mechanisms. As temperature rises, diffusion rates increase, leading to more dynamic quenching, while the strength of complexes formation decreases with higher temperatures. Consequently, static quenching diminishes at elevated temperatures due to the dissociation of loosely bound complexes (Liu, Qi, & Li, 2000). To explore the potential quenching mechanisms between β-CN and VD2, the classical Stern-Volmer equation was utilized in this study:

$$F_0 / F = 1 + Kq\tau_0 [Q] = 1 + K_{sv}[Q] \quad (3)$$

Here, F_0 and F represent the fluorescence intensities of β-CNs of donkey and bovine in the absence and presence of VD2 after correction, respectively; Kq and τ_0 are the quenching rate constant of biomolecule and average lifetime of the biomolecule without a quencher ($\tau_0 = 10^{-8}$ s), respectively; K_{SV} ($Kq\tau_0$) and [Q] are used to denote the Stern-Volmer quenching constant and the concentration of the quencher VD2, respectively. The linear plots of F_0/F against [Q] at five different temperatures (290, 297, 304, 311 and 318 K) are shown in Fig. 4A whereas Table 1 displays the K_{SV} and Kq values of the complexes formed between both β-CNs and VD2 calculated by Equation (3).

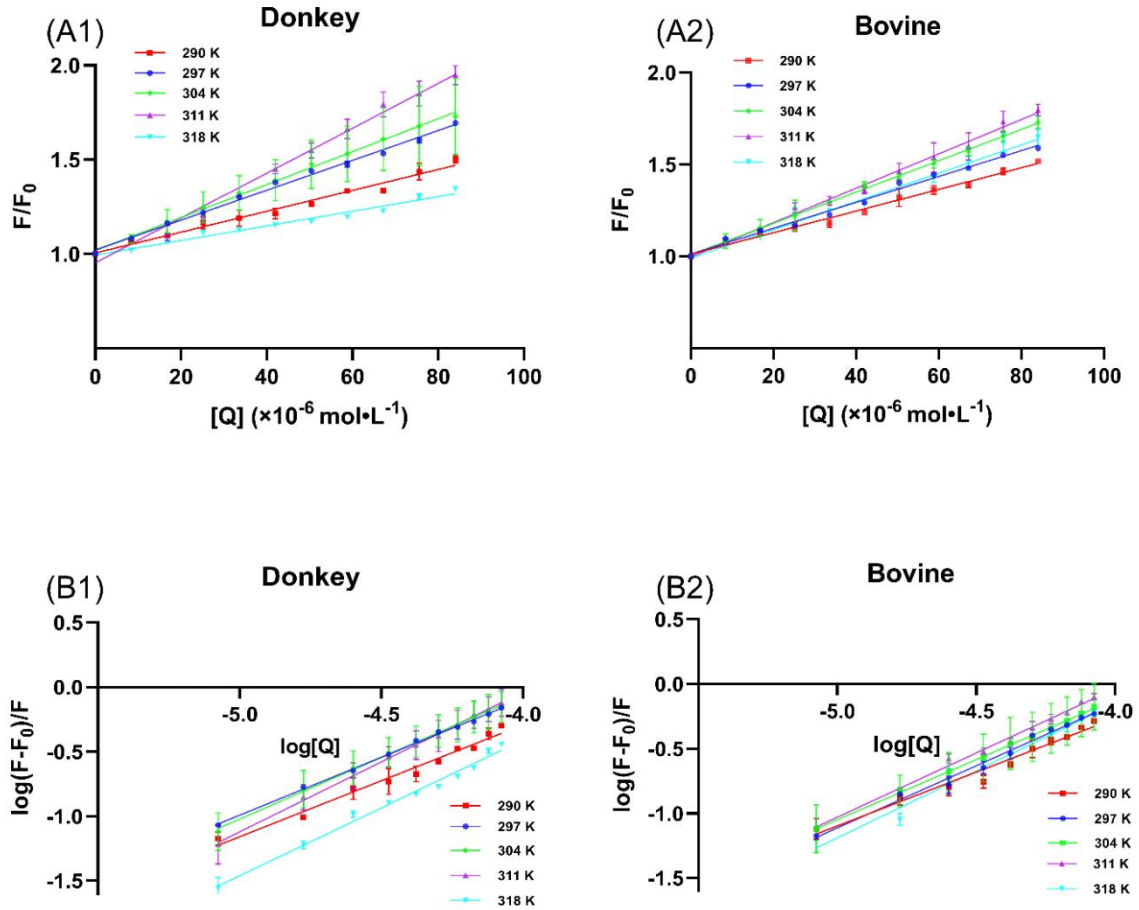

Fig. 4. Stern-Volmer plots of bovine and donkey β-CNs binding to VD2 at 290 K, 298 K, 304 K, and 310 K (A1-2).

Double logarithmic plots of bovine and donkey β-CNs interacting with VD2 at 298, 304, and 310 K (B1-2).

Table 1. The quenching and bind constant and thermodynamic parameters for the interaction of bovine and donkey β-CNs with VD2 at five different temperatures.

	Temperature (K)	$K_{sv}\times10^4$ (mol^{-1})	$K_q\times10^{12}$ ($mol^{-1}s^{-1}$)	R^2	$K_a\times10^4$ (mol^{-1})	n	R^2
Bovine	290	0.61±0.02	0.61±0.02	0.976	0.12±0.01	0.83±0.01	0.949
	297	0.77±0.02	0.77±0.02	0.992	0.20±0.01	0.87±0.00	0.981
	304	0.87±0.40	0.87±0.40	0.981	0.53±0.41	0.93±0.03	0.894
	311	0.88±0.05	0.88±0.05	0.974	0.90±0.15	1.00±0.01	0.990
	318	0.70±0.05	0.70±0.05	0.970	1.14±0.50	1.04±0.06	0.970
Donkey	290	0.56±0.00	0.56±0.00	0.964	0.15±0.00	0.87±0.00	0.954
	297	0.84±0.01	0.84±0.01	0.993	0.31±0.02	0.90±0.01	0.997
	304	0.90±0.26	0.90±0.26	0.928	0.62±0.27	0.96±0.02	0.879
	311	1.00±0.08	1.00±0.08	0.979	2.37±4.29	1.11±0.73	0.929
	318	0.38±0.00	0.38±0.00	0.968	1.63±0.5	1.15±0.03	0.980

The lowest Kq values observed for donkey and bovine β-CNs were 1.7×10^{11} $M^{-1}S^{-1}$ and 1.8×10^{11} $M^{-1}S^{-1}$, respectively, which exceed the dispersion collision quenching constant value (2.0×10^{10} $M^{-1}S^{-1}$), indicating static quenching was the dominant mechanism when VD2 bound to these proteins. However, there was an increase in Ksv values of both β-CN proteins as the temperature increased. The results was similar to those obtained from the other authors (Cheng et al., 2022; Esmaili et al., 2011; Li et al., 2020), who also found that Kq was much larger than 2.0×10^{10} $M^{-1}S^{-1}$ and K_{SV} increased with the increasing temperature between bovine β-CN and molecule ligands (luteolin, curcumin and benzoic acid derivatives).

3.3.4. Binding constant and number of binding sites

Since static quenching has been determined between β-CN-VD2 complex, the following formula can be used to calculate the binding constant (Ka) and number of binding sites (n) (Rout et al., 2020):

$$\log\frac{F0-F}{F} = LogKa + nLog[Q] \qquad (4)$$

Where, Ka is the binding constant, n is the number of binding sites, and [Q] is the concentration of VD2. F and F_0 represent the fluorescence intensities of the β-CNs with or without VD2. The binding constant and number of binding sites were calculated from the intercept and the slope based on equation (4). Table 1 summarized the Ka and n values for donkey and bovine β-CN-VD2 complexes at five different temperatures (290, 297, 304, 311 and 318 K), and the plots of log [(F_0−F)/F] versus log [Q] were presented in Fig. 2B.

The number of binding sites of both β-CNs for VD2 was all approximately equal to one, indicating that the molar ratio of VD2 combining to these proteins was 1:1. The Ka values of donkey β-CN-VD2 complex exhibited an initial increase with temperature from 290 K to 311 K, followed by a decrease at 318 K. In contrast, the Ka values of bovine β-CN-VD2 complex showed a continuous increase with temperature from 290 K to 318 K. These differences indicated that the stability of the donkey β-CN-VD2 complex formed at a high temperature of 318K was comparatively lower than that of bovine β-CN-VD2 complex. It has been shown that the increase of Ka values with increasing temperature is the result of endothermic reactions (Jiang et al., 2020). At temperatures of 290, 297, 304, and 311K, the Ka values of donkey β-CN-VD2 complex were consistently greater than those of bovine β-CN-VD2 complex, indicating a higher binding affinity of donkey β-CN-VD2 complex compared to bovine β-CN-VD2 complex. Hence, it can be inferred that the binding of donkey β-CN to VD2 was more temperature dependent than that of bovine β-CN.

3.3.5. Thermodynamic parameters and binding model

The determination of thermodynamic parameters including entropy change (ΔS) and enthalpy change (ΔH) was used to further investigate the interaction types between donkey and bovine β-CN-VD2 complexes. Generally, the binding interaction of proteins with small molecule ligands can be characterized by four main different driving forces, which are hydrogen bonding interaction, van der Waals force, electrostatic interaction and hydrophobic interaction (Bijari et al., 2017). These thermodynamic parameters could be given by the following Van't Hoff formula (Byadagi et al., 2017):

$$\log Ka = -\frac{\Delta H}{2.303RT} + \frac{\Delta S}{2.303R} \quad (5)$$

$$\Delta G = \Delta H - T\Delta S \quad (6)$$

where R, Ka and T represent gas constant (8.314 J mol $^{-1}$ K $^{-1}$), the binding constant between β-CN-VD2 complexes, and the experimental temperatures, respectively. Previous studies have reported in detail the relationship between the driving force of protein with molecule ligand and thermodynamic parameters: hydrophobic effects are the main driving force when ΔS > 0 and ΔH > 0; van der Waals forces and hydrogen bonds are confirmed the two dominant driving forces when ΔS < 0 and ΔH < 0; they are supposed to be electrostatic forces if ΔS > 0 and ΔH < 0; the electrostatic and hydrophobic interactions contributed a lot between the complexes when ΔS < 0 and ΔH > 0 (Temboot et al., 2018).

Thermodynamic parameters and Van't Hoff plot of donkey and bovine β-CN-VD2 systems were presented in Table 2 and Fig. 5, respectively. The positive values of ΔS and ΔH found in both β-CN-VD2 complexes indicated that the binding between VD2 and proteins was predominantly driven by the hydrophobic effect accompanied by an endothermic process. Meanwhile, the negative values of ΔG provided the key information that the reaction between donkey and bovine β-CN-VD2 complexes was spontaneous (He et al., 2016). These results were agreement with Cao's study (Cao

et al., 2019), who found that the hydrophobic interaction was the crucial driving force for the formation of complexes between bovine β-CN and eriocitrin (a glycosylated flavanone with strong antioxidant, antitumor, anti-allergic, antidiabetic and anti-inflammatory activities), and the reaction occurs spontaneously. In a study conducted by He et al. (2016), it was similarly observed that hydrophobic interactions played a crucial role in the formation of complexes between bovine β-CN and malvidin-3-O-glucoside (MG, a flavonoid), as evidenced by the positive values of ΔH (>0) and ΔS (>0) (He et al., 2016).

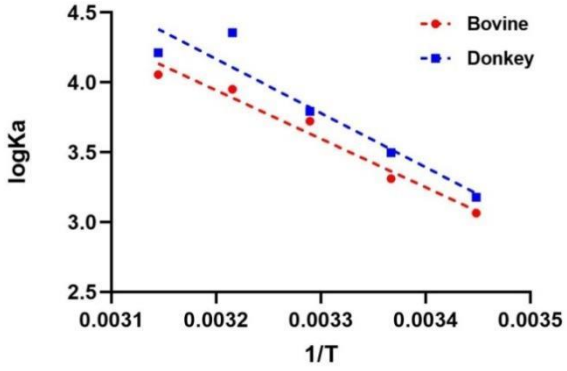

Fig. 5. Van't Hoff plot of donkey and bovine β-CN binding to VD2.

Table 2 Thermodynamic parameters of donkey and bovine β-CN-VD2 systems.

	Temperature (K)	ΔH (kJ mol^{-1})	ΔS (J mol^{-1})	ΔG (kJ mol^{-1})	R^2
Bovine	290	66.43±0.20	288.07±0.06	-17.11±0.12	0.977
	297			-19.13±0.61	
	304			-21.15±0.22	
	311			-23.16±0.17	
	318			-25.18±0.03	

Donkey	290	74.15±0.75	317.08±0.02	-17.80±0.15	0.904
	297			-20.33±0.28	
	304			-22.24±0.13	
	311			-24.14±0.01	
	318			-26.68±0.05	

3.3.6. Analysis of synchronous fluorescence spectra

Synchronous fluorescence is considered a powerful method that is extensively utilized to investigate complex mixtures of fluorophores because they can yield a much narrower bands compared with conventional excitation or emission spectra. This technique is achieved by scanning both the excitation and emission wavelengths at the same time. Synchronous fluorescence can provide characteristic information about the conformation of fluorophore molecules in the microenvironment, which will change around tyrosine (Tyr) and tryptophan (Trp) residues when wavelength intervals ($\Delta\lambda$) is set at 15 and 60 nm, respectively (He et al., 2016; Van de Weert & Stella, 2011). One of the previous studies stated that the synchronous fluorescence of the tyrosine-tryptophan mixture tends to represent tyrosine when the $\Delta\lambda$ value is small, while shows a spectrum similar to that of tryptophan at large $\Delta\lambda$ values (Bobone et al., 2014). Moreover, a blue or red shift in the position of maximum emission wavelength (λ_{max}) indicate a change in the polarity of the microenvironment surrounding Tyr or Trp residues (Mohammadi & Moeeni, 2015). Considering this, the structural change of β-CN from donkey and bovine in present study was evaluated in the absence and presence of VD2 by synchronous fluorescence spectrum measurement.

Based on information obtained from the UniProt database (https://www.uniprot.org/), all three until known isoform of the β-CN from donkey (see figure 3, Chapter 1) contains five Tyr residues that are located at position 82, 84, 90, 201, 214 (considering the isoform D2EC27, see Chapter 1,

figure 3). However, β-CN from bovine (P02666) possesses four Tyr residues at locations 75, 129, 195, 208, as well as one Trp residue at location 158.

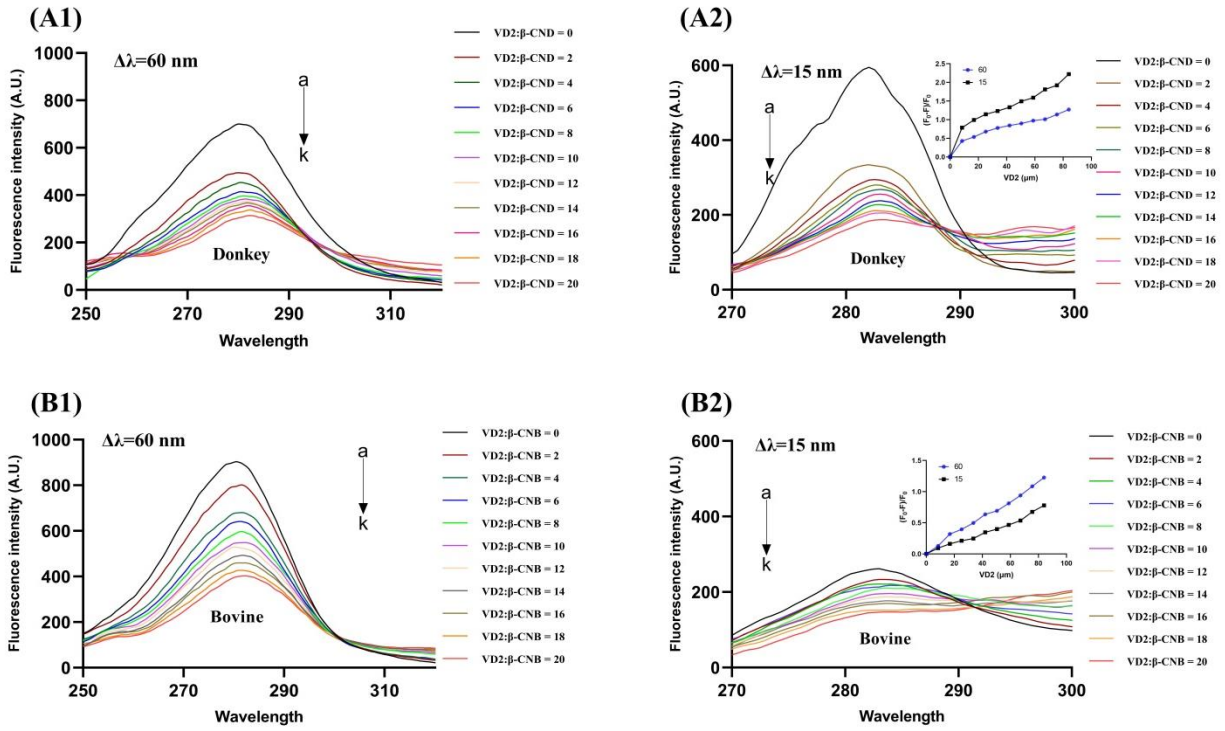

Fig. 6. Synchronous fluorescence spectra of donkey and bovine β-CN with varying concentration of VD_2 (A1-B1: Δλ = 60 nm, A2-B2: Δλ = 15 nm). Concentration of β-CN was 4.2 μM, and the letters a–k represent molar ratios VD_2: β-CN = 0, 2, 4, 6, 8, 10, 12, 14, 16, 18, and 20, respectively. Inserted (A2-B2): the quenching ability of β-CN synchronous fluorescence by VD2.

As shown in Fig.5, the synchronous fluorescence intensity of β-CN from donkey and bovine milk decreased progressively with the increase of VD2 concentration, showing that the tyrosine residues (in donkey) and both Tyr and Trp residues (in bovine) were devoted to the quenching of the intrinsic fluorescence.

Meanwhile, VD2 played different roles in the fluorescence quenching of the Tyr and Trp residues between bovine and donkey β-CNs. The quenching degree of Tyr residues of β-CN from donkey was strong (Inset in Fig. 4A), while bovine β-CN showed higher quenching degree in Trp

than Tyr (Inset in Fig. 4B). The results evidenced that there are different binding sites on β-CN proteins of bovine for the small molecule VD2 and this could occur also for donkey β-CN. Similar results were obtained in Bourassa's (2013) study that there were different binding sites of retinol and retinoic acid on β-CN proteins (Bourassa et al., 2013).

According to Fig.6 A1 and B1, at Δλ=60 nm it was observed a red shift (1.94 nm for donkey β-CN and 1.79 nm for bovine β-CN) with the increasing molar ratios of VD2 to β-CNs, while a tiny red shift also appeared in the maximum emission wavelengths of Tyr residues (Δλ=15 nm) in donkey and bovine β-CNs, which was 1.32 nm and 1.81 nm, respectively (Fig.6 A2 and B2). These results proved that the hydrophobicity around the Tyr and Trp residues in β-CNs was slightly decreased, and the polarity of these proteins increased after adding VD2. Thus, it could be confirmed that the changes occurred in the conformation of β-CN proteins and in microenvironment surrounding Tyr and Trp residues. In a study conducted by Mohammadi et al. (2015), the interaction between genistein (an isoflavone, it has been described as an angiogenesis inhibitor, antioxidant and anthelmintic) and kaempferol (a polyphenol antioxidant found in fruits and vegetables, dietary kaempferol could reduce the risk of chronic diseases, especially cancer), with bovine α-lactalbumin was examined using synchronous fluorescence spectrum. The results revealed that the conformation of bovine α-lactalbumin was changed, leading to the exposure of Tyr and Trp residues in a more polar microenvironment, which closely resembled the findings of the present research (Mohammadi & Moeeni, 2015).

3.3.7. Surface hydrophobicity

The surface hydrophobicity (S_0) of proteins has been proved to play a crucial role in determining their conformational changes and hydrophobic sites exposed to aqueous environments (Yuan et al., 2018). The S_0 values of β-CNs from donkey and bovine in the absence and presence of VD2 calculated using Eq. (2) were shown in Fig. 7.

In brief, surface hydrophobicity of both β-CNs was increased by the addition of VD2. The improved hydrophobicity of β-CNs was the result of introducing hydrophobic groups of VD2, indicating more hydrophobic regions were exposed and a decrease in polarity of the surrounding solutions in β-CN-VD2 complexes (Li et al., 2018; Wei et al., 2015). However, the hydrophobicity values showed a slight decrease as the increasing molar ratios of VD2-to-β-CN from 8:1 to 10:1,

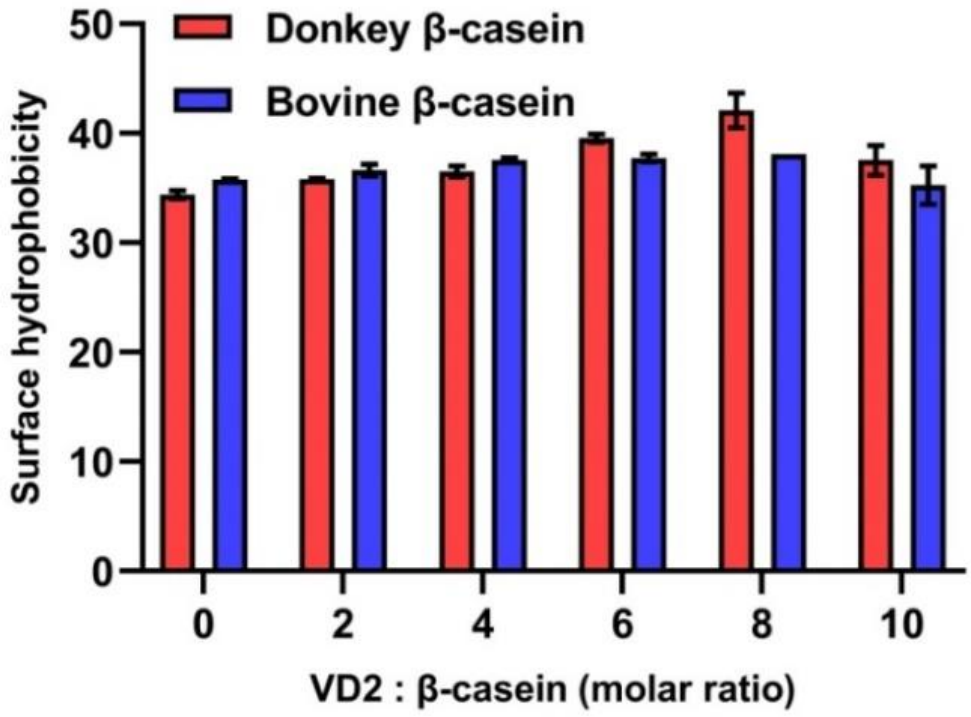

Fig. 7. Effect of VD2 on surface hydrophobicity of bovine and donkey β-CNs.

suggesting that certain hydrophobic amino acids converged inside the proteins or some amount of VD2 bound to the non-polar regions on the β-CN surfaces. Chen et al. (2021) have also reported the surface hydrophobicity of alpha-lactoglobulin was increased after interacting with VD3, indicating that the structure of the protein become compacted and more hydrophobic residues exposed to the solution (Chen et al., 2021).

3.3.8. Particle size measurement

Fig. 8 illustrates the mean hydrodynamic diameter values of donkey and bovine β-CN-VD2

complexes at different concentrations of VD2 (corresponding to the VD2 to β-CN molar ratio from 0.25 to 16), as well as the particle size of VD2 alone at the same concentration as in the complexes. The protein concentrations utilized for these measurements were 0.1, 1, and 2 mg/mL, respectively. Mean hydrodynamic diameters of all the analyzed VD2 samples were exceeded 100 nm, suggesting that vitamin aggregates in an aqueous medium as a function of its concentration. All the obtained intensity distribution curves of complexes have a sigmoidal trend in which two plateau regions can be observed. At lower VD2-to-β-CN molar ratios from 0.25 to 0.75, the mean hydrodynamic diameters of both β-CN-VD2 complexes remained relatively constant around 10 nm (forming the first plateau), resembling the dimensions of the protein in its monomeric state. The second plateau refers to the range of molar ratios (VD2-to-β-CN) at which the mean hydrodynamic diameters held steady at approximately 100 nm with reference protein concentration 0.1 mg/mL, 200 nm with reference protein concentration 1 mg/mL, and 250-300 nm with reference protein concentration 2 mg/mL, respectively. In the middle region with molar ratios ranging from 0.75 to 2 (VD2-to-β-CN), the average hydrodynamic diameters of these complexes significantly increased with the increasing concentration of VD2, inferring the formation of β-CN with VD2 complex. Hence, the particle size of β-CN-VD2 complexes at lower molar ratios of VD2-to-β-CN ranging from 0.25 to 0.75 seems to be determined only by protein concentration, while the presence of VD2 does not affect it. Conversely, at higher molar ratios ranging from 2 to 16, the particle size of these complexes seems to be determined only by VD2 concentration, showing that the particle sizes of the complexes were strongly depended on the concentration of vitamin.

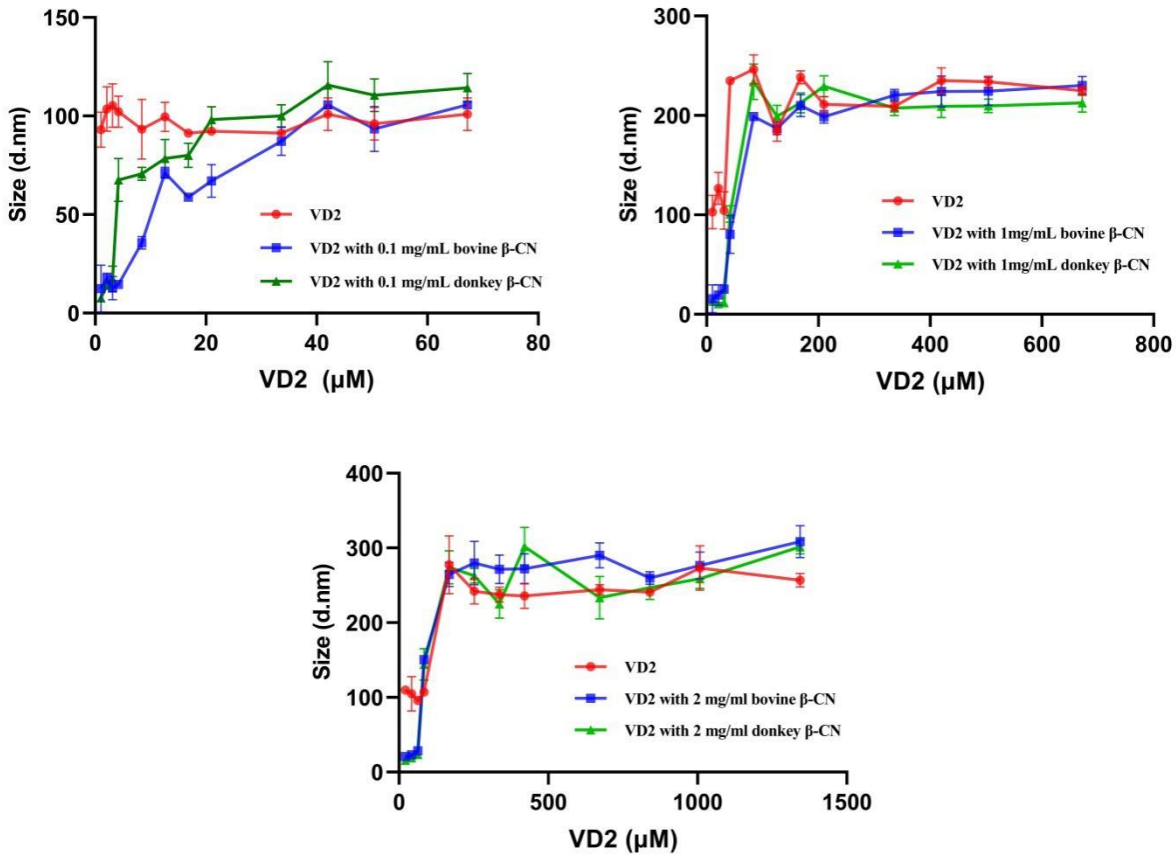

Fig.8. Mean hydrodynamic diameter vs. VD2 concentration for different β-CN concentrations: 0.1 mg/ml, 1 mg/ml, and 2 mg/ml. (The molar ratios of VD2 to protein were 0.25, 0.5, 0.75, 1, 2, 3, 4, 5, 8, 10, 12, and 16, respectively.)

Abbasi et al. (2014) investigated the particle sizes of VD3-whey protein complexes, which ranged from approximately 100 nm to 200 nm, however, the size of vitamin in the absence of protein was not measured. (Abbasi et al., 2014). Furthermore, Berino et al., (2019) worked on the interaction of vitamin D with beta-lactoglobulin at high vitamin/protein ratios (larger than 1), and they determined the particle size of vitamin aggregates (from 100 nm to 160 nm) was very much larger than that of the protein molecule (7 nm) (Berino et al., 2019). These findings are similar to that in our study. Additionally, it is worth mentioning that the DLS instrument may overlook the size of small nanoparticles when there are larger nanoparticles exhibiting higher intensity of scattered light (Hiemenz & Rajagopalan, 1997). Therefore, based on this information, we can suppose that the

detected nanoparticle size values (larger than 100 nm) in present work correspond to VD2 aggregates or the vitamin-protein complexes.

3.4. Conclusion

This study provided a comprehensive perspective on the interaction of donkey and bovine β-CN with VD2, revealing similar behavior of both proteins after the addition of VD2. Analysis of fluorescence spectroscopy observed that VD2 significantly quenched the intrinsic fluorescence intensity of both proteins via static quenching, with a slightly stronger binding affinity observed towards donkey β-CN compared to bovine β-CN. Moreover, hydrophobic interaction has mainly contributed to the binding process of β-CNs and VD2. Additionally, the enhanced surface hydrophobicity revealed that VD2 decreased the polarity of the surrounding solutions in these complexes, leading to the conformational changes in the structure of these proteins.

Furthermore, the particle size of both β-CN-VD2 complexes was determined by protein concentration at lower molar ratios of VD2-to-β-CN (0.25 to 0.75), whereas it exhibited a strong dependency on VD2 concentration at higher molar ratios (2 to 16), indicating that VD2 seems to aggregate into nanoparticles whose size is unaffected by the presence of the proteins.

In summary, the findings support the potential use of donkey β-CN characterized by hypoallergenic properties as a viable substitute for bovine β-CN, offering a novel nanocarrier system for VD2 in food applications and providing a theoretical basis for the encapsulation of this vitamin.

References

Abbasi, A., Emam-Djomeh, Z., Mousavi, M. A. E., & Davoodi, D. (2014). Stability of vitamin D3 encapsulated in nanoparticles of whey protein isolate. *Food Chemistry*, *143*, 379-383.

Arroyo-Maya, I. J., Campos-Terán, J., Hernández-Arana, A., & McClements, D. J. (2016). Characterization of flavonoid-protein interactions using fluorescence spectroscopy: Binding of pelargonidin to dairy proteins. *Food Chemistry*, *213*, 431-439.

Autier, P., Boniol, M., Pizot, C., & Mullie, P. (2014). Vitamin D status and ill health: a systematic review. *The Lancet Diabetes & Endocrinology*, *2*(1), 76-89.

Barvencik, F., & Amling, M. (2015). Vitamin-D-Stoffwechsel des Knochens. *Der Orthopäde*, *44*(9), 686-694.

Berino, R. P., Báez, G. D., Ballerini, G. A., Llopart, E. E., Busti, P. A., Moro, A., & Delorenzi, N. J. (2019). Interaction of vitamin D3 with beta-lactoglobulin at high vitamin/protein ratios: Characterization of size and surface charge of nanoparticles. *Food Hydrocolloids*, *90*, 182-188.

Bi, H., Tang, L., Gao, X., Jia, J., & Lv, H. (2016). Spectroscopic analysis on the binding interaction between tetracycline hydrochloride and bovine proteins β-casein, α-lactalbumin. *Journal of Luminescence*, *178*, 72-83.

Bijari, N., Ghobadi, S., & Derakhshandeh, K. (2017). Irinotecan binds to the internal cavity of beta-lactoglobulin: A multi-spectroscopic and computational investigation. *Journal of Pharmaceutical and Biomedical Analysis*, *139*, 109-115.

Bourassa, P., N'soukpoé-Kossi, C. N., & Tajmir-Riahi, H. A. (2013). Binding of vitamin A with milk α- and β-caseins. *Food Chemistry*, *138*(1), 444-453.

Bobone, S., van de Weert, M., & Stella, L. (2014). A reassessment of synchronous fluorescence in the separation of Trp and Tyr contributions in protein emission and in the determination of conformational changes. *Journal of Molecular Structure, 1077*, 68-76.

Buitenhuis, B., Poulsen, N. A., Gebreyesus, G., & Larsen, L. B. (2016). Estimation of genetic parameters and detection of chromosomal regions affecting the major milk proteins and their post translational modifications in Danish Holstein and Danish Jersey cattle. *BMC Genetics*, *17*(1), 114.

Businco, L., Giampietro, P. G., Lucenti, P., Lucaroni, F., Pini, C., Di Felice, G., Iacovacci, P., Curadi, C., & Orlandi, M. (2000). Allergenicity of mare's milk in children with cow's milk allergy. *Journal of Allergy and Clinical Immunology*, *105*(5), 1031-1034.

Byadagi, K., Meti, M., Nandibewoor, S., & Chimatadar, S. (2017). Investigation of binding behaviour of procainamide hydrochloride with human serum albumin using synchronous, 3D fluorescence and circular dichroism. *Journal of Pharmaceutical Analysis*, *7*(2), 103-109.

Cao, X., He, Y., Kong, Y., Mei, X., Huo, Y., He, Y., & Liu, J. (2019). Elucidating the interaction mechanism of eriocitrin with β-casein by multi-spectroscopic and molecular simulation methods. *Food Hydrocolloids*, *94*, 63-70.

Chen, W., Yu, H., Shi, R., Chenglong, M., Gantumur, M.-A., Qayum, A., Bilawal, A., Liang, G., Oh, K.-C., Jiang, Z., & Hou, J. (2021). Comparison of carrying mechanism between three fat-soluble vitamins and alpha-lactalbumin: Effects on structure and physicochemical properties of alpha-lactalbumin. *Food Hydrocolloids*, *116*, 106662.

Cheng, Y., Liu, D., Zeng, M., Chen, J., Mei, X., Cao, X., & Liu, J. (2022). Milk β-casein as delivery systems for luteolin: Multi-spectroscopic, computer simulations, and biological studies. *Journal of Food Biochemistry*, *46*(7), e14133

Esmaili, M., Ghaffari, S. M., Moosavi-Movahedi, Z., Atri, M. S., Sharifizadeh, A., Farhadi, M., Yousefi, R., Chobert, J.-M., Haertlé, T., & Moosavi-Movahedi, A. A. (2011). Beta casein-micelle as a nano vehicle for solubility enhancement of curcumin; food industry application. *LWT - Food Science and Technology*, *44*(10), 2166-2172.

Forrest, S. A., Yada, R. Y., & Rousseau, D. (2005). Interactions of vitamin D3 with bovine β-lactoglobulin A and β-casein. *Journal of agricultural and food chemistry*, *53*(20), 8003-8009.

Ghasemi, S., & Abbasi, S. (2014). Formation of natural casein micelle nanocapsule by means of pH changes and ultrasound. *Food Hydrocolloids*, *42*, 42-47.

Grossmann, R. E., & Tangpricha, V. (2010). Evaluation of vehicle substances on vitamin D bioavailability: A systematic review. *Molecular Nutrition & Food Research*, *54*(8), 1055-1061.

He, Z., Xu, M., Zeng, M., Qin, F., & Chen, J. (2016). Interactions of milk α- and β-casein with malvidin-3-O-glucoside and their effects on the stability of grape skin anthocyanin extracts. *Food Chemistry*, *199*, 314-322.

Heidebach, T., Först, P., & Kulozik, U. (2010). Influence of casein-based microencapsulation on freeze-drying and storage of probiotic cells. *Journal of Food Engineering*, *98*(3), 309-316.

Hiemenz, P., & Rajagopalan, R. (1997). Static and dynamic light scattering and other radiation scattering. *Principles of Colloid and Surface Chemistry*, 193-247.

Holick, M. F., Chen, T. C., Lu, Z., & Sauter, E. (2007). Vitamin D and Skin Physiology: A D-Lightful Story . *Journal of Bone and Mineral Research*, *22*(S2), V28-V33.

Horne, D. S. (2002). Casein structure, self-assembly and gelation. *Current Opinion in Colloid & Interface Science*, *7*(5), 456-461.

Jahanban-Esfahlan, A., & Panahi-Azar, V. (2016). Interaction of glutathione with bovine serum albumin: Spectroscopy and molecular docking. *Food Chemistry*, *202*, 426-431.

Jiang, Z., Li, T., Ma, L., Chen, W., Yu, H., Abdul, Q., Hou, J., & Tian, B. (2020). Comparison of interaction between three similar chalconoids and α-lactalbumin: Impact on structure and functionality of α-lactalbumin. *Food Research International*, *131*, 109006.

Li, M., Fokkink, R., Ni, Y., & Kleijn, J. M. (2019). Bovine beta-casein micelles as delivery systems for hydrophobic flavonoids. *Food Hydrocolloids*, *96*, 653-662.

Li, T., Hu, P., Dai, T., Li, P., Ye, X., Chen, J., & Liu, C. (2018). Comparing the binding interaction between β-lactoglobulin and flavonoids with different structure by multi-spectroscopy analysis and molecular docking. *Spectrochimica Acta Part A: Molecular and Biomolecular*

Spectroscopy, *201*, 197-206.

Li, T., Li, X., Dai, T., Hu, P., Niu, X., Liu, C., & Chen, J. (2020). Binding mechanism and antioxidant capacity of selected phenolic acid - β-casein complexes. *Food Research International*, *129*, 108802.

Liu, E. H., Qi, L. W., & Li, P. (2000). Structural relationship and binding mechanisms of five flavonoids with bovine serum albumin. *Molecules, 15*, 9092e9103.

Lou, Y.-Y., Zhou, K.-L., Shi, J.-H., & Pan, D.-Q. (2017). Characterizing the binding interaction of fungicide boscalid with bovine serum albumin (BSA): A spectroscopic study in combination with molecular docking approach. *Journal of Photochemistry and Photobiology B: Biology*, *173*, 589-597.

Malissiova, E., Arsenos, G., Papademas, P., Fletouris, D., Manouras, A., Aspri, M., Nikolopoulou, A., Giannopoulou, A., & Arvanitoyannis, I. S. (2016). Assessment of donkey milk chemical, microbiological and sensory attributes in Greece and Cyprus. *International Journal of Dairy Technology*, *69*(1), 143-146.

Moeiniafshari, A.-A., Zarrabi, A., & Bordbar, A.-K. (2015). Exploring the interaction of naringenin with bovine beta-casein nanoparticles using spectroscopy. *Food Hydrocolloids*, *51*, 1-6.

Mohammadi, F., & Moeeni, M. (2015). Analysis of binding interaction of genistein and kaempferol with bovine α-lactalbumin. *Journal of Functional Foods*, *12*, 458-467.

Pathak, M., Mishra, R., Agarwala, P. K., Ojha, H., Singh, B., Singh, A., & Kukreti, S. (2016). Binding of ethyl pyruvate to bovine serum albumin: Calorimetric, spectroscopic and molecular docking studies. *Thermochimica Acta*, *633*, 140-148.

Perinelli, D. R., Bonacucina, G., Cespi, M., Bonazza, F., Palmieri, G. F., Pucciarelli, S., Polzonetti, V., Attarian, L., Polidori, P., & Vincenzetti, S. (2019). A comparison among β-caseins purified from milk of different species: Self-assembling behaviour and immunogenicity potential. *Colloids and Surfaces B: Biointerfaces*, *173*, 210-216.

Pinto, M. S., Léonil, J., Henry, G., Cauty, C., Carvalho, A. F., & Bouhallab, S. (2014). Heating and

glycation of β-lactoglobulin and β-casein: Aggregation and in vitro digestion. *Food Research International*, *55*, 70-76.

Pludowski, P., Holick, M. F., Pilz, S., Wagner, C. L., Hollis, B. W., Grant, W. B., Shoenfeld, Y., Lerchbaum, E., Llewellyn, D. J., Kienreich, K., & Soni, M. (2013). Vitamin D effects on musculoskeletal health, immunity, autoimmunity, cardiovascular disease, cancer, fertility, pregnancy, dementia and mortality—A review of recent evidence. *Autoimmunity Reviews*, *12*(10), 976-989.

Poiffait, A., & Adrian, J. (1991). Interaction between Casein and Vitamin a during Food Processing. In M. Friedman (Ed.), *Nutritional and Toxicological Consequences of Food Processing* (pp. 61-73). Springer US.

Polzonetti, V., Pucciarelli, S., Vincenzetti, S., & Polidori, P. (2020). Dietary intake of vitamin D from dairy products reduces the risk of osteoporosis. *Nutrients*, *12*(6), 1743.

Raza, M., Ahmad, A., Yue, F., Khan, Z., Jiang, Y., Wei, Y., Raza, S., He, W. W., Khan, F. U., & Qipeng, Y. (2017). Biophysical and molecular docking approaches for the investigation of biomolecular interactions between amphotericin B and bovine serum albumin. *Journal of Photochemistry and Photobiology B: Biology*, *170*, 6-15.

Rout, J., Swain, B. C., Mishra, P. P., & Tripathy, U. (2020). Spectroscopic insight into the interaction of dopamine with spherical gold nanoparticles. *Journal of Photochemistry and Photobiology B: Biology*, *203*, 111770.

Semo, E., Kesselman, E., Danino, D., & Livney, Y. D. (2007). Casein micelle as a natural nano-capsular vehicle for nutraceuticals. *Food Hydrocolloids*, *21*(5-6), 936-942.

Shaghaghi, M., Dehghan, G., Rashtbari, S., Sheibani, N., & Aghamohammadi, A. (2019). Multispectral and computational probing of the interactions between sitagliptin and serum albumin. *Spectrochimica Acta Part A: Molecular and Biomolecular Spectroscopy*, *223*, 117286.

Shapira, A., Assaraf, Y. G., & Livney, Y. D. (2010). Beta-casein nanovehicles for oral delivery of

chemotherapeutic drugs. *Nanomedicine: Nanotechnology, Biology and Medicine*, *6*(1), 119-126.

Temboot, P., Usman, F., Ul-Haq, Z., Khalil, R., & Srichana, T. (2018). Biomolecular interactions of amphotericin B nanomicelles with serum albumins: A combined biophysical and molecular docking approach. *Spectrochimica Acta Part A: Molecular and Biomolecular Spectroscopy*, *205*, 442-456.

van de Weert, M., & Stella, L. (2011). Fluorescence quenching and ligand binding: A critical discussion of a popular methodology. *Journal of Molecular Structure*, *998*(1), 144-150.

Vincenzetti, S., Polidori, P., Mariani, P., Cammertoni, N., Fantuz, F., & Vita, A. (2008). Donkey's milk protein fractions characterization. *Food Chemistry*, *106*(2), 640-649.

Wang, Y., Zhu, M., Liu, F., Wu, X., Pan, D., Liu, J., Fan, S., Wang, Z., Tang, J., Na, R., Li, Q. X., Hua, R., & Liu, S. (2016). Comparative Studies of Interactions between Fluorodihydroquinazolin Derivatives and Human Serum Albumin with Fluorescence Spectroscopy. *Molecules*, *21*(10).

Wei, Z., Yang, W., Fan, R., Yuan, F., & Gao, Y. (2015). Evaluation of structural and functional properties of protein–EGCG complexes and their ability of stabilizing a model β-carotene emulsion. *Food Hydrocolloids*, *45*, 337-350.

Yuan, X., Li, X., Zhang, X., Mu, Z., Gao, Z., Jiang, L., & Jiang, Z. (2018). Effect of ultrasound on structure and functional properties of laccase-catalyzed α-lactalbumin. *Journal of Food Engineering*, *223*, 116-123.

Zeng, L., Ding, H., Hu, X., Zhang, G., & Gong, D. (2019). Galangin inhibits α-glucosidase activity and formation of non-enzymatic glycation products. *Food Chemistry*, *271*, 70-79.

Zhang, D., Zhang, X., Liu, Y.-C., Huang, S.-C., Ouyang, Y., & Hu, Y.-J. (2018). Investigations of the molecular interactions between nisoldipine and human serum albumin in vitro using multi-spectroscopy, electrochemistry and docking studies. *Journal of Molecular Liquids*, *258*, 155-162.

Zhu, M., Wang, L., Wang, Y., Zhou, J., Ding, J., Li, W., Xin, Y., Fan, S., Wang, Z., & Wang, Y. (2018). Biointeractions of Herbicide Atrazine with Human Serum Albumin: UV-Vis, Fluorescence and Circular Dichroism Approaches. *International Journal of Environmental Research and Public Health*, *15*(1).

Zimet, P., Rosenberg, D., & Livney, Y. D. (2011). Re-assembled casein micelles and casein nanoparticles as nano-vehicles for ω-3 polyunsaturated fatty acids. *Food Hydrocolloids*, *25*(5), 1270-1276.

CHAPTER 4 - Bovine and donkey beta-casein monomers and micelles as delivery vehicles for resveratrol

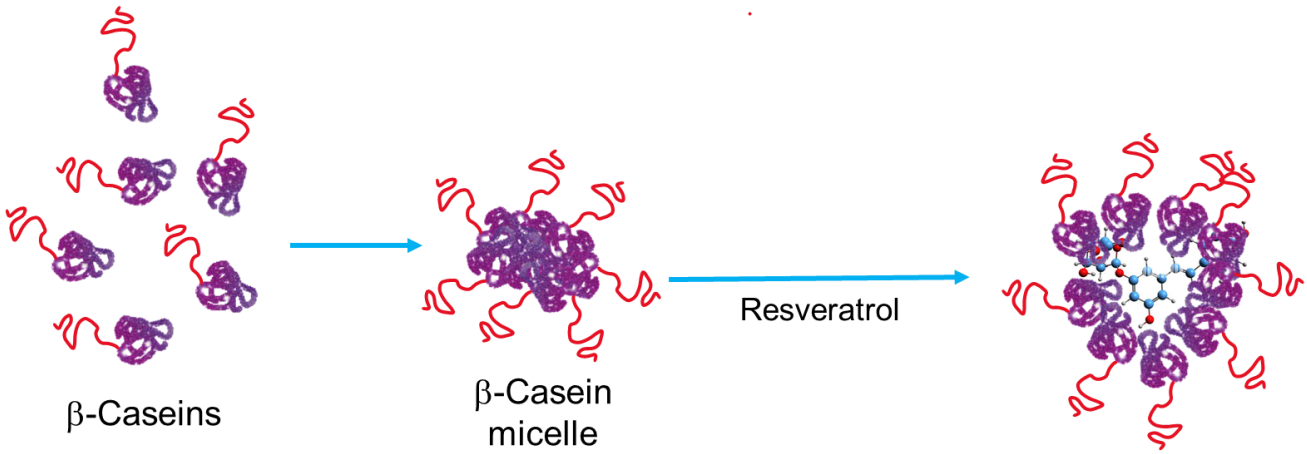

Abstract

Recently, β-casein (β-CN) micelles have emerged as natural nanocarriers for enhancing the bioavailability of hydrophobic compounds during delivery. Hypoallergenic β-CN isolated from donkey milk has demonstrated similar self-assembling behaviour compared to the bovine counterpart. Resveratrol is a natural polyphenol that has vast health benefits but faces the challenges of low and variable oral bioavailability. The aim of this study was to investigate the interaction mechanism between donkey β-CN and resveratrol, as well as to explore the potential of these protein nanoparticles for encapsulation of resveratrol. The obtained results were compared with that of bovine β-CN. Analysis of fluorescence spectroscopy showed that resveratrol quenched the intrinsic fluorescence of both β-CNs in a static quenching mode. The interaction of resveratrol with both β-CNs was a spontaneous reaction mainly driven by hydrophobic interaction, and the number of binding sites was approximately equal to 1. Moreover, fluorescence emission spectra of resveratrol,

DLS particle characterization, and HPLC encapsulation efficiency (EE) experiments have shown that resveratrol could be encapsulated into donkey and bovine β-CN micelles of a concentration higher than 40 μM. With an increase in protein concentration from 40 μM to 80 μM, the EE of resveratrol within donkey β-CNs increased from 54.81% to 82.01%, while in bovine β-CNs it increased from 45.74% to 80.23%. These findings could be useful for the development of donkey β-CN-based nano-delivery systems for the polyphenols.

Keywords: Donkey β-CN; Resveratrol; Interaction; Encapsulation; Spectroscopy

4.1. Introduction

Resveratrol (trans-resveratrol), known as trans-3,5,4'-trihydroxystilbene, is a lipophilic polyphenolic compound that is abundant in grape skins, peanuts, and red wine (Walle et al., 2004). Several studies have shown that resveratrol has potential beneficial effects on human health, including neuro- and cardio protection, anti-inflammatory, anti-carcinogenic, antioxidant, and anti-obesity effects, which has generated interest in its application as a nutraceutical ingredient within food and pharmaceutical fields (Catalgol et al., 2012; Rute et al., 2013; Svajger & Jeras, 2012). Nevertheless, the clinical application efficiency of this bioactive ingredient is facing challenges due to its poor water-solubility, low oral bioavailability, and chemical instability (Patel et al., 2011). Various strategies have been developed to enhance the solubility and bioavailability of resveratrol, including the utilization of nanoparticles (Pandita et al., 2014), emulsions (Davidov-Pardo & Mcclements, 2015) and liposomes (Zhao et al., 2019). In particular, milk protein-based delivery systems have shown great potential in incorporating polyphenols and hydrophobic compounds into functional foods, due to their specific structural and functional diversity, thereby protecting them against degradation caused by UV light or exposure to oxygen (Patel et al., 2012).

The protein β-casein (β-CN), containing five phosphoserine residues, is widely recognized as the primary component among the four caseins (α_{S1} -casein, α_{S2} -casein, β-casein, and κ-casein)

found in bovine milk (Portnaya et al., 2008). At the natural pH of about 6.6, the N-terminal region of β-CN is hydrophilic and highly negative-charged, while the C-terminal domain is predominantly hydrophobic and nearly uncharged. Due to its prominent amphiphilic structure, β-CN exhibits surfactant-like properties and has the ability to self-associate, forming stable micelles with a diameter of approximately 13 nm in aqueous solutions under varies physiological conditions, including temperature, pH, solvent composition, and ionic strength (Bachar et al., 2012; Mikheeva et al., 2003; Portnaya et al., 2006). Furthermore, the amphiphilic structure of β-CN has been proposed to be similar to that of an amphiphilic block copolymer (Horne, 2002). The block copolymer micelles were more stable than low-molecular-weight surfactant micelles due to their low critical micellization concentration (ranging from 0.05% to 0.2% wt/vol) that provides assurance against spontaneous disassembly and content leakage into the solution.

β-CN micelles, characterized by a hydrophobic core and a hydrophilic corona, have been employed as natural nanocarriers for polyphenols (e.g., resveratrol, naringenin, and curcumin), lipid-soluble vitamins (e.g., vitamin D3), and water-insoluble drugs (e.g., celecoxib) (Cheng et al., 2020; Esmaili et al., 2011; Li et al., 2019; Ranadheera et al., 2016). These bioactive compounds and drugs could be encapsulated inside the hydrophobic core of the re-assembled β-CN micelles, thus being stabilized and protected by this protein against degradation while improving their delivery efficiency.

In addition, earlier investigations have indicated that hydrophobic compounds have considerable binding affinities for hydrophobic regions in β-CN, resulting in the formation of intermolecular complexes primarily driven by hydrophobic interactions, hydrogen bonding force, and van der Waals interactions (Livney, 2010). Polyphenols, including trans-resveratrol, genistein, and curcumin, have been demonstrated to successfully bind to β-CN, forming protein-ligand complexes with binding constants of 2.3×10^4 M^{-1}, 3.0×10^4 M^{-1}, and 3.0×10^4 M^{-1}, respectively (Bourassa, 2013). Moreover, the binding of polyphenols to β-CN was also found to modify the protein's secondary conformation through decreasing α-helix structure, and in vitro, this protein was

identified as a potential carrier for polyphenol transport. The complexes with β-CN could effectively prolong the photo-isomerization of trans-resveratrol to cis-resveratrol, which showed a better protective effect on the stability of both isomers during storage compared to β-CN micelles (Cheng et al., 2020).

Basing on all the donkey β-caseins characteristics described in previous chapters, including their hypoallergenic properties, and their self-assembling behaviour similar to the bovine β-casein, in the current work, the binding mechanisms, surface hydrophobicity of donkey β-CN complexed with resveratrol has been detected through fluorescence quenching spectroscopy and fluorescence spectroscopy using the extrinsic probe ANS (8-Anilinonaphthalene-1-sulfonate). Furthermore, the encapsulation efficiency of resveratrol into β-CN micelles was evaluated by using high-performance liquid chromatography (HPLC). Moreover, the particles size of the resveratrol-containing β-CN micelles was investigated by using dynamic light scattering (DLS). All the obtained results were analyzed and then compared to that of bovine β-CN.

4.2. Materials and methods

4.2.1. Materials

β-CN from bovine milk (purity ≥ 90 %), resveratrol (trans isomer, ≥ 99 %), 1-Anilinonaphthalene-8-sulfonic acid (ANS, purity ≥ 95%), Carboxymethyl cellulose (CM52, Whatman, Merck, Darmstadt, Germany), and Methanol (HPLC grade) were purchased from Sigma-Aldrich Co. (St. Louis, MO). All other chemical reagents used in the study were of analytical purity.

4.2.2. Purification of donkey β-CN

Individual donkey milk samples were collected from lactating jennies reared on the biggest farms located in the Azienda Agricola Mamma Asina, Colmurano, Marche region, Italy. The obtained donkey milk was immediately stored at 4 °C before being used. β-CN from donkey milk

was purified following the protocol described in section 2.2. All the solutions were prepared using ultrapure water.

4.2.3. Preparation of β-CN and resveratrol mixtures

The β-CN stock solutions of bovine and donkey milk were prepared with gentle stirring at a concentration of 500 μM (12 mg/mL) in phosphate buffer (50 mM, pH 7.0), then stored overnight at 4°C to ensure full hydration. The solution of resveratrol at 2 mM was freshly prepared in 70% ethanol, and then diluted with phosphate buffer to the final concentration of 200 μM. The mixture of β-CN and resveratrol was prepared by dropwise addition of various volumes of the above resveratrol diluent into a β-CN solution of 10 μM (below the CMC values) under gentle magnetic stirring for 2 h before analysis. The concentration of the protein was kept constant at 10 μM during the experiment and the final concentrations of resveratrol were 0, 0.5, 1, 5, 10, 15, 20, 30, 40, 60, 80, 100, 120, and 160 μM, respectively. All the above solutions were prepared in dark and were immediately used. The final content of ethanol was < 1% v/v.

4.2.4. UV-Vis absorption spectroscopy experiments

UV absorbance spectra of both bovine and donkey β-CN in the absence or presence of resveratrol were recorded at wavelengths between 200 and 600 nm with a UV-2450 spectrophotometer (Shimadzu) at the temperature of 298 K. The β-CN concentration was constant at 10 μM, while the concentrations of resveratrol were increased from 0 to 60 μM.

4.2.5. Fluorescence emission spectroscopy measurements of β-CN

At the temperature of 298 K, 305 K, and 312 K, fluorescence measurements of both bovine and donkey β-CN were performed with a Perkin-Elmer fluorescence spectrophotometer (LS-55) equipped with a 1 cm path length cuvette. The intrinsic fluorescence spectra of β-CN at 10 μM in the absence or presence of different concentrations of resveratrol (from 0.5 μM to 160 μM) were

scanned from 200 nm to 600 nm at an exaction wavelength of 295 nm. The excitation and emission slit widths were both set 2.5 nm. Since resveratrol has absorption in the detection range, the raw fluorescence intensity was corrected by the following equation: $F = F_{det} \times 10^{(\mathrm{Aex+Aem})/2}$. Here F and F_{det} denote the corrected and detected fluorescence intensities, respectively, whereas Aex and Aem represented the absorption of resveratrol in the excitation and emission wavelengths, respectively (Qi et al., 2021).

In order to investigate the effect of the presence of resveratrol on the conformational change in bovine and donkey β-CN proteins, the synchronous fluorescence spectrometry method was used. This method can simultaneously scan the excitation and emission wavelengths，and keep a fixed wavelength difference Δλ (Δλ = λ emission - λ excitation) between them. In present study, synchronous fluorescence spectra of β-CN were collected in wavelength between 270–300 nm for Δλ = 15nm (for tyrosine) and between 250-300 nm for Δλ = 60nm (for tryptophan).

Fluorescence emission spectra of resveratrol in the absence or presence of β-CN were measured from 330 to 600 nm with an excitation of 320 nm at the temperature of 305 K.

4.2.6. Determination of surface hydrophobicity

ANS was used as a fluorescence probe to determine the surface hydrophobicity of β-CN with a fluorescence spectrophotometer according to the method of Uruakpa (Uruakpa & Arntfield, 2006). ANS stock solution was prepared at the concentration of 8 mM in phosphate buffer (50 mM, pH 7.0) in the dark.

The samples were obtained by adding different volumes of resveratrol stock solution to achieve the final concentrations of resveratrol of 0, 5, 10, 15, 20, 30, and 40 μM, while the concentration of β-CN ranged from 5 to 40 μM. Ten microliters of ANS stock solution was added to 1 mL β-CN-resveratrol mixture, which was gently shaken for 1 min and then incubated in dark for 15 min before being assessed. The emission fluorescence spectra were collected from 400 to 600 nm at the

excitation wavelength of 390 nm and the bandwidths for excitation and emission were set at 5 and 2.5 nm, respectively. The measurements were performed in triplicate at the temperature of 298 K. The initial slope (S_0) of the fluorescence intensity (F) versus β-CN concentration (C) was used as an index of the protein surface hydrophobicity: $S_0 = \frac{F}{c}$ (1)

4.2.7. Preparation of resveratrol loaded β-CN micelles.

β-CN solutions from bovine and donkey milk at various concentrations (40, 80, 160, 200, 300, and 400 μM) were obtained by diluting 500 μM protein stock solution with phosphate buffer (50 mM, pH 7.0). A final resveratrol concentration of 20 μM was achieved by adding 50 μL of 200 μM resveratrol stock solution to a series β-CN solution. Then the mixture was incubated for 2 h with slightly shaking at the temperature of 305 K (above CMT) to form the micelles. After centrifugation at 3000 g for 20 min at about 305 K, no precipitation was shown in the samples suggesting a total dissolution of resveratrol. Experiments were performed in dark and the volume percentage of ethanol in the mixture was < 1% v/v.

4.2.8. Encapsulation efficiency (EE %) determination by HPLC

The isoelectric precipitation method described in previous study of Zimet was used to determine the encapsulation efficiency of resveratrol (Zimet et al., 2011). In order to precipitate protein, 10 % acetic acid (v/v) was added to the mixture to adjust the pH to 4.6. Then the solutions were centrifuged at 3000 g for 20 min. The protein precipitate was re-suspended in 50 mM phosphate buffer (pH 7.0). The re-suspended protein and the supernatant containing free resveratrol were retained for further analysis.

Twenty microliters of the obtained supernatants were directly injected into an HPLC instrument (Agilent 1100 series) equipped with a Mediterranea SEA C18 column (5 μm, 2.1 × 250 mm; Sigma Aldrich, St. Louis, MO) using a UV detector at 306 nm. The column was equilibrated in Buffer A

solution (99.9 % H_2O + 0.5 % Acetic acid) and elution was achieved by the following gradient steps with Buffer B solution (99.9 % Methanol + 0.5 % Acetic acid): % B = 0-100, time = from 0 to 25 min; % B = 100, time = from 25 to 27 min; % B = 0-100, time = from 27 to 30 min; 5 min of post-run. The flow rate was 1 mL/min. Resveratrol in concentrations of 5 to 60 μM was used to make a calibration curve. The amounts of resveratrol in supernatant were detected by using the peak areas according to the calibration curve. The EE % was calculated by the following equation:

$$EE\% = \frac{\text{Total amount of added } resveratrol - Amount\ of\ resveratrol\ in\ supernatant}{\text{Total amount of added } resveratrol} \times 100 \quad (2)$$

4.2.9. Dynamic light scattering analysis (DLS)

Particle size of both donkey and bovine β-CN in the absence and presence of resveratrol was measured by using Dynamic Light Scattering (DLS) instrument (Malvern Instrument Worcestershire, UK). The β-CN concentration in β-CN-resveratrol complex solution that prepared using the method described in Section 4.2.3 was increased from 2 μM to 20 μM (lower than the CMC). The β-CN micelles containing resveratrol were used the same as that prepared by Section 4.2.7 with β-CN concentration increasing from 40 μM to 400 μM. In addition, the re-suspended precipitate obtained in Section 2.8 was detected. The resveratrol concentration in all systems was 20 μM. The experiment was conducted at the temperature of 298 K with a scattering angle of 173°.

4.3. Results and discussion

4.3.1. Fluorescence quenching of β-CN by resveratrol.

The sensitivity of the photophysical properties of the fluorophores to the polarity of their surrounding environment makes fluorescence an effective method for exploring intermolecular interactions. Therefore, the utilization of protein intrinsic fluorescence has been prevalent in studying the structure and dynamics of proteins in aqueous environments (Jiang et al, 2008). The intrinsic fluorescence spectra of both donkey and bovine β-CN-resveratrol complexes are shown in

Fig. 1. In phosphate buffer at pH 7.0, the maximum fluorescence emission wavelength of donkey and bovine

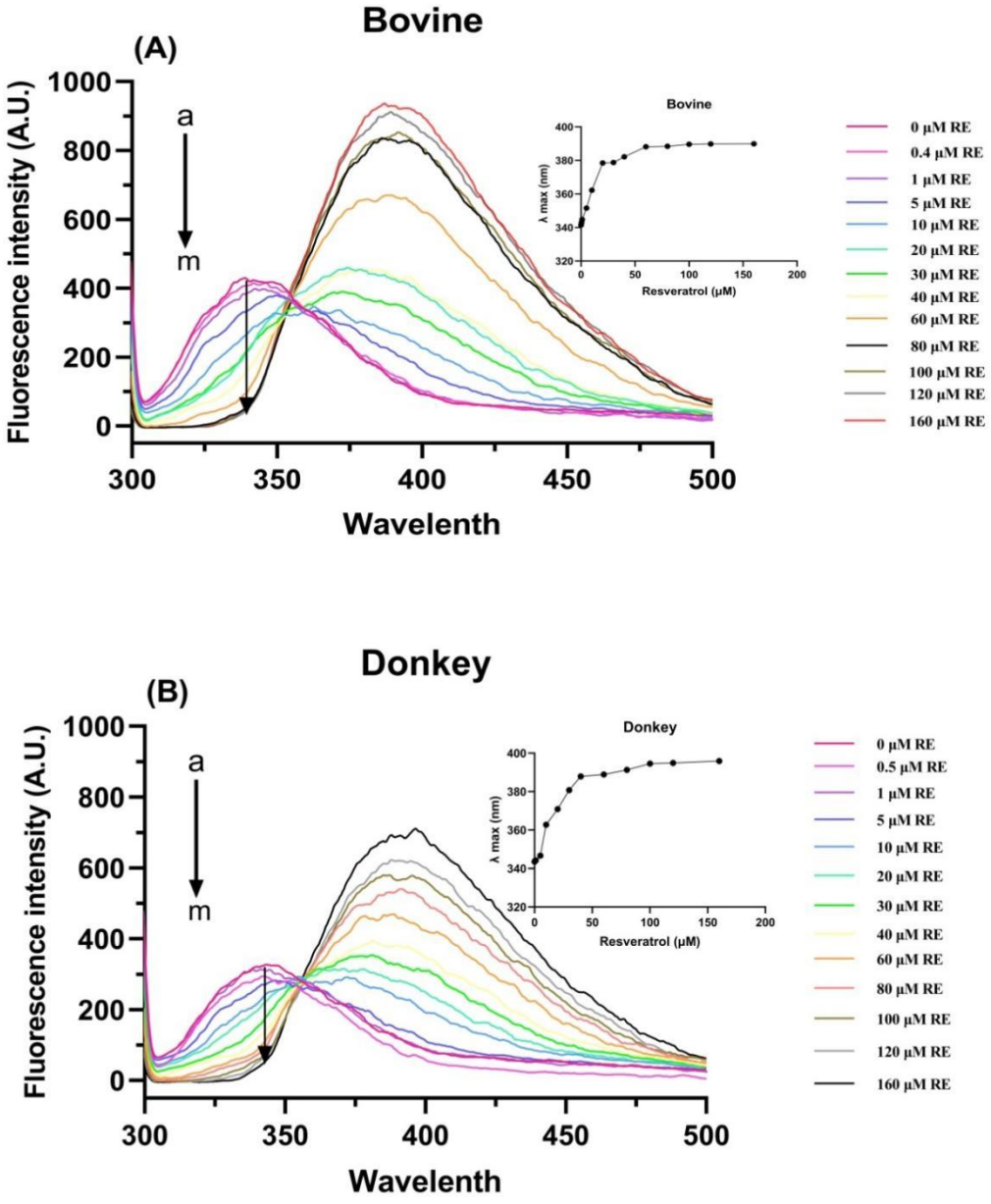

Fig. 1. The effect of resveratrol on fluorescence spectra of bovine and donkey β-CN (T = 298 K, pH = 7.0, λ ex = 295 nm). Letters of a-m represent the concentrations of resveratrol varied from 0, 0.5, 1, 5, 10, 20, 30, 40, 60, 80, 100, 120, and 160, respectively. The concentration of β-CN was 10 μM. Inset: The λ max of β-CN in the absence or presence of resveratrol at various concentrations.

β-CN was detected at approximately 341 and 338 nm, respectively. A fluorescence quenching of both proteins was observed upon the addition of resveratrol, and the fluorescence intensity of β-CNs decreased significantly with the increase of resveratrol concentration. These findings suggested that an interaction appeared between β-CNs and resveratrol (Chen et al, 2021). Additionally, the fluorescence spectrum of donkey β-CN exhibited a λ_{max} of approximately 340 nm. As the concentration of resveratrol increasing to 60 μM, the fluorescence spectrum gradually shifted to longer wavelengths of approximately 385 nm (Inset in Fig. 1A), corresponding to the spectrum of resveratrol alone (~383 nm) in 75% ethanol reported in the literature (Li et al, 2008). This occurred red-shift of the protein λ_{max} indicated the exposure of the fluorophores to a more polar environment due to the interaction between β-CNs and resveratrol. At resveratrol concentrations higher than 60 μM, the maximum fluorescence emission peak remained stable at 385 nm, and the fluorescence intensity was increased owing to the contribution from the resveratrol fluorophore (Liang et al., 2008). As expected, bovine β-CN exhibited the same behavior as donkey β-CN. These findings regarding the interaction between resveratrol and β-CNs are consistent with a previous study, which reported resveratrol induced a gradual decrease in the fluorescence intensity of bovine β-CN accompanied by a red shift at λ_{max} as the concentration of resveratrol increasing to 20 μM (Cheng et al. 2020). Furthermore, the results obtained in the present study agree with previous findings obtained by Cheng and co-workers (2018b) on the effect of different resveratrol concentration (from 0 to 30 μM) on globular proteins such as bovine serum albumin, β-lactoglobulin or α-lactalbumin.

In order to explore the quenching mechanism between resveratrol and β-CN, a comprehensive fluorescence experiment was performed at various temperatures (297, 304, and 311 K). The quenching constant was determined by the equation of Stern-Volmer (Jiang et al. 2004):

$$F_0 / F=1+Kq\tau_0 [Q]=1+K_{sv}[Q] \quad (3)$$

Here F_0 and F represent the fluorescence intensities in the absence and presence of quencher, respectively; [Q], Kq, and τ_0 are the concentration of the quencher, the bimolecular reaction rate constant and lifetime of the biomolecule without a quencher ($\tau_0 = 3.3\times10^{-8}$ s), respectively; K_{SV}

represents the Stern-Volmer quenching constant that is calculated by linear regression of a plot of F_0 /F against [Q].

The Stern-Volmer plots for the quenching of bovine and donkey β-CNs by resveratrol at pH 7.0 were displayed in Fig. 3 A1 and A2, respectively, and the calculated parameters were shown in Table 1. The plots of F_0/F vs [Q] were liner for both β-CN-resveratrol complexes and decreased as increasing temperature from 297 to 311 K. As the temperature increased, the quenching constants of resveratrol for both β-CNs decreased and exceeded the limiting diffusion rate constants (Kq = 2 × 10^{10} L/mol/s). According to these results, the quenching mechanism of both β-CNs by resveratrol was predominant static quenching (Zhang, Que, Pan, & Guo, 2008).

4.3.2. Binding constant and number of binding sites

Based on static quenching, the binding constants (Ka) and numbers of binding sites (n) between both β-CNs and resveratrol can be determined via the following formula:

$$\text{Log } [(F0-F)/F]=\log Ka + n\log[Q] \quad (4)$$

It can be seen that the Ka values for donkey and bovine β-CN-resveratrol complexes increased as a function of temperature (Table 1), showing that the interaction between these proteins and resveratrol was endothermic. The binding of resveratrol to β-CN proteins was facilitated by an

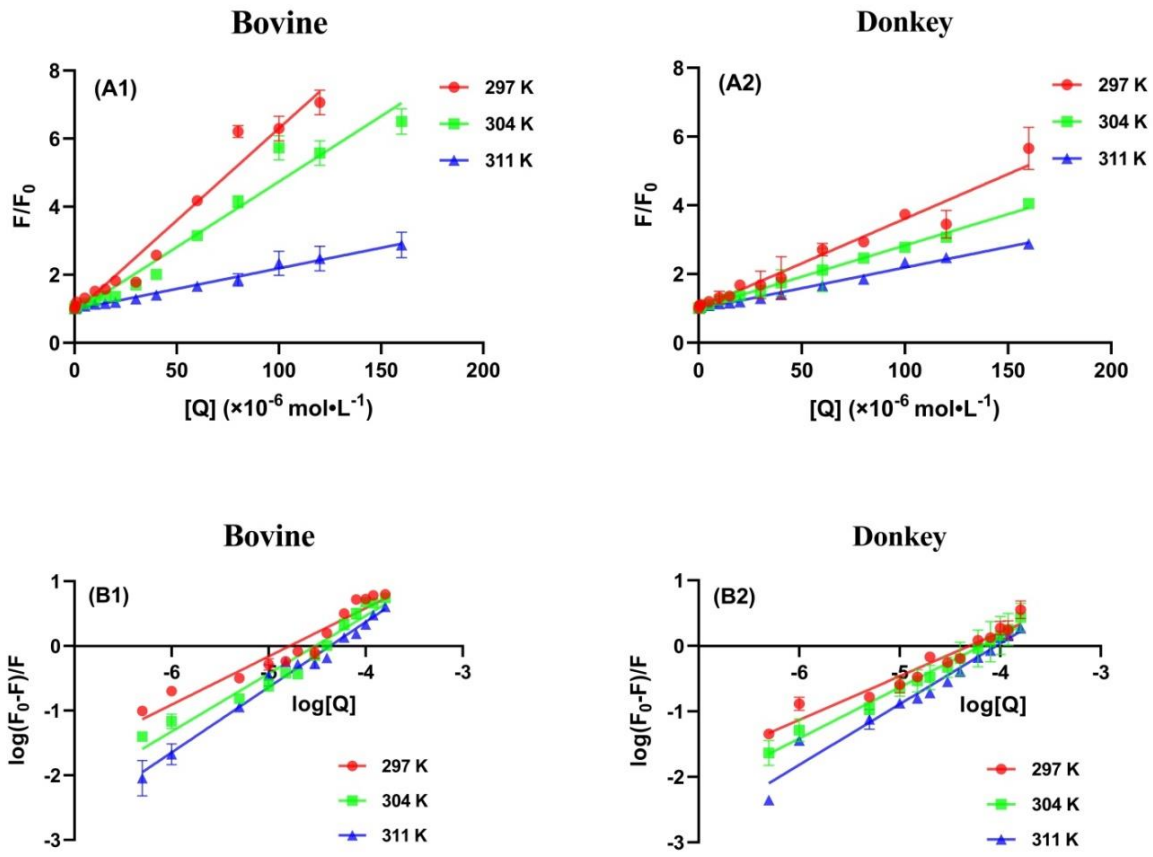

Fig. 3. Stern-Volmer plots of bovine and donkey β-CN binding to resveratrol at 297 K, 304 K, and 310 K (A1-2); The plot of log (F_0-F)/F as a function of log [resveratrol] for calculation of number of bound resveratrol molecules (n) in resveratrol-β-CN complexes at 298, 304, and 310 K (B1-2).

increase in temperature (Jiang et al. 2020). Generally, Ka values of bovine β-CN-resveratrol complexes were larger than that of donkey β-CN-resveratrol complexes. Furthermore, the numbers of binding sites (n) were almost equal to 1.0, indicating that there was only one resveratrol molecule bound to per donkey or bovine β-CN molecule. Bourassa et al. (2013) reported that resveratrol bund to bovine β-CN via hydrophobic interactions with the number of binding sites were approximately equal to 1.0, which was similar to that in present study (Bourassa et al. 2013).

Table 1. The quenching constants, binding constants, and thermodynamic parameters for the interaction of bovine and donkey β-CNs with resveratrol at different temperatures.

	Temperature (K)	$K_{sv}\times10^4$ (L mol^{-1})	$K_q\times10^{12}$ (L mol^{-1} s^{-1})	R^2	$K_a\times10^4$ (L mol^{-1})	n	R^2
Bovine	297	5.25±0.01	5.25±0.01	0.965	0.44±0.00	0.75±0.01	0.919
	304	3.69±0.05	3.69±0.05	0.964	0.57±0.01	0.83±0.01	0.911
	311	2.45±0.10	2.45±0.10	0.956	3.01±0.15	1.01±0.45	0.968
	297	2.60±0.17	2.60±0.17	0.940	0.16±0.09	0.73±0.02	0.951
Donkey	304	1.80±0.90	1.80±0.90	0.976	0.29±0.22	0.78±0.05	0.981
	311	1.19±0.10	1.19±0.10	0.984	0.59±0.10	0.93±0.01	0.957

4.3.3. Thermodynamics

To elucidate the interaction forces between β-CNs and resveratrol, mainly including hydrophobic forces, van der Waals forces, electrostatic interactions, hydrogen bonds, and steric resistance repulsive force, the thermodynamic parameters were determined and analyzed using the binding constants acquired through fluorescence quenching (Moeiniafshari et al. 2015). The investigation of the thermodynamic parameters of the systems provides insights into the nature of the interaction. By examining the temperature dependence of the binding constant, valuable information regarding the magnitude and sign of the enthalpy change (ΔH), entropy change (ΔS), and change in Gibbs free energy (ΔG) of the systems can be obtained upon the introduction of resveratrol. Therefore, the Van't Hoff Equations can typically be utilized to calculate ΔH, ΔS, and ΔG,

$$\ln Ka=-\frac{\Delta H}{RT}+\frac{\Delta S}{R} \quad (5)$$

$$\Delta G=\Delta H-T\Delta S \quad (6)$$

where T and R represent the absolute temperature and gas constant (8.314 J mol^{-1} K^{-1}),

respectively. The obtained values for donkey and bovine β-CN-resveratrol complexes are documented in Table 2. The negative Δ*G* values confirmed that the interaction between both donkey and bovine β-CNs and resveratrol was spontaneous. Furthermore, the hydrophobic interactions apparently play main roles in formation of both β-CN-resveratrol complexes, as evidenced by the positive Δ*H* and Δ*S* values. Moeiniafshari et al. (2015) emphasized that the binding of bovine β-CN

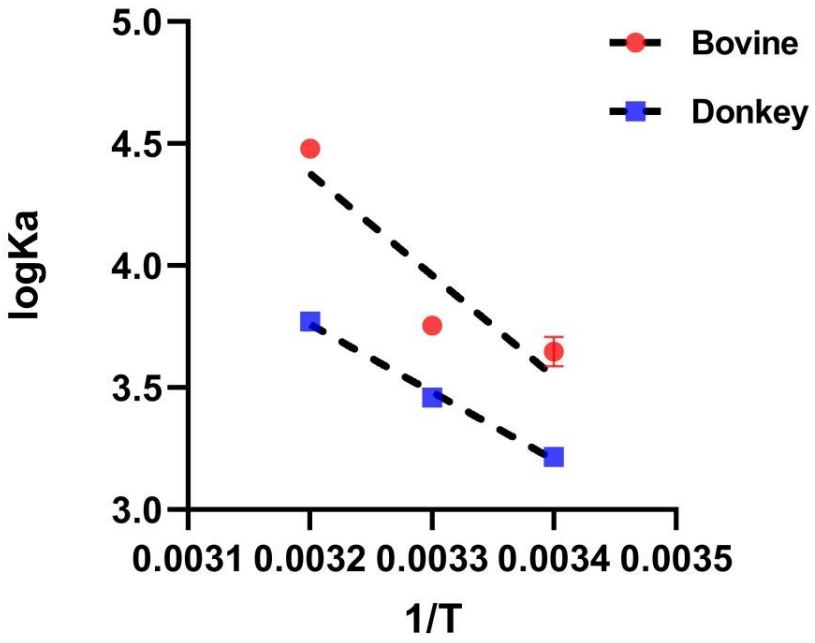

Fig. 4. Van't Hoff plot of donkey and bovine β-CN binding to resveratrol.

to naringenin occurred spontaneously (Δ*G* < 0), and the hydrogen bonds, hydrophobic interactions, and van der Waals forces played a key role for the complex formation based on positive Δ*S* > 0 and Δ*H* < 0 (Moeiniafshari et al. 2015).

Table 2. Thermodynamic parameters of donkey and bovine β-CN- resveratrol systems.

	Temperature (K)	△H ×10^4 (kJ mol^{-1})	△S×10^4 (J mol^{-1})	△G×10^4 (kJ mol^{-1})	R^2

Bovine	297	10.44	0.42	-2.02±0.61	0.934
	304			-2.31±0.62	
	311			-2.60±1.17	
Donkey	297	7.00	0.30	-1.82±0.83	0.993
	304			-2.03±0.23	
	311			-2.24±0.11	

4.3.4. Synchronous fluorescence analysis

Synchronous fluorescence spectroscopy is considered an effective technique for characterizing the changes in the microenvironment surrounding tyrosine (Tyr) and tryptophan (Trp) residues,

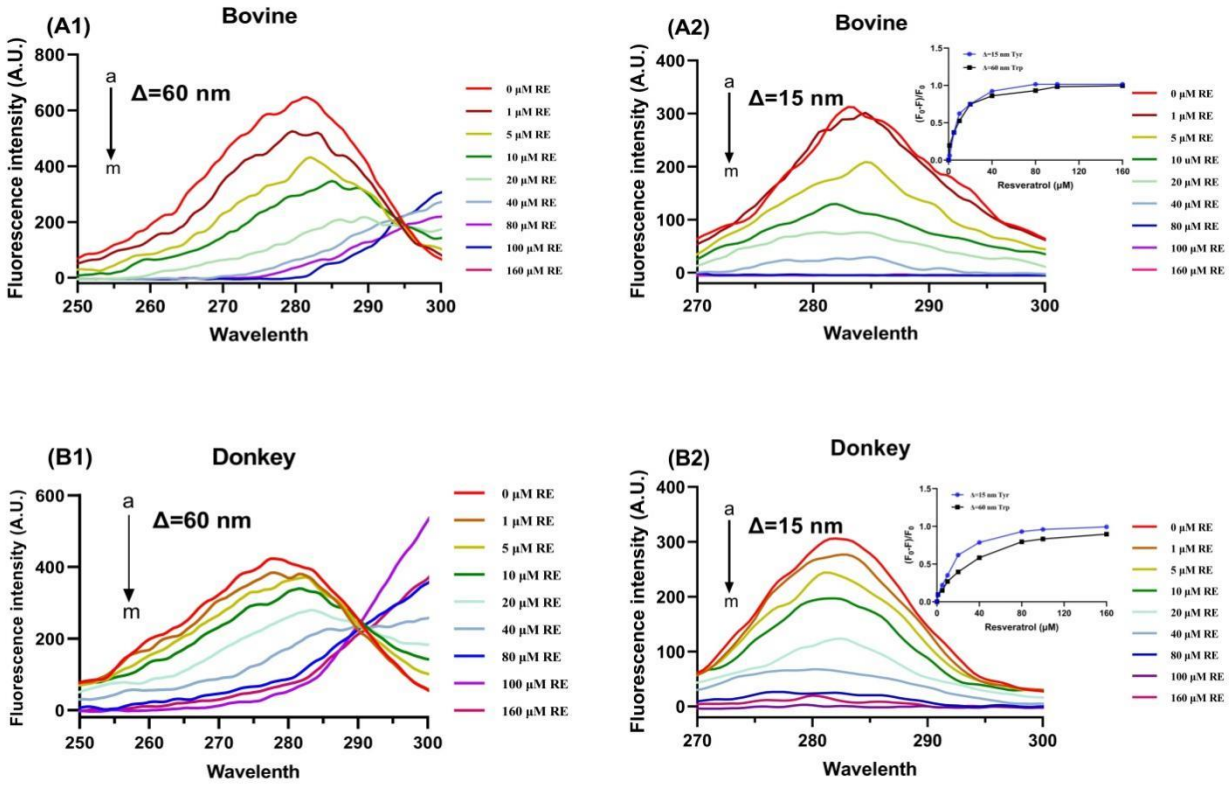

Fig. 5. Synchronous fluorescence spectra of bovine and donkey β-CN with varying concentration of resveratrol (A1-B1: Δλ = 60 nm, A2-B2: Δλ = 15 nm). Letters of a-m represent the concentrations of resveratrol varied from 0, 0.5, 1, 5, 10, 20, 30, 40, 80, 100, 120, and 160, respectively. The concentration of β-CN was 10 μM. Inserted (A2-B2): the quenching ability of β-CN synchronous fluorescence by resveratrol.

which is achieved by fixing the wavelength interval ($\Delta\lambda = \lambda_{em} - \lambda_{ex}$) at 15 nm and 60 nm, respectively (Wang et al. 2022). Therefore, this technique was used in present study to assess the impact of resveratrol with different concentrations on the conformation of donkey and bovine β-CNs.

Fig. 5 illustrates the synchronous fluorescence spectra obtained from both β-CN proteins with various concentrations of resveratrol. It could be found that the synchronous fluorescence spectra exhibited similar changes in both β-CN-resveratrol complexes. With increasing concentrations of resveratrol, the synchronous fluorescence intensity of donkey and bovine β-CNs decreased progressively accompanied with a red shift at Δλ = 15 and 60 nm, providing a plausible evidence that both Tyr and Trp residues could play a role in the quenching of the intrinsic fluorescence and that the polarity of the microenvironment around Tyr or Trp residues of these proteins was altered (Wang et al. 2022). Furthermore, β-CN displayed a stronger fluorescence quenching ability for Tyr compared to Trp residues as observed from inserted Fig. 5 A2 and B2. These results agree with a previous work carried out by Cao et al. (2019) where it was found that the fluorescence intensity was decreased gradually with the addition of different concentrations of eriocitrin. Additionally, these authors observed a slight decrease in polarity around Trp residues, while the polarity around Tyr residues remained unchanged, showing the microenvironment of β-CN was altered by the interaction with eriocitrin (Cao et al. 2019).

4.3.5. Surface hydrophobicity

Surface hydrophobicity plays a crucial role as a primary indicator for predicting and evaluating

alterations in the protein tertiary structure, as it is the key driving force for protein folding and significantly influences both protein structure and function (Yuan et al. 2018). The surface hydrophobicity (S_0) of donkey and bovine β-CN in the absence and presence of resveratrol was calculated by Eq. (1) and presented in Fig. 6. Generally, the surface hydrophobicity of both β-CN-resveratrol complexes was higher than that of β-CN proteins and increased with increasing resveratrol concentration from 0 to 20 μM, which can be explained by exposing more hydrophobic regions hidden inside the protein to the solution and the polarity of β-CN was reduced after introducing resveratrol. Furthermore, as the resveratrol concentration increased from 20 to 40 μM, the surface hydrophobicity of the complexes decreased slightly but still more than that of β-CNs alone. The decrease in surface hydrophobicity could be attributed to certain hydrophobic regions converged inside the proteins, suggesting an increase in the polarity of β-CN and a change in the polarity of the surrounding solution with the addition of resveratrol into β-CNs' solution (Li et al. 2018). Moreover, the binding of resveratrol molecules to non-polar regions on the surface of β-CN

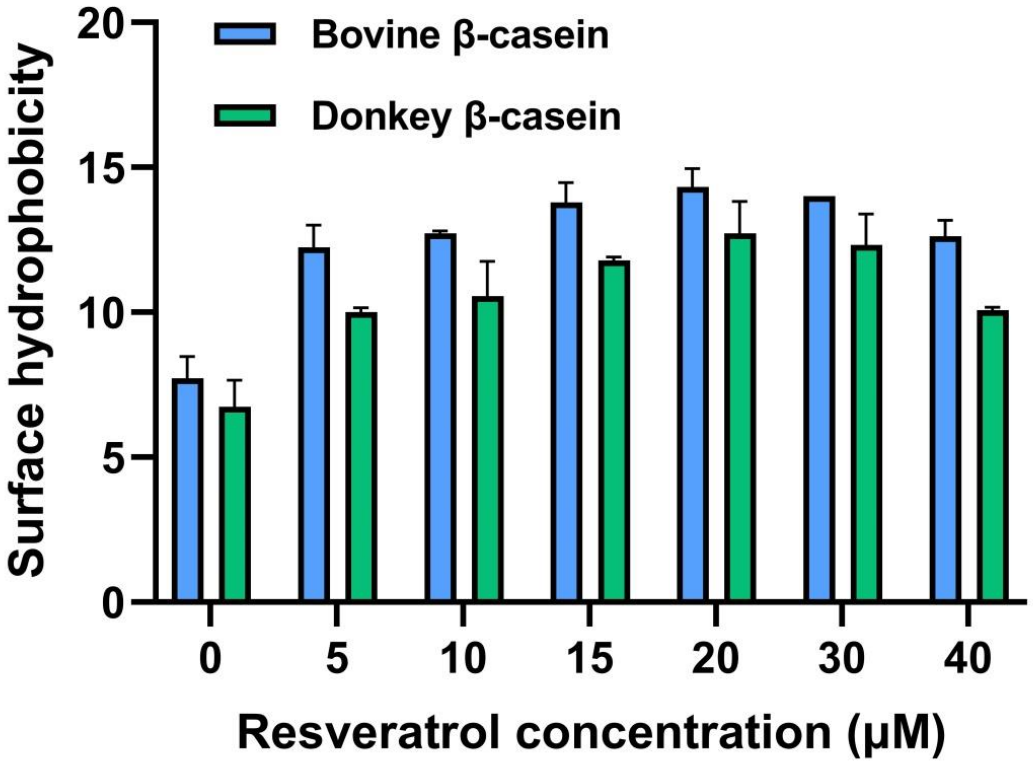

Fig. 6. Effect of resveratrol on surface hydrophobicity of bovine and donkey β-CNs.

may also reduce the overall surface hydrophobicity of the protein (Li et al. 2020). In particular, Li et al. (2020) demonstrated that the surface hydrophobicity decreased significantly ($p<0.05$) after adding phenolic acids including three benzoic acid derivatives and three cinnamic acid derivatives. However, researchers reported in previous studies that the surface hydrophobicity of β-lactoglobulin was enhanced by the addition of ferulic acid (Jia et al. 2017). The surface hydrophobicity of protein generally depends on its amino acid composition and sequence, size and shape, as well as the presence of intermolecular or intramolecular cross-links (Jiang et al. 2015).

4.3.6. Encapsulation of resveratrol within β-CN micelles

4.3.6.1. Microenvironment of resveratrol

Fig. 7 displays fluorescence emission spectra of resveratrol in the absence and presence of donkey and bovine β-CNs. Resveratrol had a maximum wavelength at 411 nm in phosphate buffer at pH 7.0, and the binding to both β-CNs at concentrations of 2 μM and 5 μM did not significantly alter its fluorescence intensity and λ_{max}. This result revealed that the formation of protein-resveratrol complexes could not change the mi-croenvironment of this polyphenol and the binding sites of resveratrol to β-CN were hydrophilic. As the β-CN concentration increased from 20 μM to 200 μM, the resveratrol fluorescence intensity significantly enhanced accompanied by a an obvious blue shift (Inset in Fig. 7), which implied that resveratrol is transferred from the hydrophilic environment of the aqueous solution to a more hydrophobic environment (Cheng et. al, 2020).

However, when the β-CN concentration increase from 200 μM to 400 μM the fluorescence intensity in the case of donkey β-CN is slightly more pronounced compared to that of bovine β-CN. It has been repored that the critical micelle concentrations (CMC) of donkey and bovine β-CN in 50 mM HEPES buffer at pH 7.3 were 0.44 mg/mL and 0.57 mg/mL, respectively (Perinelli et al. 2019), suggesting that donkey β-CN appears to be more prone to forming micelles.

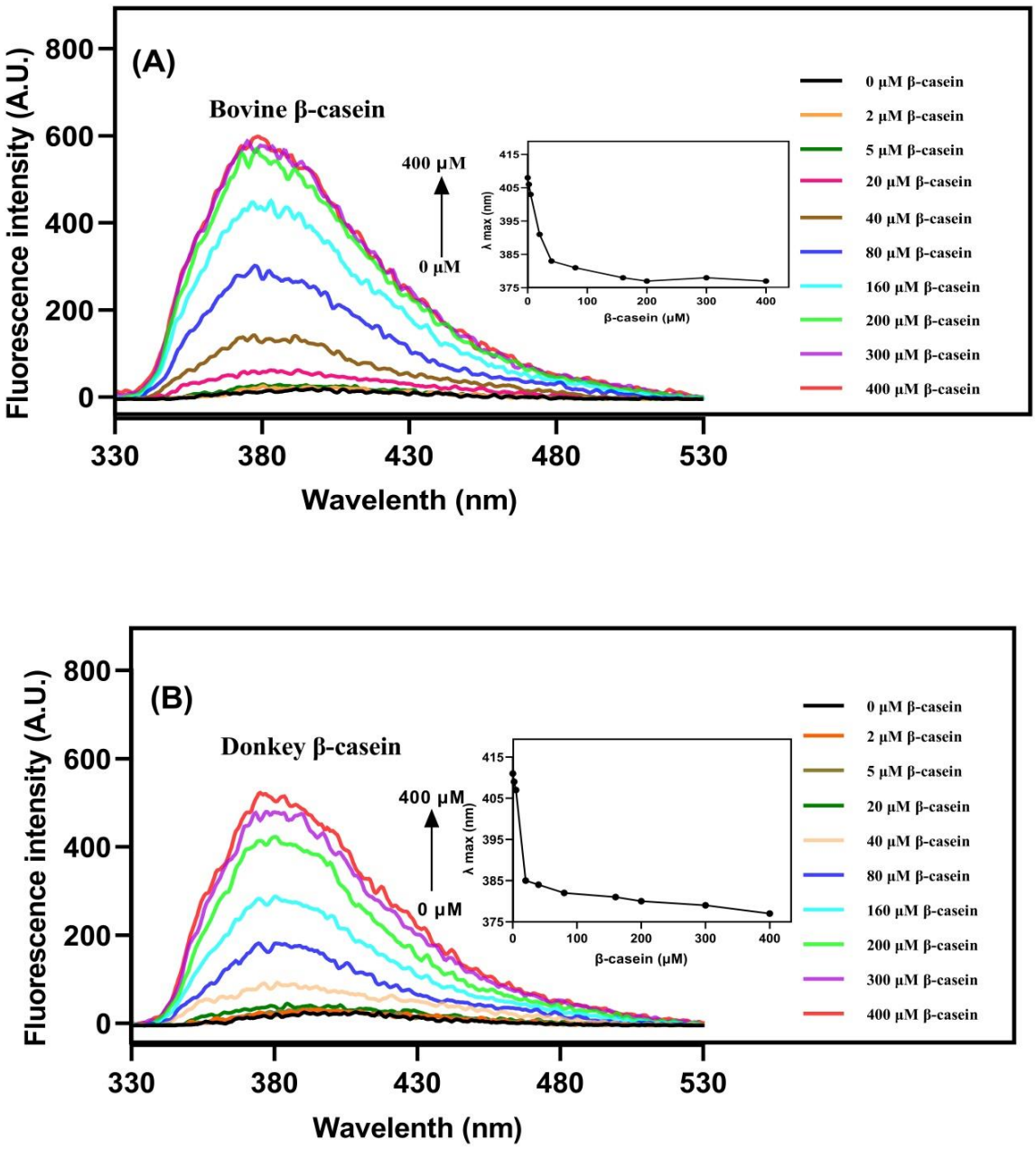

Fig. 7. Fluorescence emission spectra of resveratrol, free and bound to bovine and donkey β-CN at various concentrations (from 0 to 400 μM) in phosphate buffer at pH 7.0. The concentration of resveratrol was 20 μM. Inset: The fluorescence intensity normalized by pure resveratrol and λ_{max} of resveratrol in the absence or presence of β-CN at various concentrations.

When β-CN micelles are formed, fluorescence intensities of resveratrol in the presence of 40 μM donkey and bovine β-CN were about 1.9 and 3.2 times that of resveratrol alone, respectively,

and the values reached about 24.7 and 30.8 times as the protein concentration was 400 μM. The enhanced fluorescence intensity of resveratrol might due to the fact that the entrapment of resveratrol within β-CN micelles could restrict the mobility of the polyphenol to reduce somewhat the nonradiative decay of energy. Thereby, we can suppose that resveratrol could be entrapped into both donkey and bovine β-CN micelles, when the β-CN concentration is higher than 40 μM, which is consistant with a previous study found in the literature (Cheng et al. 2020).

4.3.6.2. Particle size

Fig. 8 shows the average hydrodynamic diameter values of resveratrol loaded β-CNs from donkey and bovine, control samples of pure β-CNs solution, and resuspended precipitate (Section 2.9). At low protein concentrations from 5 μM to 20 μM, both β-CNs were monomeric, with a particle size of around 10 nm. When protein concentrations were in the range of 40 μM to 400 μM, the hydrodynamic diameter of a pure donkey and bovine β-CN solutions was found to be approximately 16-25 nm and 25-30 nm, respectively, indicating the formation of protein micelles (Portnaya et. al, 2006). An interesting observation was that, the particle size of resveratrol loaded

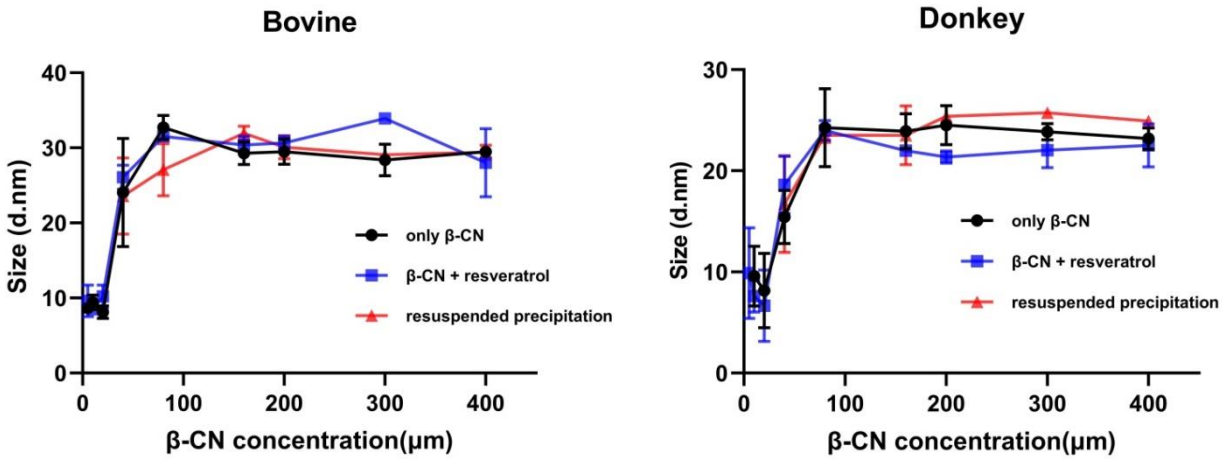

Fig. 8. Hydrodynamic diameters of donkey and bovine β-CN at various concentrations (from 5 μM to 400 μM) in

the absence and presence of resveratrol, as well as the hydrodynamic diameters of the resuspended precipitate (concentration of protein was from 40 μM to 400 μM).

protein micelles was similar to that of pure proteins, indicating that the presence of resveratrol did not affect the particle size of these proteins. Moreover, particle sizes of resuspended precipitate with protein concentration from 40 μM to 400 μM were detected to be in good agreement with those of total resveratrol loaded both β-CNs and pure proteins. Hence, these results revealed that the addition of resveratrol had no significant effect on the size of donkey and bovine β-CN monomers and micelles, as well as resveratrol could be entrapped within these protein micelles. The finding is consistent with the study of Cheng et al. (2020), which demonstrated both trans- and cis- resveratrol could be encapsulated into β-CN micelles.

4.3.6.3. Encapsulation Efficiency

The encapsulation efficiency (EE) of 20 μM resveratrol within donkey and bovine β-CN micelles has been detrmined at various β-CN concentrations by RP-HPLC as described in the section 4.2.8 and is presented in Fig. 8.

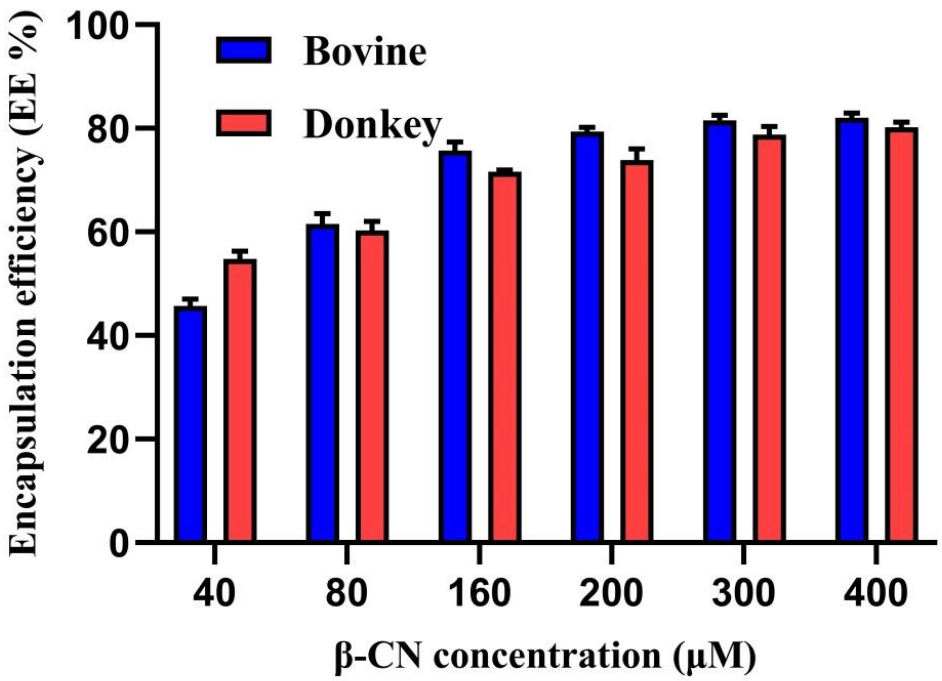

Fig. 9. Encapsulation efficiency of resveratrol in the presence of various concentrations (from 40 to 400 μM) of donkey and bovine β-CNs.

When protein concentrations increased from 40 μM to 80 μM, the EE of resveratrol in donkey and bovine β-CNs increased from 54.81 % to 82.01 % and from 45.74 % to 80.23 %, respectively. Similaly, Cheng et al. (2020) demonstrated that an increase in β-CN concentrations lead to a corresponding increase in EE (Cheng et al. 2020). In addition, in the presence of β-CN at the concentrations of 40 μM, 80 μM, and 200 μM, the EE values of resveratrol were approximately 38 %, 49 %, and 69 %, respectively, which were slightly higher than those observed in both donkey and bovine β-CN proteins at same concentrations in present study.

4.4. Conclusions

In this work it was shown that donkey β-CN can bind resveratrol to form the protein-polyphenol mono complex or β-CN-resveratrol diligand complex, exhibiting similar properties compared to bovine β-CN. Resveratrol spontaneously binds both β-CNs with with a ratio 1:1

(resveratrol: β-CN), and hydrophobic force appears to be the primary driving force in the formation of β-CN-resveratrol complexes. The polarity of microenvironment of both β-CNs was altered in the presence of resveratrol, as evidenced by synchronous fluorescence spectra and surface hydrophobicity.

Furthermore, fluorescence emission spectra of resveratrol suggested that resveratrol could be entrapped into both β-CN micelles at the protein concentrations higher than 40 μM, and transferred to a more hydrophobic environment. Particle size experiments have shown the formation of β-CN micelles upon addition of resveratrol by supporting that resveratrol could be encapsulated. Additionally, the encapsulation efficiency of resveratrol was enhanced with the increase in both β-CN concentrations.

In conclusion, the binding and encapsulation of resveratrol exhibit similar behavior in both donkey and bovine β-CN proteins. These results may help in the design of donkey β-CN-based delivery systems for resveratrol, and in particular provide new insights that β-CN isolated from donkey milk with hypoallergenicity might act as a new transporter of polyphenol bioactive substances. Further studies are required to quantify release kinetics of resveratrol, and stability of the formed nanoparticles during their processing and storage.

References

Bachar, M., Mandelbaum, A., Portnaya, I., Perlstein, H., Evenchen, S., Barenholz, Y., & Danino, D. (2012). Development and characterization of a novel drug nanocarrier for oral delivery, based on self-assembled (beta)-casein micelles.

Bourassa. (2013). Binding Sites of Resveratrol, Genistein, and Curcumin with Milk α- and β-Caseins. *The Journal of Physical Chemistry B*, *117*(5), 1287-1295.

Catalgol, B., Batirel, S., Taga, Y., & Ozer, N. K. (2012). Resveratrol: French Paradox Revisited. *Frontiers in Pharmacology*, *3*(article 141), 141.

Cao, X., He, Y., Kong, Y., Mei, X., Huo, Y., He, Y., & Liu, J. (2019). Elucidating the interaction mechanism of eriocitrin with β-casein by multi-spectroscopic and molecular simulation methods. Food Hydrocolloids, 94, 63–70.

Cheng, H., Dong, H., Wusigale, & Liang, L. (2020). A comparison of β-casein complexes and micelles as vehicles for trans-/cis-resveratrol. *Food Chemistry*, *330*, 127209.

Cheng, H., Fang, Z., Wusigale, Bakry, A. M., Chen, Y. T., & Liang, L. (2018b). Complexation of trans- and cis-resveratrol with bovine serum albumin, beta-lacto-globulin or alpha-lactalbumin. *Food Hydrocolloids, 81*, 242-252.

Chen, W. , Yu, H. , Shi, R. , Ma, C. , & Hou, J. . (2021). Comparison of carrying mechanism between three fat-soluble vitamins and alpha-lactalbumin: effects on structure and physicochemical properties of alpha-lactalbumin. *Food Hydrocolloids, 116*(7), 106662.

Davidov-Pardo, G., & Mcclements, D. J. (2015). Nutraceutical delivery systems: Resveratrol encapsulation in grape seed oil nanoemulsions formed by spontaneous emulsification. *Food Chemistry*, *167*(jan.15), 205-212.

Esmaili, M., Ghaffari, S. M., Moosavi-Movahedi, Z., Atri, M. S., Sharifizadeh, A., Farhadi, M., . . . Moosavi-Movahedi, A. A. (2011). Beta casein-micelle as a nano vehicle for solubility enhancement of curcumin; food industry application. *LWT - Food Science and Technology*,

44(10), 2166-2172.

Horne, D. S. (2002). Casein structure, self-assembly and gelation. *Current Opinion in Colloid & Interface Science*, *7*(5-6), 456-461.

Jiang, X. Y. , Li, W. X. , & Cao, H. . (2008). Study of the interaction between trans-resveratrol andbsa by the multi-spectroscopic method. *Journal of Solution Chemistry, 37*(11), 1609-1623.

Jiang, M., Xia, M. X., Zheng, D., Liu, Y., Li, X. Y., & Chen, X. (2004). Spectroscopic studies on the interaction of cinnamic acid and its hydroxyl derivatives with human serum albumin. *Journal of Molecular Structure, 692*, 71–80.

Jiang, Z., Li, T., Ma, L., Chen, W., Yu, H., Abdul, Q., ... & Tian, B. (2020). Comparison of interaction between three similar chalconoids and α-lactalbumin: Impact on structure and functionality of α-lactalbumin. *Food Research International*, *131*, 109006.

Jia, J., Gao, X., Hao, M., & Tang, L. (2017). Comparison of binding interaction between β-lactoglobulin and three common polyphenols using multi-spectroscopy and modeling methods. Food Chemistry, 228, 143–151.

Jiang, L., Wang, Z., Li, Y., Meng, X., Sui, X., Qi, B., et al. (2015). Relationship between surface hydrophobicity and structure of soy protein isolate subjected to different ionic strength. *International Journal of Food Properties, 18*(5), 1059–1074.

Li, M., Fokkink, R., Ni, Y., & Kleijn, J. M. (2019). Bovine beta-casein micelles as delivery systems for hydrophobic flavonoids. *Food Hydrocolloids*, *96*(NOV), 653-662.

Li, T., Hu, P., Dai, T., Li, P., Ye, X., Chen, J., & Liu, C. (2018). Comparing the binding interaction between β-lactoglobulin and flavonoids with different structure by multi-spectroscopy analysis and molecular docking. *Spectrochimica Acta Part A: Molecular and Biomolecular Spectroscopy*, *201*, 197-206.

Li, T., Hu, P., Dai, T., Li, P., Ye, X., Chen, J., & Liu, C. (2018). Comparing the binding interaction between β-lactoglobulin and flavonoids with different structure by multi-spectroscopy

analysis and molecular docking. *Spectrochimica Acta Part A: Molecular and Biomolecular Spectroscopy*, *201*, 197-206.

Liang, L. , Tajmir-Riahi, H. A. , & Subirade, M. . (2008). Interaction of beta-lactoglobulin with resveratrol and its biological implications. *Biomacromolecules, 9*(1), 50.

Livney, Y. D. (2010). Milk proteins as vehicles for bioactives. *Current Opinion in Colloid & Interface Science*, *15*(1-2), 73-83.

Mikheeva, L. M., Grinberg, N. V., Grinberg, V. Y., Khokhlov, A. R., & De Kruif, C. G. (2003). Thermodynamics of Micellization of Bovine β-Casein Studied by High-Sensitivity Differential Scanning Calorimetry. *Langmuir*, *19*(7), 2913-2921.

Moeiniafshari, A. A., Zarrabi, A., & Bordbar, A. K. (2015). Exploring the interaction of naringenin with bovine beta-casein nanoparticles using spectroscopy. *Food Hydrocolloids*, *51*, 1-6.

Pandita, D., Kumar, S., Poonia, N., & Lather, V. (2014). Solid lipid nanoparticles enhance oral bioavailability of resveratrol, a natural polyphenol. *Food Research International*, *62*, 1165-1174.

Patel, A. R., Heussen, P. C. M., Hazekamp, J., Drost, E., & Velikov, K. P. (2012). Quercetin loaded biopolymeric colloidal particles prepared by simultaneous precipitation of quercetin with hydrophobic protein in aqueous medium. *Food Chemistry*, *133*(2), 423-429.

Patel, K. R., Scott, E., Brown, V. A., Gescher, A. J., & Brown, K. (2011). Clinical trials of resveratrol. *Annals of the New York Academy of Sciences*, *1215*(1), 161-169.

Perinelli, D. R., Bonacucina, G., Cespi, M., Bonazza, F., Palmieri, G. F., Pucciarelli, S., . . . Vincenzetti, S. (2018). A comparison among β-caseins purified from milk of different species: Self-assembling behaviour and immunogenicity potential. *Colloids and surfaces B: Biointerfaces*, *173*, 210-216.

Portnaya, I., Benshoshan, E., Cogan, U., Khalfin, R., Fass, D., Ramon, O., & Danino, D. (2008). Self-assembly of bovine beta-casein below the isoelectric pH. *Journal of Agricultural & Food Chemistry*, *56*(6), 2192-2198.

Portnaya, I., Cogan, U., Livney, Y. D., Ramon, O., & Danino, D. (2006). Micellization of bovine beta-casein studied by isothermal titration microcalorimetry and cryogenic transmission electron microscopy. *Journal of Agricultural & Food Chemistry*, *54*(15), 5555-5561.

Qi, X., Xu, D., Zhu, J., Wang, S., Peng, J., Gao, W., & Cao, Y. (2021). Studying the interaction mechanism between bovine serum albumin and lutein dipalmitate: Multi-spectroscopic and molecular docking techniques. *Food Hydrocolloids*, *113*, 106513.

Ranadheera, C. S., Liyanaarachchi, W. S., Chandrapala, J., Dissanayake, M., & Vasiljevic, T. (2016). Utilizing unique properties of caseins and the casein micelle for delivery of sensitive food ingredients and bioactives. *Trends in Food Science & Technology*, *57*, 178-187.

Rute, A., Neves, Marlene, Lúcio, Susana, Martins, . . . Reis. (2013). Novel resveratrol nanodelivery systems based on lipid nanoparticles to enhance its oral bioavailability. *International journal of nanomedicine*.

Svajger, U., & Jeras, M. (2012). Anti-inflammatory effects of resveratrol and its potential use in therapy of immune-mediated diseases. *International Reviews of Immunology*, *31*(3), 202-222.

Uruakpa, F. O., & Arntfield, S. D. (2006). Surface hydrophobicity of commercial canola proteins mixed with κ-carrageenan or guar gum. *Food Chemistry*, *95*(2), 255-263.

Walle, T., Hsieh, F., Delegge, M. H., Jr, O. J., & Walle, U. K. (2004). HIGH ABSORPTION BUT VERY LOW BIOAVAILABILITY OF ORAL RESVERATROL IN HUMANS. *Drug Metabolism & Disposition the Biological Fate of Chemicals*, *32*(12), 1377.

Wang, Q., Pan, M. H., Chiou, Y. S., Li, Z., Wei, S., Yin, X., & Ding, B. (2022). Insights from alpha-Lactoalbumin and beta-Lactoglobulin into mechanisms of nanoliposome-whey protein interactions. *Food Hydrocolloids*, *125*, 107436.

Yuan, X., Li, X., Zhang, X., Mu, Z., Gao, Z., Jiang, L., et al. (2018). Effect of ultrasound on structure and functional properties of laccase-catalyzed α -lactalbumin. Journal of Food Engineering, 223, 116–123.

Zhao, Y., Cao, Y., Sun, J., Liang, Z., & Zhang, S. (2019). Anti-breast cancer activity of resveratrol encapsulated in liposomes. *Journal of Materials Chemistry B*, *8*(1).

Zhang, G., Que, Q., Pan, J., & Guo, J. (2008). Study of the interaction between icariin and human serum albumin by fluorescence spectroscopy. Journal of Molecular Structure, 881, 132–138.

Zimet, P., Rosenberg, D., & Livney, Y. D. (2011). Re-assembled casein micelles and casein nanoparticles as nano-vehicles for ω-3 polyunsaturated fatty acids. *Food Hydrocolloids*, *25*(5), 1270-1276.

CHAPTER 5 - Overall Conclusions

Caseins are a family of proteins constituted by α-caseins (αs-1 and αs-2 caseins), β-caseins and κ-caseins. β-caseins, in particular, show a temperature and concentration-dependent self-assembling behavior. Recently, β-CN micelles have been suggested as natural nanocarriers for the delivery of hydrophobic compounds, promoting their bioavailability. Until now, all studies regarding both chemical-physical characterization and applications of β-CNs have been performed using the protein of bovine origin. However, it could be interesting to exploit the use of β-CNs from other milk sources. Bovine β-CN has been considered one of the major responsible of Cow Milk Protein Allergy (CMPA) and the use of hypoallergenic donkey milk (DM) may help to avoid this problem.

Therefore, in CHAPTER 2 of this thesis work, the self-assembling behavior, secondary structure, and surface hydrophobicity of purified donkey β-CN in terms of pH, temperature, and buffer concentration were firstly investigated, and then in comparison with commercial bovine β-CN. Fluorescence spectra analysis of donkey and bovine β-CN proteins indicates that their ANS (8-anilino-1-naphthalenesulfonic acid) binding characteristics are significantly influenced by pH and temperature, suggesting that the tertiary structure undergoes rearrangement when exposed to hydrophobic regions, especially at lower pH (pH 6.0) and higher temperatures (50°C). Furthermore, according to circular dichroism (CD) analysis, both pH and temperature can impact the ordered secondary structure of donkey and bovine β-CNs, predominantly represented by the increasing α-helix and poly (Pro)II helix-like conformations. These structural features together could lead to pH, temperature, and ionic strength dependence of CMC and CMT. The results of this work can provide structural information and insight on critical parameters promoting intra and inter-molecular interactions involved in micellization for the development of β-CNs based nanocarriers useful to encapsulate bioactive compounds for pharmaceutical and nutraceutical applications.

Thus, based on the structural information of donkey β-CN mentioned above, the bioactive molecule vitamin D2 (VD2) was chosen to explore its interaction with donkey β-CN, as presented in

Chapter 3. Interaction mechanisms between donkey and bovine β-CNs with VD2 were studied at high vitamin/protein molar ratios using fluorescence and Dynamic Laser Light Scattering (DLS) techniques. The results showed that VD2 effectively quenched the intrinsic fluorescence of both donkey and bovine β-CNs through a static quenching mechanism, with a similar number of binding sites for the proteins. The addition of VD2 increased the surface hydrophobicity of both proteins. Furthermore, the DLS results indicated that at increasing concentrations of VD2, this molecule seems to aggregate into nanoparticles whose size is unaffected by the presence of the proteins, suggesting that VD2 cannot be encapsulated into β-CN micelles. These findings reveal the potential use of hypoallergenic donkey β-CN as a delivery system for hydrophobic vitamins, particularly in non-fat food enrichment.

The interaction between donkey and bovine β-CNs with the lipophilic polyphenolic compound resveratrol was analyzed by the protein fluorescence spectrum, and the results indicated that resveratrol effectively interacted with both β-CN proteins, and its interaction mechanism was similar to that occurred for β-CNs and VD2 (see CHAPTER 4). Interestingly, analysis of the resveratrol fluorescence spectrum showed that it could be encapsulated within both β-CNs' micelles, particularly at concentrations exceeding 40 μM. HPLC analysis revealed that with the increase in protein concentration from 40 μM to 80 μM, the encapsulation efficiency of resveratrol within donkey β-CN micelles increased from 54.81% to 82.01%, whereas in bovine β-CN micelles, it increased from 45.74% to 80.23%. Future research should be carried out to explore the release kinetics of resveratrol and the stability of the resulting nanoparticles during processing and storage.

In summary, the self-assembly properties and structural changes of purified β-CN obtained from hypoallergenic donkey milk at different pH, temperature, and ionic strength were similar to those of commercial bovine β-CN. Based on this structural information, the bioactive molecules VD2 and resveratrol can effectively interact with both β-CN proteins. Moreover, resveratrol could be successfully encapsulated within the β-CN micelles. The results of this study suggest the possibility of developing delivery systems for hydrophobic bioactive compounds using β-CN

purified from hypoallergenic donkey milk, highlighting the potential of this protein as an innovative and promising vehicle for enhancing the enrichment and bioavailability of various bioactive substances in food products.

ACKNOWLEDGEMENTS

Since September 2018, I embarked on a journey at University of Camerino to pursue a double master's degree. I successfully obtained my master's degree in June 2020, and commenced my doctoral studies in November 2020. Throughout these five years at Camerino, I have always been profoundly grateful and exceptionally delighted to be a part of UNICAM. First of all, I would like to express my sincere gratitude to my supervisors **Prof. Paolo Polidori, Prof. Silvia Vincenzetti,** and **Prof. Stefania Pucciarelli.** Under your guidance, I have completed my doctoral project efficiently. I remember when I started my PhD study, you always patiently showed me to do experiments and read literatures step by step. When I encountered difficulties, you would help me solve them together and always gave me encouragement and confidence, which made me feel very warm, like family. Your serious attitude towards research and your love for life have left a deep impression on me and encouraged me to continue on this path of my PhD study. You always encourage me to participate in various courses, conferences, and learn new experimental skills. Whenever I need you, you are always there, as you said 'Jingjing, I am here!'. You also remind me to take time to relax and enjoy life. No matter how beautiful words can express your help to me and my gratitude to you in the past five years. I am lucky enough to be your student, thanks a lot!

I'd like to express my gratitude to my **family** for their unwavering support and constant presence, standing by my side. I'm also thankful for my friends and colleagues. Also thanks to **Dr. Diego Romano Perinelli**, for helping me with my experiments, analyzing the data, and reviewing the article. Thanks to **Prof. Valeria Polzonetti and Dr. Sofia Renzi**.

Finally, I would like to thank my Chinese supervisors **Prof. Guiqin Liu and Prof. Lanjie Li** for their guidance in my study and concern in my life. I really appreciate that **Liaocheng University** give me an opportunity to study and supported my research in UNICAM.